University of Nevada, Reno

**Exploring Adaptation-Based Techniques to Create
Comfortable Virtual Reality Experiences**

A Dissertation Submitted in Partial Fulfillment

of the Requirements for the Degree of Doctor of Philosophy in

Computer Science and Engineering

by

Isayas Berhe Adhanom

Dr. Eelke Folmer / Dissertation Advisor

May 2022

The Graduate School

We recommend that the dissertation prepared under our supervision by

Isayas Berhe Adhanom

entitled

**Exploring Adaptation-Based Techniques to Create
Comfortable Virtual Reality Experiences**

be accepted in partial fulfillment of the requirements for the degree of

Doctor of Philosophy

Eelke Folmer, Ph.D. – Advisor

Paul MacNeilage, Ph.D. – Committee Member

David Feil-Seifer, Ph.D. – Committee Member

Alireza Tavakkoli, Ph.D. – Committee Member

Nicholas Murray, Ph.D. – Graduate School Representative

David Zeh, Ph.D. – Dean, Graduate School

May 2022

ABSTRACT

Virtual reality (VR) is transitioning from research to widespread consumer use. However, VR sickness - a type of motion sickness associated with VR usage - is believed to be a major impediment to the mass adoption of VR and it is estimated to affect more than two-thirds of VR users. Previous research also shows that VR sickness affects some vulnerable groups, such as women, more severely than other groups. Although several strategies have been developed to mitigate VR sickness, most of them are not equally effective for all users since the effectiveness of any particular strategy varies across individuals. There are also concerns that some widely used VR sickness mitigation strategies, such as field-of-view (FOV) restriction, may have negative consequences on women. This thesis aims: 1) to provide theoretical understanding of the aspects of VR systems that cause VR sickness to affect some user more than others, with focus on sex differences, and 2) to develop adaptation-based strategies that could mitigate VR sickness for all VR users irrespective of their differences.

Towards these goals, I first investigate the effectiveness of FOV restriction in reducing VR sickness across genders, and it's effects on women's spatial navigation ability. Then, based on findings from the first set of studies, I develop and empirically evaluate a novel adaptive eye gaze-contingent FOV restrictor that allows users to have a wider visual field while blocking their peripheral FOV. The wider visual field would be beneficial for women's spatial navigation performance in virtual environments. Finally, I provide a novel standardized adaptation based training paradigm that supplements existing VR sickness mitigation techniques by allowing the user to best prepare themselves for continued VR use. Evaluation of this strategy suggests that it could reduce and even eliminate VR sickness in susceptible individuals irrespective of their individual differences.

ACKNOWLEDGEMENTS

I would like to express my sincere gratitude to my advisor Professor Eelke Folmer. Thank you for taking a chance on me and for your mentorship, guidance, kindness, and generosity. I could never have done any of this research without the opportunities you gave me. For that, I am very grateful. Furthermore, I would like to sincerely thank my second advisor Dr. Paul MacNeilage for his invaluable mentorship, advice, and encouragement as I ventured into the intersection of Computer Science and Cognitive Psychology. I am also grateful to my advising committee members, Dr. David Feil-Seifer, Dr. Alireza Tavakkoli, and Dr. Nicholas Murray without whom this journey would not be complete. I would like to thank them for their insightful feedback on my research.

The work in this thesis would not be possible without the numerous collaborators whom I have had the pleasure to work with. I would like to thank everyone who contributed to my research from my co-authors to my research participants. Special thanks go to Majed Al Zayer who selflessly mentored me during my early years as a Ph.D. student, and who still continues to support my career pursuits.

An enormous thank you goes to my family. To my parents, I would not be where I am today without your constant support and your life-long sacrifices. To my siblings, thank you for the constant support and for celebrating every small success I had along the way. I specially want to thank my brother Yonas for always being a rock of moral, financial, and spiritual support.

I dedicate this thesis to my partner and the love of my life Semhar whose unconditional love and support carried me through the ups and downs of my Ph.D. journey, and to my lovely sons Jacob and Joseph. Thank you for believing in me and for helping me persevere.

TABLE OF CONTENTS

LIST OF TABLES

LIST OF FIGURES

Chapter 1

Introduction

Virtual Reality (VR) holds great promise to revolutionize the way we interact with computers. With the growing interest in immersive virtual worlds, such as the Metaverse, VR has the potential to be the next transformational computing platform. However, widespread adoption of VR is currently hindered by the fact that many users suffer from VR sickness [91], which involves a suite of symptoms including nausea, sweating, increased heart rate, dizziness, and disorientation.

VR sickness is a type of motion sickness specific to VR [114]. Motion sickness (MS) is experienced as a result of motion patterns of an organism that result in symptoms that include dizziness, cold sweating, headache, increased salivation, and nausea [91]. Visually induced motion sickness (VIMS) is a related phenomenon that has induced symptoms similar to those of MS without being subject to physical motion [99]. VIMS is a common adverse effect that results from exposure to computer simulations in general and VR experiences in particular. Several terms have been given to VIMS in the literature [91], the most common of which are: simulator sickness, cybersickness, and VR sickness. We choose to use the term "VR sickness" to refer to VIMS from this point forward.

Several theories have attempted to explain the cause of VR sickness. Some theories attribute VR sickness symptoms to a sensory conflict [146] while others believe that it is a result of a failure to maintain postural stability while being immersed in the virtual environment [150]. Other less prominent theories include the eye-movement theory [53] and the poison theory [179]. None of these theories is

complete, though the sensory conflict theory is the most widely accepted one.

It is estimated that up to 67% of adults may experience mild to severe symptoms [33] of VR sickness. However, VR sickness does not affect all users equally. Previous research shows that women are more likely to experience VR sickness than men [75, 120, 134, 67, 64], and that people with disabilities such as Multiple Sclerosis are affected differently by VR sickness than people without these disabilities [15]. This has the potential to negatively impact the adoption of VR among these vulnerable users and could impede these users from realizing the full potential of VR. Despite this, few suitable interventions that are tailored towards women [111] or people with disabilities [15] have been proposed.

To date, most research on alleviating sickness and discomfort in VR has focused on improving VR hardware and software without giving much consideration to human factors, such as sex, age, and disability status of users, that have been shown to affect the incidence and severity of VR sickness. In general, existing VR sickness mitigation strategies fall short at accommodating the individual differences between users. To address these challenges, in this thesis, I, and my collaborators, conducted a series of studies.

First, we conducted two studies to explore and better understand how sex differences could cause differences in the incidence of VR sickness and the effectiveness of widely used VR sickness mitigation strategies. The results from the first set of studies gave us the fundamental insight that adaptation, where either the virtual environment changes based on the user's behaviour, or the user adapts their behaviour towards the environment, holds the key to alleviating VR sickness for all users irrespective of their differences. Therefore, we explored two types of adaptation: 1) stimulus adaptation, where we adapt the virtual stimulus in real-time

based on the users behavior, focusing on eye-gaze behaviour, and 2) perceptual adaptation, where we develop training paradigms to allow each user to gradually adapt to the VR sickness causing virtual stimulus.

We developed prototypes for both types of adaptation and conducted user studies to empirically evaluate them. The first prototype was an adaptive gaze-contingent (foveated) FOV restriction mechanism that responds to the user's eye gaze movements in real-time. Evaluation of this prototype showed that this prototype is effective at reducing VR sickness while allowing users to have a wider visual field, removing one of the major problems with current FOV implementations. Finally, we introduced a new paradigm for VR sickness mitigation that aims to tackle VR sickness through training or perceptual adaptation. This allows users susceptible to VR sickness to better adapt to VR sickness through training allowing them to gradually adapt to the VR sickness causing stimulus, thereby increasing VR accessibility for those prone to sickness. Below, I present summaries of the studies I conducted as part of this thesis.

Chapter 2: Field-of-View Restriction to Reduce VR Sickness Does not Impede Spatial Learning in Women

Field-of-view (FOV) restictiction is a widely used strategy to reduce vection-induced VR sickness. Motion from optical flow is primarily detected by the rods on the periphery of the retina [182]. Blocking the perception of peripheral motion by reducing the user's FOV during locomotion [159, 106] is therefore considered an effective strategy to reduce VR sickness. FOV restriction -also known as "tunneling" -is already widely used in popular VR experiences like Google Earth VR and

is recommended by both Google's [3] and Oculus' [130] VR design guidelines as a feasible strategy for reducing VR sickness. However, these design guidelines seem to conflict directly with results from prior studies [41, 173] that found that women benefit from spatial navigation using a larger FOV.

In this study, I explore the effectiveness of FOV restriction and evaluate how FOV restriction could affect women differently compared to men. I specifically explored spatial learning and how it is affected by FOV restriction given that no studies have investigated this yet. In this study, we used the Morris Water Maze (MWM) to evaluate spatial learning and memory of our participants. First introduced by Richard Morris in 1981 [118], the Morris Water Maze (MWM) task has been one of the gold standards in behavioral neuroscience to evaluate spatial learning and memory in rodents [17]. Studies on human spatial learning and memory have used a virtual version of the MWM [17]. Our study found that a gender difference in spatial learning ability exists between men and women, but an FOV restrictor did not impede spatial learning in either sex.

Chapter 3: The Effect of a Foveated Field-of-view Restrictor on VR Sickness

From our first study (see Chapter 2) on FOV restriction, we were able to identify that existing FOV restrictor implementations use a head-fixed restrictor where the effect is applied to the center of the head-fixed FOV which is only updated by the user's head gaze. With this approach, peripheral motion stimulation is only optimally blocked when the head and eye gaze align, i.e, when the user is looking at the center of the HMD. However, this may not always be the case; for example,

the user's eye gaze may shift to eccentric targets in the visible field that are blocked by the restrictor. In such a case, the effectiveness of the FOV restrictor is impeded because the user's peripheral vision is not fully blocked by the restrictor exposing it to optical flow, which could increase VR sickness, and the restrictor could fall on the users foveal region, which could break immersion. These issues have the potential to affect women more than men, as women have a wider FOV [99, 104].

In this study [7] we developed a new type of adaptive FOV restrictor, one where the restrictor is gaze responsive. This foveated FOV restrictor assures that peripheral vision always remains blocked from any optical flow, which could lower VR sickness, and makes it impossible for a user to look at the restrictor itself, allowing users to visually explore a larger portion of the virtual environment during locomotion. Our evaluation of the new system showed that there was a significant difference in eye gaze behavior, as measured by eye gaze dispersion, with the foveated FOV restrictor allowing participants to have a wider visual scan area compared to the head-fixed FOV restrictor (the widely used approach), which confined their eye gaze to the center of the FOV. Although it needs further research, this has the potential to increase spatial navigation performance of users, especially women.

Chapter 4: GazeMetrics: An Open-Source Tool for Measuring the Data Quality of HMD-based Eye Trackers

As virtual reality (VR) garners more attention for eye tracking research, knowledge of accuracy and precision of head-mounted display (HMD) based eye trackers becomes increasingly necessary. It is tempting to rely on manufacturer-provided in-

formation about the accuracy and precision of an eye tracker. However, unless data is collected under ideal conditions, these values seldom align with on-site metrics. Therefore, best practices dictate that accuracy and precision should be measured and reported for each study. To address this issue, we provide a novel open-source suite for rigorously measuring accuracy and precision for use with a variety of HMD-based eye trackers. This tool is customizable without having to alter the source code, but changes to the code allow for further alteration. The outputs are available in real time and easy to interpret, making eye tracking with VR more approachable for all users.

Chapter 5: VR Sickness Adaptation with Ramped Optic Flow Transfers from Abstract To Realistic Environments

Many VR sickness mitigation strategies involve consistently modifying the visual stimulus to reduce its impact on the user, but this customised approach can have drawbacks in terms of complexity of implementation and non-uniformity of user experience. This study presents a novel alternative approach that involves training the user to better tolerate the adverse stimulus by tapping into natural adaptive perceptual mechanisms. In this study, we recruited users with limited VR experience that reported susceptibility to VR sickness. Baseline sickness was measured as participants navigated a rich and naturalistic visual environment. Then, on successive days, participants were exposed to optic flow in a more abstract visual environment, and strength of the optic flow was successively increased by increasing the visual contrast of the scene, because strength of optic flow and the resulting vection are thought to be major causes of VR sickness. Sickness measures

decreased on successive days, indicating that adaptation was successful. On the final day, participants were again exposed to the rich and naturalistic visual environment, and the adaptation was maintained, demonstrating that it is possible for adaptation to transfer from more abstract to richer and more naturalistic environments. These results demonstrate that gradual adaptation to increasing optic flow strength in well-controlled, abstract environments allows users to gradually reduce their susceptibility to sickness, thereby increasing VR accessibility for those prone to sickness.

1.1 Publications

The work included in this dissertation has resulted in the following publications:

- The work presented in Chapter 2 has resulted in the following publications:

  Isayas Berhe Adhanom, Majed Al-Zayer, Paul Macneilage, and Eelke Folmer. (2021). Field-of-view restriction to reduce VR sickness does not impede spatial learning in women. ACM Transactions on Applied Perception (TAP), 18(2), 1-17.

  Majed Al-Zayer, Isayas Berhe Adhanom, Paul Macneilage, and Eelke Folmer. (2019). The effect of field-of-view restriction on sex bias in vr sickness and spatial navigation performance. In Proceedings of the 2019 CHI Conference on Human Factors in Computing Systems (pp. 1-12).

- The work presented in Chapter 3 has resulted in the following publication:

  Isayas Berhe Adhanom, Nathan Navarro Griffin, Paul MacNeilage, and Eelke Folmer. (2020, March). The effect of a foveated field-of-view restrictor on VR sickness. In

2020 IEEE conference on virtual reality and 3D user interfaces (VR) (pp. 645-652). IEEE.

- The work presented in Chapter 4 has resulted in the following publication:

  Isayas Berhe Adhanom, Samantha C. Lee, Eelke Folmer, and Paul MacNeilage. (2020, June). Gazemetrics: An open-source tool for measuring the data quality of HMD-based eye trackers. In ACM symposium on eye tracking research and applications (pp. 1-5).

- The work presented in Chapter 5 is in review for publication at Frontiers in Virtual Reality.

Chapter 2

Field-of-View Restriction to Reduce VR Sickness Does not Impede Spatial Learning in Women

2.1 Introduction

Virtual reality (VR) has enjoyed significant popularity in recent years and has finally emerged from research labs into consumer's hands. Though consumer VR headsets have significantly advanced in terms of tracking, latency, refresh rate, resolution and optics, VR sickness is still considered a major barrier to the mass market success of VR. VR sickness is a type of motion sickness specific to the domain of VR [114] and may involve a suite of symptoms including nausea, pallor, sweating, stomach awareness, increased heart rate, drowsiness, disorientation, and general discomfort [90]. There is substantial evidence that women are more susceptible than men to sickness caused by simulators [75, 134, 67, 64] and virtual reality [120] which might have contributed to a low adoption rate (<5%) of VR technology among women [186].

A likely trigger of VR sickness is vection, i.e., the visually-induced illusion of self-motion [94]. Self-motion perception combines visual, vestibular and proprioceptive afferents and these systems are usually in agreement. When using real walking using positional tracking, users generally experience no VR sickness as vestibular and proprioceptive signals are generated that match the presented optical flow [107]. However, when navigating VR using a game controller, the absence
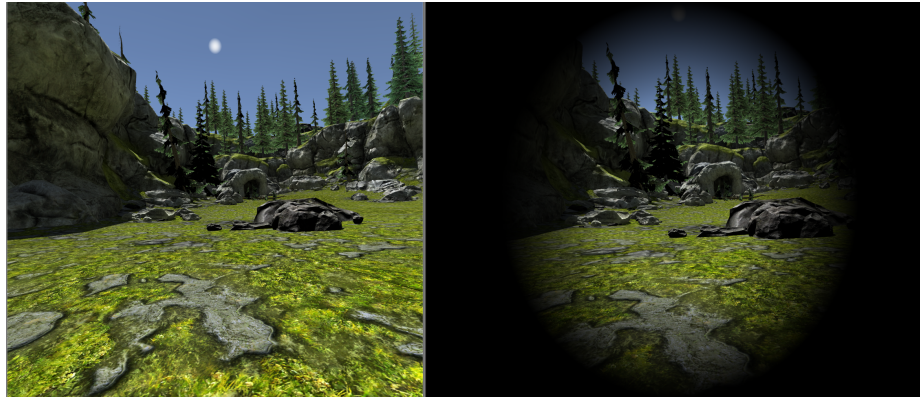
Figure 2.1: Self-motion from optical flow is driven strongly by motion at the periphery of the retina. Blocking peripheral motion by reducing the field-of-view during locomotion (right image) mitigates sensitivity to visual-vestibular conflict and VR sickness.

of any real physical movement in spite of visual self-motion leads to a sensory conflict [140], which can induce VR sickness [94].

Self-motion from optical flow is driven strongly by motion at the periphery of the retina [189]. An effective strategy for reducing VR sickness is to reduce the user's field-of-view (FOV) during locomotion (see Figure 2.1) as this reduces stimulation of the periphery by visual motion [159, 106]. However, related studies found that applying an FOV restrictor on desktop 3D environments impedes spatial navigation performance [103, 123, 142], and this effect was significant for women [41].

Spatial learning is the process of encoding spatial information about an environment to enable efficient navigation and to develop a mental representation of this environment. Sex differences in spatial learning have been well documented [187]. Although the biological factors that cause this difference remain unclear, men and women employ different strategies in spatial learning, e.g., men rely primarily on geometric information (e.g., turns and distance travelled) while women rely primarily on landmarks (e.g. salient objects seen along the path travelled)

[193, 157]. Though men exhibit better spatial learning performance on certain tasks [42, 49], on desktop 3D environments this sex difference can be mitigated by providing women with a larger FOV which is thought to work by increasing their ability to use landmarks [41, 173].

Sex differences should be considered in the design of interactive systems [20]. FOV restriction is already a widely used strategy [130], but we currently do not know whether it impedes spatial learning in women. Changes in availability of spatial learning cues might have significant implications for the general accessibility of VR. Our paper aims to provide insight into this complex relationship.

2.2 Background

VR sickness (also known as cybersickness or simulator sickness) is a type of motion sickness that is specific to the domain of VR [114]. There are several theories that aim to explain VR sickness -but these theories are neither exclusive nor exhaustive [94, 148]. The sensory conflict theory [146] attributes VR sickness to a conflict between the visual, vestibular, and proprioceptive senses. The postural instability theory [151] links VR sickness to a disruption of postural stability caused by the motion patterns of the visual stimulus of the virtual experience [151]. The eye movement theory suggests that rapid involuntary eye movements evoked by optical flow or visual patterns can innervate the vagal nerve and cause VR sickness [54]. The poison theory suggests VR sickness symptoms like nausea and vomiting are due to an incorrect application of a survival mechanism that becomes active when the body is poisoned [179]. The sensory conflict theory, however, seems to be the most widely accepted theory [91, 99].

Among individual traits that have been shown to increase the vulnerability to VR sickness [99, 166, 104, 71], sex is commonly reported, with the observation that women are more susceptible to VR sickness than men [146, 166, 120, 184]. Hormonal differences [37], physiological differences [71], under-reporting of sickness symptoms by men [23], and differences in FOV [99, 104] have all been proposed as explanations of this sex disparity in the incidence of VR sickness.

An improperly calibrated interpupillary distance (IPD) on a VR headset could lead to eye strain which is a symptom of VR sickness as measured by the widely used Simulation Sickness Questionnaire's oculomotor discomfort score [90]. US women have an IPD range of [52–76 mm] [74] while popular VR headsets support a minimum IPD range of [58–60] mm. It has been shown that improperly calibrated IPDs could be a reason why women tend to become VR sick more than men [165].

Various methods have been proposed to reduce the incidence of VR sickness. Due to recent advances, tracking inaccuracy and rendering latency are no longer significant causes of VR sickness on consumer VR platforms -though these are still problematic on mobile VR platforms. Real walking using positional tracking generally doesn't cause VR sickness, but its use is bounded by available tracking space.

To travel larger distances, users must rely on artificial locomotion technique (ALT). Examples include partial gait techniques like walking-in-place [178], arm-swinging [115] or gait negation techniques like omnidirectional treadmills [44] or low friction surfaces [171]. See [12] for an extensive survey of ALTs. Teleportation is a widely used ALT that circumvents sensory conflict because it instantly translates the virtual viewpoint which avoids any optical flow generation. Though it is a standard ALT in many VR experiences, there are significant concerns with using teleportation such as low presence [28] and spatial disorientation [36, 88, 22]. For

multiplayer games, having avatars being discontinuously represented when they teleport is an issue as it makes it difficult to follow or chase other players [76].

VR sickness can also be reduced by drugs [104], but effectiveness is limited due to adverse side effects [71]. An alternative is to use behavioral interventions that either regulate the user's behavior (e.g., head movements or breathing), or manipulate the visual stimuli [91]. There is some evidence that balance training can prevent motion sickness symptoms [154]. Manipulation of the visual stimuli has been achieved by controlling the FOV [27, 93, 106, 61, 25], using independent backgrounds and rest frames [145, 51], dynamically controlling travel velocity [174], freezing the virtual viewpoint rotations [89], and blurring non-salient virtual objects [125].

The effect of FOV on participants' performance and quality of user experience in VR has been the focus of several studies. Reducing the FOV was shown as an effective intervention to reduce the incidence of VR sickness [159, 106, 27, 93]. Dynamic FOV restriction [61] applies an FOV restrictor as a function of the users linear and angular velocities [61] which allows users to experience the full FOV when there is no optical flow. Other studies showed that larger FOV can increase the sense of presence [159, 106, 103]. However, on desktop 3D environments, FOV restriction was shown to impede spatial learning performance [191, 123, 142] with a greater negative impact on women [41, 173]. Even though prior studies used desktop environments, their findings are highly relevant to VR given that the FOV of consumer VR headsets (up to 110°) is still well below the human binocular FOV (up to 190°) [79].
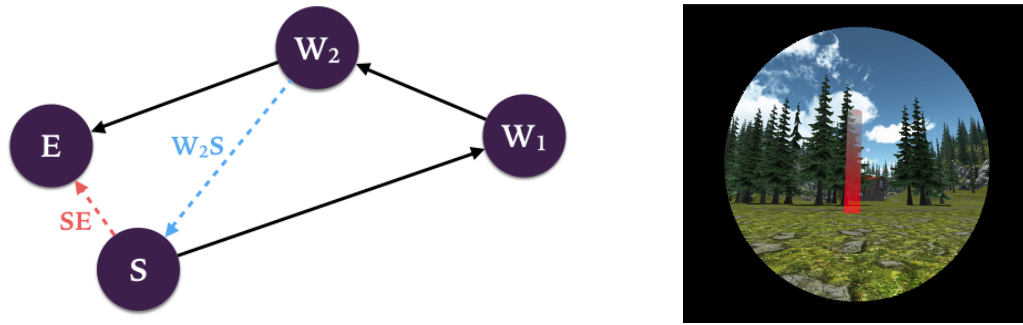
Figure 2.2: Left: the triangle completion task. S = starting position, E = estimated position, W_1 = first waypoint, W_2 = second waypoint, $\vec{W_2S}$ = the vector from the second waypoint to the starting position, and $\vec{SE}$ = the vector from the starting position to the estimated position, which indicates the error of the path integration. **Right: FOV restrictor showing the waypoint users must navigate to.**

2.2.1 Prior Work

In closely related earlier work [10], we investigated whether dynamic FOV restriction affects path integration ability differently in women versus men. Path integration is one component of spatial navigation and refers to the process of integrating self-motion (using inertial/visual/auditory cues) over time to obtain an estimate of one's current position relative to a starting point [108]. Participants performed a triangle completion task [109], which is a standardized navigation task for assessing path integration ability. This task required participants to travel from a starting position to two consecutive waypoints (see Figure 2.2) shown one after the other, which are non collinear with the starting position and which form two adjacent legs of a triangle. After arriving at the second waypoint, participants were then asked to navigate back to the starting position (S) and confirm their location (E). The distance between (S) and (E) is an indication of the path integration error. Similar to prior FOV studies [27, 93, 106, 61, 25], participants used a controller for navigation as this is most likely to induce VR sickness. We recruited 28 participants (14 females) in our study and found that a dynamic FOV restrictor was effective

in reducing VR sickness in both sexes –as measured using the simulator sickness questionnaire (SSQ). Contrary to our expectations, FOV restriction did not impede path integration ability in men or women.

2.2.2 Study Overview

A limitation of our earlier study was that path integration is considered to be only one component of spatial navigation which also involves skills like spatial learning, spatial memory, and constrained route planning [153]. For spatial navigation, women reportedly rely more on landmarks to cognitively map spaces [193, 157]. Applying an FOV restrictor can block peripheral landmarks which might impede spatial learning to a larger extent than path integration ability. In this paper we specifically explore spatial learning and how it is affected by FOV restriction using a virtual Morris Water Maze (MWM) [17] given that no studies have investigated this yet.

2.3 Methods

2.3.1 Participants

We recruited 31 participants, with normal or corrected to normal vision, but three women exited the study due to severe discomfort. This resulted in a final sample of 28 participants (14 women) who completed the study (minimum: 18, maximum: 42, mean age: 22.96, SD: 5.41) and whose data was considered in our analysis. We balanced the sex of participants in order to assess the role of sex in spatial learning

	1	2	3	4	5	
Never						*Very frequently*

How frequently do you use VR?

	1	2	3	4	5
Women	35.7% (5)	42.8% (6)	14.3% (2)	7.2% (1)	0.0% (0)
Men	42.8% (6)	28.5% (4)	7.2% (1)	7.2% (1)	14.3% (2)
Total	39.3% (11)	35.6% (10)	10.7% (3)	7.1% (2)	7.1% (2)

How frequently do you get motion or VR sick?

	1	2	3	4	5
Women	50.0% (7)	21.4% (3)	7.2% (1)	21.4% (3)	0.0% (0)
Men	50.0% (7)	42.8% (6)	7.2% (1)	0.0% (0)	0.0% (0)
Total	50.0% (14)	32.1% (9)	7.2% (2)	10.7% (3)	0.0% (0)
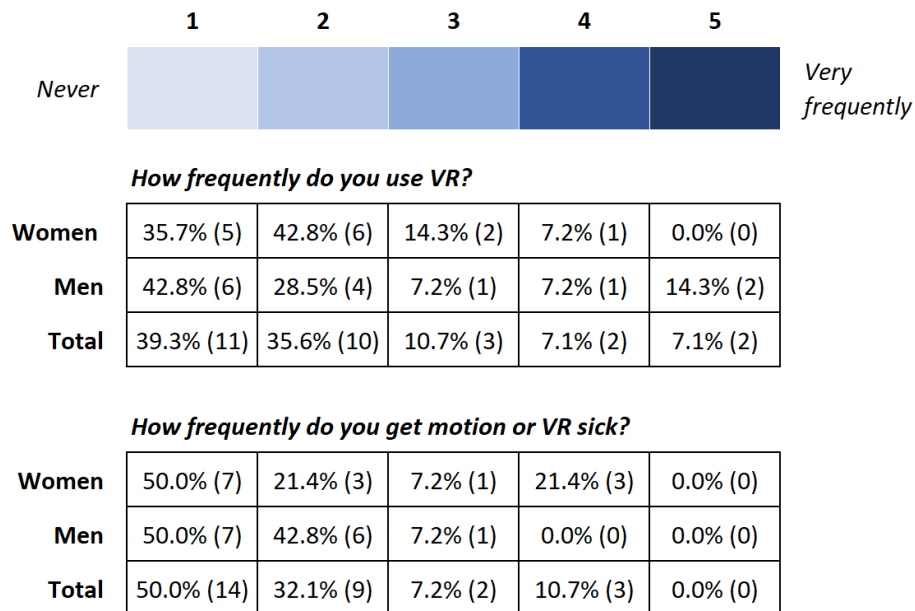
Figure 2.3: Summary of participants ratings of their frequency of using VR and their tendency of getting motion or VR sick on a scale of 1 (never) to 5 (very frequently). The results are reported in the form of *percentage (count)*.

and VR sickness incidence. We asked participants to rate their frequency of using VR on a scale of 1 (rarely) to 5 (very frequently) as well as their frequency of getting motion or VR sick and the results broken down by sex are listed in Figure 2.3. Participants were recruited at the University of Nevada through flyers and word of mouth. Each participant was given a $15 Amazon gift card as compensation for their participation. This study was approved by the University of Nevada's Institutional Review Board.

A power analysis, with power set at 0.8, α set at 0.05, and estimated effect size set at 0.28, indicated that 28 participants would be required to have adequate power. The effect size was estimated based on effect sizes found in other similar virtual reality studies, and in our closely related previous work [10, 61]. Power analysis was performed with G*Power 3 [57].

2.3.2 Materials

Equipment

We used the HTC Vive as the VR headset in this study which has a 110° diagonal FOV, 90Hz refresh rate, 2160×1200 pixels of combined resolution, adjustable interpupillary distances, and six-degrees of freedom tracking for position and orientation, respectively. The headset was powered by a computer having a 3.4GHz AMD Ryzen 7 eight-core processor with 16GB memory and NVIDIA GeForce GTX 1080 Ti graphics card running Windows 10. We were able to achieve a frame rate close to 90 fps for our MWM simulation. An Xbox 360 controller was used for omni-directional locomotion using the left thumb-stick and for selection participants used the A button. This controller was more familiar to participants and more suitable for our study than the Vive track-pad as the thumb-stick offers better haptic feedback and granularity of control.

Tasks

Virtual Morris Water Maze Task   First introduced by Richard Morris in 1981 [118], the MWM task has been one of the gold standards in behavioral neuroscience to evaluate spatial learning and memory in rodents [17]. Studies on human spatial learning and memory have used a virtual version of the MWM [17]. Briefly, the task tests the quality of the subject's spatial learning through their ability to remember the location of a hidden object in reference to distal cues that are not co-located with the hidden object [118]. This task can be used to investigate which mechanism is more dominant during spatial navigation, path integration or landmark based navigation [108]. Previous work has reported sex differences
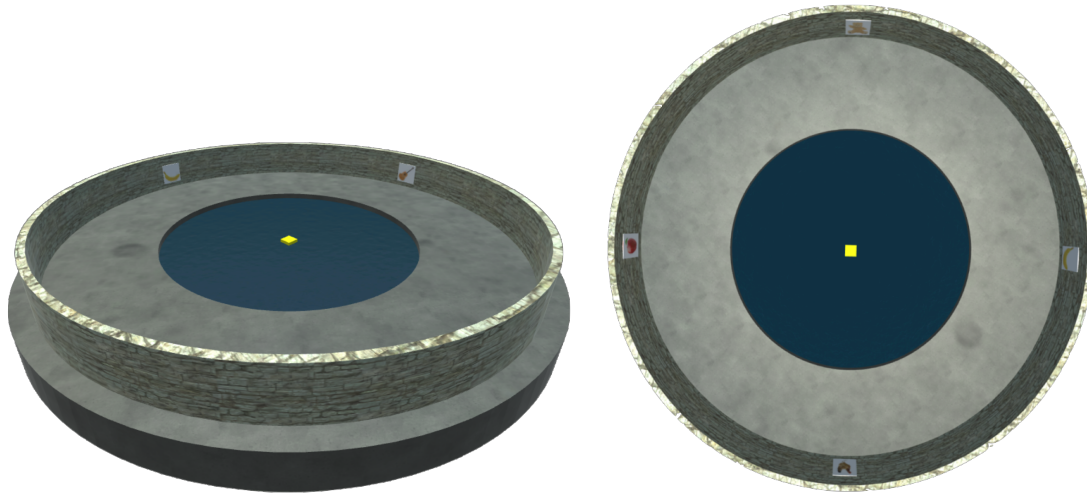
Figure 2.4: Left: Depiction of the Virtual MWM we used in this study with one location of the platform location shown in yellow and landmarks on the walls. Right: Third-person view of the water maze used in the object placement task.

in performance of the MWM task with men relying more on path integration and women relying more on landmark-based navigation [193, 157]. We believe findings achieved using the MWM task generalize to navigating any virtual environment as this typically relies on a combination of path integration and landmark based navigation.

For locomotion input we used a controller because previous studies that have evaluated the effectiveness of FOV restriction also used a controller and found this to induce VR sickness [159, 106, 27, 93, 61]. In each trial, participants started from a starting position at the edge of the pool while facing the wall (see Figure 3). Participants were then asked to move around in the pool to find a hidden platform under the water surface within 1 minute. The platform was found when participants crossed its location under the water surface. This was indicated to the participant using sound feedback and by the platform raising up, which elevated their viewpoint. If the platform was not found within 1 minute, participants heard a different feedback sound and the platform was made visible. When that happened, partici-

pants were asked to move towards the platform until they reached it. Participants then continued on to the next trial after 5 seconds.

To assess spatial learning over time, participants were asked to locate the hidden platform over several trials grouped in blocks. Within a block of trials, the location of the platform was fixed but the starting point changed on each trial. In blocks that followed, the location of the platform, the sequence of starting positions, and the landmarks were changed. Participants went through 6 blocks of 6 trials each for every FOV condition. Starting positions were separated by 30° and a random sequence of starting positions was created for each block of trials.

Object Placement Task   For navigation, humans generally rely on a combination of two distinct strategies defined by the spatial memory process they rely on, e.g., allocentric and egocentric navigation [32]. Where egocentric navigation relies on learned associations between the observer and landmarks (self-referenced), allocentric navigation relies more on a cognitive map of the environment (world-referenced). Because our assumption is that an FOV restrictor may impede the observation of landmarks, this would primarily affect allocentric learning. To evaluate this, we used an additional task where we tested participants' ability to estimate the location of the platform using an object placement task. This task was modeled after the relative vector discrimination (RVD) task proposed by Starrett and Ekstrom [169]. Spatial memory is never purely egocentric or allocentric [60] and the RVD task was designed in such a way that the optimal solution relies on allocentric information. With the RVD task, after finding the platform, participants were presented with a bird's-eye view of the arena and had to place a platform in the remembered location.

Virtual Environment

We modeled our virtual MWM exactly after the one used in [17]. The virtual environment consists of a 42m-wide circular pool filled with opaque water below which is a hidden 2m × 2m × 2m cubic platform. When made visible, the platform is elevated 1m above the water surface. The pool is positioned at the center of an open-roof 75m-wide circular arena with a wall that is 8m-high. Placed on the wall of the arena are four 2D images distributed evenly. Each of these images act as a distal cue that participants can use to remember the position of the platform. Distances were mapped such that 1 Unity unit equals 1m. Participants experienced the environment at a first-person-view and achieved navigation using the thumb-stick of the Xbox 360 controller at a speed that varied between 0 and 4.2m/s. Omni-directional steering was achieved using the same thumb-stick at a direction relevant to the virtual viewpoint's forward vector. Participants always started the virtual experience from a point at the edge of the pool. To ensure that participants always stay in the pool, the water surface was made 1m below the pool wall. We used Blender to design the virtual environment that was imported to Unity3D, the virtual world generator used to run the study. We used the FOV restrictor developed by SixWays [175] and configured it as explained in the previous section. Our implmentation of the virtual MWM and the FOV restrictor can be found on Github [1]. Figures 2.5 and 2.4 show first-person and third-person views of the virtual environment, respectively.

---

[1] https://github.com/isayasMatter/virtual-morris-water-maze

2.3.3 Design

We used a 2×2 mixed factorial design in which sex and FOV condition were the independent variables. Sex was the between-subjects variable with two levels: Men and Women. FOV condition, the within-subjects variable, also had two levels: no FOV restriction (RN) and dynamically changing FOV (RY). We use a dynamic FOV restriction [63] as unlike a static FOV restrictor this allows users to experience the full FOV while they are stationary. We considered eight dependent variables in this study. Four of these measured spatial learning: learning rate, distance traveled, placement error, and placement latency. The remaining four were the SSQ [90] scales: Total Severity (TS), Nausea (N), Oculomotor Discomfort (O), and Disorientation (D). Each participant experienced two sessions, one for each FOV condition. To minimize the transfer of VR sickness symptoms across sessions, each session was conducted on a separate day with at least 24 hours of rest between sessions. Most participants returned the next day but due to scheduling conflicts the maximum time one participant returned for the second session was 4 days.

Each session contained six blocks of trials with each block containing six platform search trials and one object placement task. The order of blocks was changed across sessions to minimize learning effects. Half of the participants started with the RN condition (Group A) while the other half started with the RY condition (Group B). We alternated the assignment of men and women to each group to ensure that both groups had an equal number of men and women.

Each participant experienced two FOV conditions in this study: the full FOV allowed by the VR headset (RN) and the dynamic FOV restriction (RY) (see Figure 2.5). Similar to Fernandes and Feiner [61] and Bolas et al. [25], we dynamically
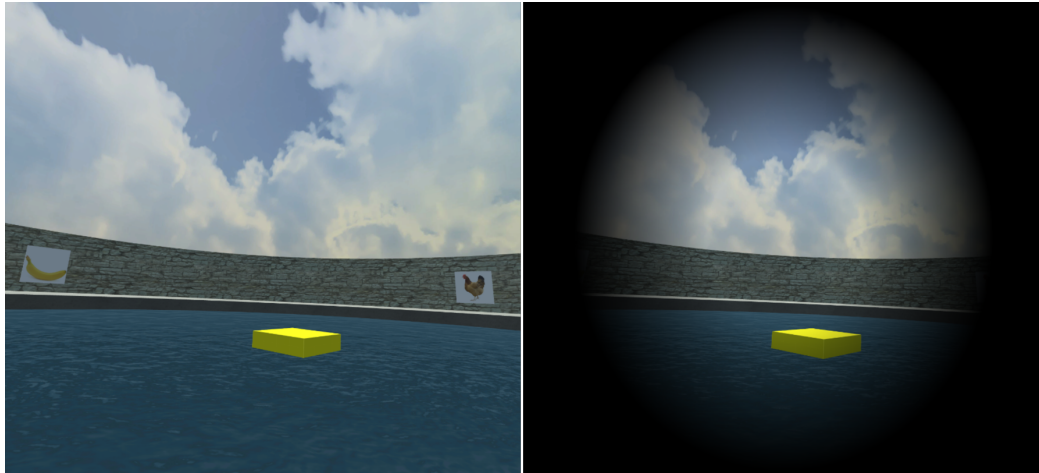
Figure 2.5: Visual conditions used in the study. Left: Morris Water Maze with no restrictor. Right: Water maze shown using an FOV restrictor.

manipulated the FOV as a function of the participant's linear and angular speeds using a black texture with a transparent circular cutoff (Figure 2.5). The restrictor narrowed down the FOV as a response to and increase in linear or angular movements by manipulating the radius of the circular cutoff according to the following formula [175]:

$$FOV_{r,t} = FOV_{r,t-1} \times [1 - (RF_{max} \times max(\frac{v_t}{v_{max}}, \frac{\omega_t}{\omega_{max}}))] \tag{2.1}$$

where $FOV_{r,t}$ and $FOV_{r,t-1}$ are the radii of the circular cutoff at times t and $t-1$, respectively. RF_{max} is the maximum restriction applied to $FOV_{r,t-1}$ at the peak linear or angular speeds. v_t and v_{max} are the current and maximum virtual linear speeds, respectively. ω_t and ω_{max} are the current and maximum virtual angular speeds, respectively. We empirically chose a value of 0.75 for RF_{max} to match the tunneling effect used in common VR experiences such as Google Earth VR. Through preliminary trials, we found the values 4.2m/s and $180°/sec$ suitable for v_{max} and ω_{max}, respectively. To make participants less distracted, the edges of the restrictor were

feathered and FOV restriction was applied gradually over time.

2.3.4 Measurements

Virtual MWM Task

We measured participants' performance in the virtual MWM task in terms of learning rate and distance traveled. We quantify learning rate as the mean of slopes of the normalized search completion (t_n) times across blocks. For each search trial, we calculated t_n as follows:

$$t_n = \frac{t_c}{\vec{IP}} \tag{2.2}$$

where t_c is the trial completion time and $\vec{IP}$ is the absolute distance between the starting position and the hidden platform position. We performed this normalization to factor out the time needed to travel directly to the platform from the search time. Because no place learning takes place during the first trial of a block, we excluded the first trial from the learning rate calculation. Because we are interested in the performance difference between the beginning and the end of a block, the slope was calculated from the second and last trials. A steep negative slope indicates learning. The distance traveled was measured as the mean distance traveled across all trials.

Object Placement Measures

We measured object placement performance in terms of placement error and placement time. The placement error was measured as the Euclidean distance between

the estimated platform position and its actual position. The placement time was measured as the elapsed time from the start of the task until the participant presses the controller's A button.

Simulator Sickness Questionnaire Measures

We measured VR sickness symptoms through the SSQ and scored them according to the procedure prescribed by Kennedy and Lane [90] to obtain the weighted Total Severity (TS), Nausea (N), Disorientation (D), and Oculomotor discomfort (O) scores.

2.3.5 Procedure

The study was conducted in a quiet space void of obstacles. On the first day, upon their arrival, participants were greeted and seated for an orientation at which participants were familiarized with the goal of the study, its duration, collected data, and tasks. The participants' IPD was then measured using a ruler and was used to calibrate the VR headset's IPD. We asked participants whether they could properly converge using this setting and if this wasn't the case, we let them adjust the IPD settings until they could. The IPD of the headset (HTC Vive) used in this study was limited to a value that varied between 60.9mm and 75.4mm. Accordingly, participants' measured IPD was rounded up or down to the limits of the headset's IPD when their IPD was outside the range of the headset's IPD. Participants were then asked to stand at the center of the tracking space to take part in the training session, whose goal was to familiarize participants with the controls, the virtual environment, and the tasks. The training session consisted of one block of three

platform search trials followed by an object placement task. For training purposes, participants were informed that the platform shall be positioned at the center of the virtual pool for all three search trials. To familiarize participants with the unsuccessful search scenario, we asked participants not to move during the first training trial until the deadline has passed, which we set for 20 seconds only for the training session. While they were briefed about the platform search task, we pointed out to participants the location of the four landmarks that could be used to remember the location of the platform. Navigation generally relies on a combination of path integration and landmark navigation and we encouraged participants to use landmarks since we anticipated this process to be affected by FOV restriction.

Participants were also encouraged to strike a balance between estimation time and accuracy while performing the placement task. Each participant performed six blocks, each consisting of six platform search trials and one placement task. Participants filled in a SSQ at the end of the session. On the second day, participants performed six experiment blocks, and then filled in another SSQ at the end of the trial. Participants then filled a post-study questionnaire at which they provided their age, sex, frequency of experiencing motion or VR sickness (five-point Likert scale), and their experience with VR (five-point Likert scale). On average, the duration of the study took approximately one hour divided between day one (≈ 40 minutes) and day two (≈ 20 minutes).

2.4 Results

We report on the analysis of results of our 28 participants who fully completed our study. Table 2.1 gives a summary of the results in terms of means and standard

Condition	No restrictor (RN)			FOV restrictor (RY)		
Sex	Women	Men	Total	Women	Men	Total
Virtual MWM						
Learning rate	-.01 (.1)	-.03 (.1)	-.02 (.1)	-.01 (.1)	-.09 (.1)	-.05 (.1)
Distance	39.78 (8.0)	38.26 (8.6)	39.02 (8.2)	39.61 (6.2)	37.34 (8.4)	38.48 (7.4)
Object Placement						
Accuracy	3.04 (.9)	3.38 (1.4)	3.21 (1.2)	2.81 (1.0)	3.02 (1.3)	2.91 (1.2)
Time	8.84 (2.4)	10.53 (4.4)	9.69 (3.6)	9.36 (3.8)	10.92 (5.2)	10.14 (4.5)
Simulator Sickness Questionnaire						
SSQ Total Score	27.52 (27.9)	23.78 (28.7)	25.65 (27.6)	15.76 (18.2)	16.56 (17.8)	16.16 (17.6)
SSQ Disorientation	33.81 (41.1)	24.86 (37.9)	29.33 (39.1)	19.89 (27.14)	15.91 (26.1)	17.90 (26.2)
SSQ Nausea	25.21 (26.1)	22.49 (23.6)	23.85 (24.4)	12.95 (17.4)	14.31 (14.4)	13.63 (15.7)
SSQ Oculomotor	17.33 (18.7)	16.78 (22.7)	17.05 (20.4)	10.83 (11.4)	13.54 (16.3)	12.18 (13.9)

Table 2.1: Quantitative measures of virtual MWM, Object placement, and simulator sickness questionnaire in terms of *mean (standard deviation).*

deviations. For all our analyses, all our data was tested for normality using a Shapiro-Wilk test, and Levene's test for homogeneity of variances was used to test for homogeneity of variances amongst groups.

2.4.1   Virtual Water Maze Task

Spatial performance in the virtual MWM task was measured in terms of learning rate and distance traveled. Figures 2.6 and 2.7 show summary of the results. There was homogeneity of variances in our MWM task data, as assessed by Levene's test of homogeneity of variance (p > .05).

A two-way mixed ANOVA did not detect a significant interaction between sex and FOV condition ($F_{1,26} = 2.41, p = .13, \eta_p^2 = .085$) with respect to *learning rate*. No significant difference was found between FOV conditions ($F_{1,26} = 1.86, p = .19, \eta_p^2 = .067$) while women had significantly slower learning rate than men ($F_{1,26} = 4.21, p = .050, \eta_p^2 = .139$). This p-value was exactly 0.050 (truncated out to three decimal places) and is therefore considered significant given that p is significant
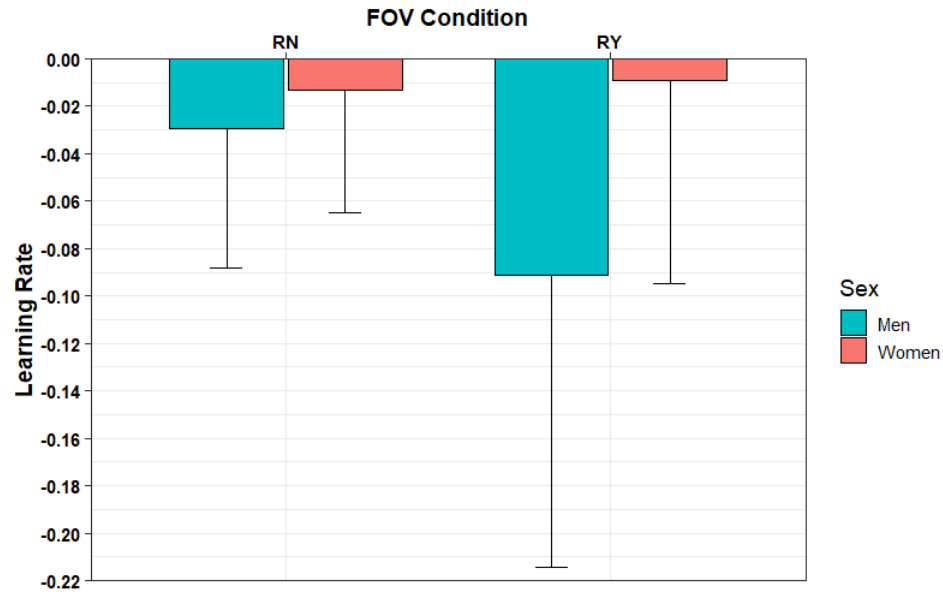
Figure 2.6: Average learning rate shown in terms of the slope and summarized by sex and FOV condition. RN= No FOV restriction. RY = Dynamic FOV restriction. Error bars show standard deviation.

for p≤ α [87].

A two-way mixed ANOVA did not find a significant interaction between sex and FOV condition ($F_{1,26} = .05, p = .83, \eta_p^2 = .002$) with respect to *distance traveled*. No significant main effect of sex ($F_{1,26} = .6, p = .45, \eta_p^2 = .023$) or FOV condition ($F_{1,26} = .10, p = .75, \eta_p^2 = .004$) was detected either.

2.4.2 Object Placement Task

We measured performance in the object placement task in terms of their estimation accuracy of the platform location and time delay to provide the estimation. Figures 2.8 and 2.9 show summary of the results. A Levene's test of homogeneity of variance showed that there was homogeneity of variances (p > .05) across groups in our placement task data.
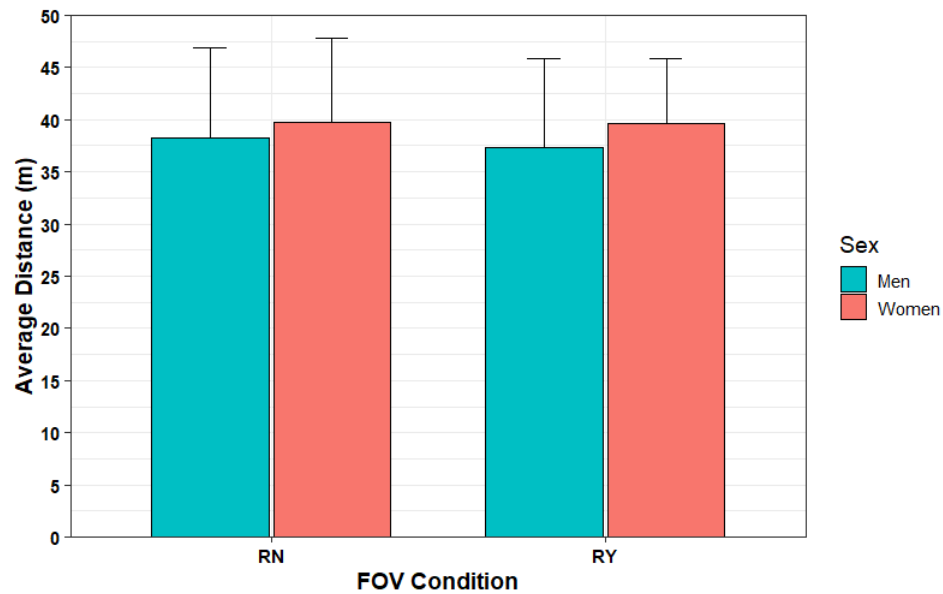
Figure 2.7: Average distance traveled summarized by sex and FOV condition. RN= No FOV restriction. RY = Dynamic FOV restriction. Error bars show standard deviation.

A two-way mixed ANOVA did not find a significant interaction effect between sex and FOV condition ($F_{1,26} = .13, p = .72, \eta_p^2 = .005$) with respect to *placement accuracy*. No significant effect of sex ($F_{1,26} = .47, p = .50, \eta_p^2 = .018$) or FOV condition ($F_{1,26} = 2.28, p = .14, \eta_p^2 = .081$) was found either.

A two-way mixed ANOVA did not find a significant interaction effect between sex or FOV condition ($F_{1,26} = .01, p = .92, \eta_p^2 = .000$) with respect to *placement time*. No significant effect of sex ($F_{1,26} = 1.33, p = .26, \eta_p^2 = .049$) or FOV condition ($F_{1,26} = .54, p = .47, \eta_p^2 = .020$) was found either.

2.4.3 Simulator Sickness Questionnaire

Levene's test was conducted to assess the equality of variances in our SSQ data, and the test showed that there was homogeneity of variances (p > .05) across the
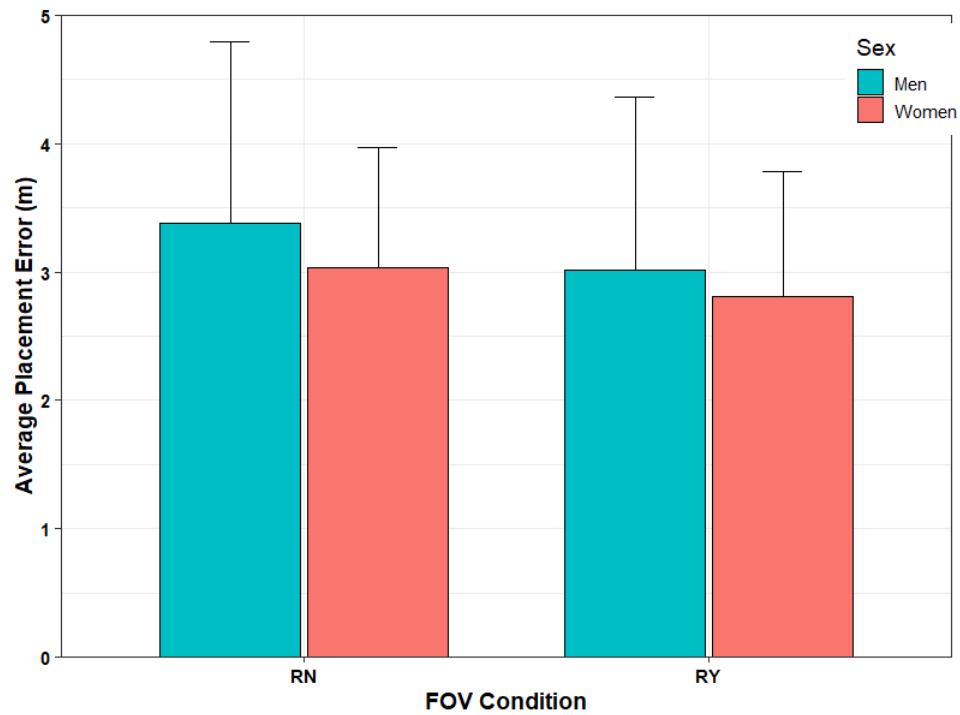
Figure 2.8: Object placement accuracy in terms of placement error and summarized by sex and FOV condition. RN= No FOV restriction. RY = Dynamic FOV restriction. Error bars show standard deviation.

groups. A two-way mixed ANOVA did not find an interaction effect between sex and FOV condition with respect to the TS ($F_{1,26} = .32, p = .58, \eta_p^2 = .012$), N ($F_{1,26} = .33, p = .57, \eta_p^2 = .013$), O ($F_{1,26} = .175, p = .68, \eta_p^2 = .007$), and D ($F_{1,26} = .213, p = .649, \eta_p^2 = .008$) scores. No significant main effect of sex was found on the TS ($F_{1,26} = .03, p = .86, \eta_p^2 = .001$), N ($F_{1,26} = .01, p = .92, \eta_p^2 = .000$), O ($F_{1,26} = .031, p = .86, \eta_p^2 = .001$), and D ($F_{1,26} = .31, p = .58, \eta_p^2 = .012$) scores. FOV restriction resulted in significantly lower TS ($F_{1,26} = 8.30, p = .008, \eta_p^2 = .242$), N ($F_{1,26} = 8.31, p = .008, \eta_p^2 = .242$), O ($F_{1,26} = 6.30, p = .019, \eta_p^2 = .195$) and D ($F_{1,26} = 4.50, p = .044, \eta_p^2 = .147$) scores. Figure 2.10 shows a summary of the results.

Seven participants (all women) had IPDs less than 60.9mm, which is the minimum IPD of the VR headset we used in this study. We analysed the IPD results
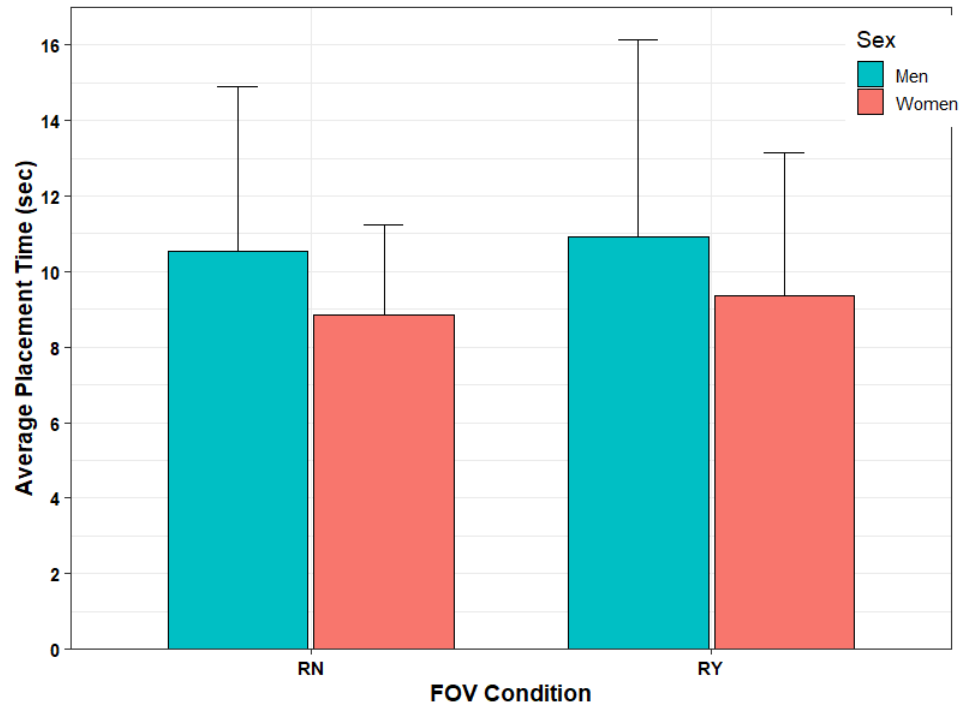
Figure 2.9: Object placement time summarized by sex and FOV condition. RN= No FOV restriction. RY = Dynamic FOV restriction. Error bars show standard deviation.
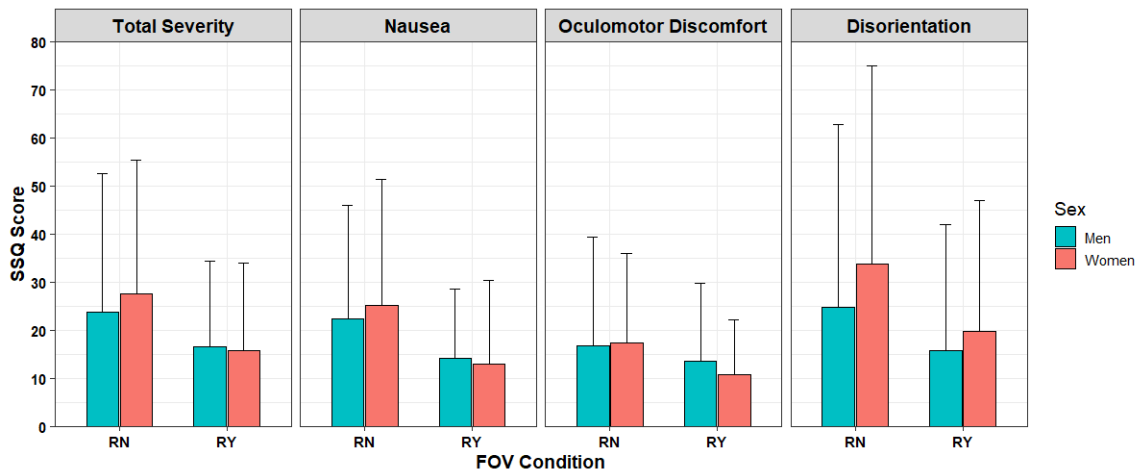
Figure 2.10: The weighted total severity, nausea, oculomotor discomfort, and disorientation SSQ scores summarized by sex and FOV condition. RN= No FOV restriction. RY = Dynamic FOV restriction. Error bars show standard deviation.

to check if improper IPD calibration due to the headset limitation could have led

to eye strain that would, in turn, lead to oculomotor discomfort. We did not find,

however, a significant difference between the Oculomotor Discomfort scores of the seven women in question and the rest of the participants ($t_{27} = -1.94$, $p = .062$).

2.5 Discussion

2.5.1 Spatial Learning

Similar to previous studies [17, 139] that explored sex differences using a virtual MWM task, our study found a significant sex difference in spatial learning, with women showing a significantly lower learning rate. This is quantified in terms of improvement in place learning over time, given fixed distal landmarks.

Also similar to these previous studies [17, 139], we did not observe any significant differences between men and women in the object placement task (i.e., spatial memory retrieval). Previous research suggests that having participants experience the object placement task from a third-person view makes performance depend more on allocentric information (e.g., landmarks) than the virtual MWM task [169]. The narrower sex difference in performance of the object placement task could be a consequence of women using landmark-based navigation more often than men do [157]. Participants took part in the object placement task after several repetitions of the virtual MWM task. This might have given participants enough time to learn the position of the platform by the time they started the object placement task, which might be another reason why no sex difference was found in the object placement task. This is in line with a previous study which suggests that environment familiarity through repetition can lead to reduced observations of sex differences in spatial abilities [127].

Our findings are important because unlike earlier virtual MWM studies [17, 139] that used desktop 3D environments, our study used a VR headset, which offers a different spatial information fidelity profile than desktop VR [169]. Thus, our findings are applicable to today's consumer VR platforms.

2.5.2 FOV restriction

Our analysis did not find a significant effect of FOV restriction on spatial learning. On the surface, this seems to contradict previous studies on desktop platforms which showed that restricting FOV impedes spatial navigation performance of both sexes in general [103, 123, 142] and of women in particular [41, 173]. There are, however, key differences in our study that might explain why we obtained different results. We used a VR headset that has an FOV of 110°. Participants in previous studies, however, experienced VR using a desktop monitor with significantly lower FOV. Moreover, the FOV was fixed throughout the experiment session in earlier studies. The restrictor that we used, however, only gets narrowed as a response to participants' linear or angular head movement, giving participants an opportunity to experience the full FOV provided by the headset while their head is stationary. However, when looking around to find the next waypoint, an FOV restrictor is applied based on angular head velocity. Our study investigated dynamic FOV restriction in comparison to the baseline condition of no FOV restriction, we believe future research should compare fixed vs. dynamic FOV restriction.

These two differences in the degree of FOV and the behavior of the FOV restrictor might have given both men and women a fair chance in performing equally across FOV conditions in our study.

2.5.3 VR Sickness

The use of a dynamic FOV restrictor was effective in reducing VR sickness for both sexes while it did not impede spatial learning. However, unlike previous studies [75, 120, 134, 67, 64, 166], we did not find a significantly greater report of VR sickness in women compared to men based on any of the SSQ scores. Besides issues regarding experimental conditions and hardware a possible reason for this could be due to the nature of the navigation task used in our study. Generally, VR experiences with involuntary movements are more likely to induce VR sickness than VR experiences where the user controls their movements [116, 168] –though a recent study using a driving simulators found a contradictory result [183]. In our study, participants were standing up and could rotate their view with their head which minimizes visual-vestibular conflict. Earlier studies that found sex differences used involuntary movements (i.e., roller coaster) or used fixed head positions with the viewpoint updated by a controller which could have exacerbated VR sickness incidence. An implication of this decision is providing participants with limited proprioceptive and vestibular input which might have reduced the magnitude of sensory conflict, which might have led to low VR sickness scores across sexes.

Out of the 31 participants we recruited for this study, three participants exited due to severe discomfort on the first session. Two of these participants experienced VR with a full FOV, while the third experienced it with the FOV dynamically restricted. It is interesting to note that all of those who exited were women with very limited experience using VR. Two of these participants also reported having frequent occurrences of motion or VR sickness. Since frequent exposure to VR can reduce the symptoms of VR sickness and past experience with VR sickness [166, 99]

can influence the incidence of VR sickness, these two factors might at least partially explain why these participants exited the study. Although our choice of number of participants matches previous similar studies [61], most of the effect sizes revealed a medium to large effect size [40]. A larger number of participants could increase the effect size and make our results and findings more certain. Therefore, as future work, we plan to expand the study by recruiting more participants.

Our results indicate that an FOV restrictor used with high-end consumer VR headsets seems to be effective for both sexes in reducing VR sickness without impeding spatial learning. Our results complement earlier findings on this relationship [10], but this prior study only evaluated path integration ability. Combining results from both studies provides strong evidence that FOV restrictors can be safely used to minimize VR sickness with no adverse side effects on spatial navigation performance.

Chapter 3

The Effect of a Foveated Field-of-view Restrictor on VR Sickness

3.1 Introduction

Virtual Reality (VR) has finally emerged from research labs into consumers' hands. In less than a decade, consumer VR headsets have significantly advanced in terms of tracking, latency, refresh rate, resolution and optics. However, VR sickness is still preventing many people from using VR. VR sickness is considered a type of motion sickness that is specific to the domain of VR [114] and may involve various symptoms including nausea, pallor, sweating, stomach awareness, increased heart rate, drowsiness, disorientation, and general discomfort [90]. Up to 67% of adults may experience mild to severe symptoms [33], but there is growing evidence that women are more likely to experience VR sickness than men [120, 67].

Though various theories have been postulated that aim to explain VR sickness (see related work), the most likely trigger of VR sickness is generally considered to be vection, i.e., the visually-induced illusion of self-motion [26]. Self-motion perception involves inputs from the visual and vestibular systems and usually these inputs are in agreement. When walking around in VR with the viewpoint updated using positional tracking, users generally don't experience VR sickness because vestibular and proprioceptive afferents from walking are generated that match the perceived optical flow. VR sickness typically occurs when there is visual self motion, but no real physical movement which leads to sensory conflict [140]. This

can happen when users try to navigate VR using a game controller with steering and rate control activated using a thumbstick. Teleportation avoids optical flow generation as it instantly translates the user's viewpoint and thus avoids sensory conflicts. Despite its wide usage, teleportation is considered to offer a low presence [28] while the absence of optical flow can lead to spatial disorientation [22]. For multiplayer games, discontinuous avatar representations present a challenge for gameplay design as it is impossible to follow or chase other players [76].

To be able to still use a controller for navigation, a widely used solution to reduce vection-induced VR sickness is to reduce the field-of-view (FOV) during locomotion. Because motion from optical flow is primarily detected by the periphery of the retina [189], the idea is to block the peripheral stimulation by applying an opaque texture with a transparent circular hole to the center of the user's FOV within the HMD (see Figure 3.1:left). This strategy is also known as tunneling as it gives users the impression that they are traveling through a tunnel. Restrictors can be implemented fairly non-intrusively with users barely observing their presence [61]. Various studies have found FOV restriction to be effective in reducing vection, visual-vestibular conflict and resulting VR sickness [159, 106, 27, 93, 61]. FOV restriction is already widely used in popular VR experiences and is recommended by Google's and Oculus' VR design guidelines [4, 130].

Eye tracking isn't widely available on consumer VR headsets, therefore existing FOV restrictor implementations use a fixed restrictor where the effect is applied to the center of the head-fixed FOV which is only updated by the user's head gaze. Peripheral motion stimulation is most optimally blocked when the head and eye gaze align, i.e, when the user is looking at the center of the HMD. However, this may not always be the case; for example, the user's eye gaze may shift to eccentric
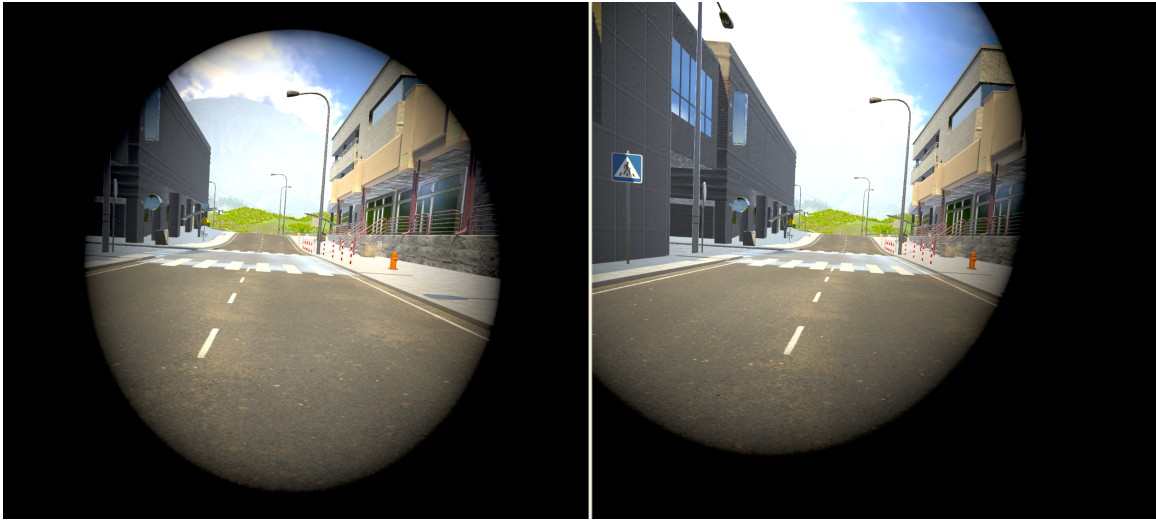
Figure 3.1: **FOV restriction during locomotion is a widely used strategy to mitigate visual-vestibular conflict and VR sickness. A limitation of existing implementations is that they use a viewport fixed restrictor (left). In this paper we explore the effectiveness of a foveated restrictor (right) that moves with the user's eye gaze.**

targets in the visible field that are blocked by the restrictor.

In this example, the effectiveness of a FOV restrictor is impeded because the user's peripheral vision is not fully blocked by the restrictor exposing it to optical flow, which could increase VR sickness. Because the restrictor is head-fixed, the user's gaze is confined to a very small region because there is nothing to see where the restrictor is applied. This head-fixed FOV restrictor is a somewhat unnatural implementation that does not appropriately leverage known properties of the human visual system. Namely foveal vision offers high resolution centrally, with resolution that drops toward the periphery.

In this paper we evaluate a new type of FOV restrictor, one where the restrictor is gaze responsive. This foveated FOV restrictor assures that peripheral vision always remains blocked from any optical flow, which could lower VR sickness, and makes it impossible for a user to look at the restrictor itself, allowing users to

visually explore a larger portion of the virtual environment during locomotion.

3.2   Related Work

VR sickness is still considered a major hurdle for the large scale adoption of VR. A number of theories have been proposed that aim to explain VR sickness-but these theories are neither exclusive nor exhaustive [94]. We discuss these as well as various solutions that have been proposed to mitigate VR sickness.

The eye movement theory suggests that rapid involuntary eye movements evoked by optical flow or visual patterns can innervate the vagal nerve and cause VR sickness [54]. This happens when an image moves contrary to the user's expectations and unnatural eye motions are required to keep the scene image stable on the retina. To judge space, positions, and orientations around them, a person must select a reference frame within which to make judgements. A rest-frame can be defined as a specific reference frame that the observer chooses and that appears to be stationary [144]. Many VR experiences are devoid of such a rest-frame, but involuntary eye movements can be reduced when a rest frame is added. For example: in a driving or flying simulator one can add a heads-up display (HUD). For other VR experiences a HUD might break presence, therefore a virtual nose [192], or an independent background [144] can be used.

The postural instability theory [151] links VR sickness to a disruption of posture stability caused by the motion patterns of the visual stimulus of the virtual experience [151]. Repeated exposure to VR would allow users to better control posture and balance and in due time VR sickness will dissipate.

The sensory conflict theory [146] attributes VR sickness to a conflict between the visual, vestibular, and proprioceptive senses. VR sickness results from a sensory disagreement between expected motion and motion that is actually experienced. An evolutionary explanation [179] as to why conflict leads to sickness is that the brain interprets sensory conflict as a sign of intoxication which then triggers nausea/vomiting/sweating as self-defense responses.

The sensory conflict theory is currently the most widely accepted VR sickness theory [91, 99]. Due to recent advances, tracking inaccuracy and rendering latency are no longer significant causes of visually induced VR sickness on consumer VR platforms -though these are still problematic on mobile VR platforms.

Sensory conflict can be reduced by avoiding optical flow generation, for example by using teleportation. Teleportation is a widely used alternative locomotion technique that allows users to safely navigate beyond the confines of available tracking space but it has issues with low presence [28] and spatial disorientation [22]. A controller is the defacto input technique for navigating 3D environments on desktop/console platforms but using a controller in VR is likely to cause VR sickness [181].

Several studies [159, 106, 103] suggest a positive relationship between FOV size and presence but that negative relationship to VR sickness exists, i.e. using a larger FOV increases presence but also increases VR sickness. Self-motion from optical flow is driven most strongly by motion at the periphery of the retina [182, 189]. Blocking peripheral motion stimulation by reducing the user's FOV (i.e. tunneling) during locomotion is an effective strategy to reduce VR sickness [159, 106, 27, 93, 61]. FOV restriction has been found to be equally effective for both men and women and does not impede path integration ability [10]. Other

strategies to reduce optical flow generation include blurring non-salient virtual objects [125] and optical flow analysis to filter out content that increases optical flow [105]. Optical flow can also be minimized by dynamically controlling the travel velocity [65, 174]. FOV restriction seems to be the most widely implemented strategy to reduce VR sickness and can be found in many popular VR experiences (e.g., Google Earth VR). However, current implementations of FOV restriction do not take the user's eye gaze position into consideration, and could therefore be less effective when the user's eye gaze and head gaze are not aligned. An abandoned patent application exists [58] that describes a foveated FOV restrictor, but to date no studies have evaluated the effectiveness of such a restrictor, which is what our paper contributes.

3.3   Design of foveated FOV Restrictor

To implement a foveated FOV restrictor (FV) that responds to the user's eye gaze, we first implement a fixed FOV restrictor (FX) based on the strategy of Bolas et al [25], Fernandes, and Feiner [61] to dynamically manipulate the FOV in response to changes in the participant's linear and angular velocities in the virtual environment. After the fixed restrictor we implement a method to manipulate it's position in the VE based on the user's eye gaze position.

For both FOV restriction conditions (FX and FV), the FOV was decreased as the participant's speed or angular velocity increases. To restrict the FOV, we used a black texture with a fully transparent circular cut-off. The circular cut-off is defined by an inner and outer radius that together form an annulus. We call the region between these two radii the feathering region. In this region the opacity

of the circular cut-off increases linearly from completely transparent to completely opaque. The inner radius of the circular cut-off is calculated using the following formula [175].

$$FOV_{r,t} = FOV_{r,t-1} \times [1 - (RF_{max} \times max(\frac{v_t}{v_{max}}, \frac{\omega_t}{\omega_{max}}))] \qquad (3.1)$$

$FOV_{r,t-1}$ is the radius of the circular cut-off at time $t-1$. RF_{max} is the amount of restriction applied to $FOV_{r,t-1}$ at the maximum virtual speed. v_t and ω_t are the virtual linear and angular virtual speeds, respectively, at time t. v_{max} and ω_{max} are linear and angular virtual speeds, respectively, at which the maximum FOV restriction is applied. We set RF_{max} to 0.75 for both conditions, which is equivalent to a minimum FOV of 55° on the HTC Vive Pro Eye with a FOV of around 110°. We empirically found that this value is close to the max FOV restriction applied by popular VR experiences such as Google Earth VR [5]. We specifically chose this value as to be able to maximally suppress VR sickness. The outer radius is always set to be $RF_{max} + 0.1$, which indicates that the feathering region covers about 11° of the FOV on the HTC Vive Pro Eye. The value of v_{max} was set to 1.4 m/s, a value that matches the average preferred walking speed of humans [117]. We empirically found 180°/sec worked best as a maximum angular speed to ensure a frequent FOV restriction as a response to the dynamics of head movement. The FOV restriction was applied gradually over 0.15 seconds and the edges of the circular cut-off were feathered as these factors were found to make the restrictor less noticeable to the participants [61].

For the fixed FOV restrictor the center of the restrictor was always fixed at the center of the user's viewport, or at $(0,0)$ in normalized screen coordinates, where

the lower left corner of the viewport is represented by (-1,-1) and the upper right corner is represented by (1,1). For the foveated FOV restrictor the center of the circular cut-off is moved in response to the user's eye gaze. The user's eye gaze position in normalized coordinates was used to move the center of the circular cut-off accordingly at every frame update. To ensure that the movements of the FOV restrictor are smooth and subtle to the user, the eye gaze positions are smoothed using Unity's smooth damp algorithm with a smooth-time parameter of 0.15 seconds. Eye gaze smoothing also helps us avoid jerky movement of the restrictor during blink events. Finally, to avoid blocking large parts of the VE by the foveated restrictor, we ensure that the center of the restrictor does not move beyond the central 20° of visual angle. We chose this value because it is the threshold for gaze shifts that do not involve head movements [136].

3.4   User Study

Based on the arguments presented in the introduction, our study aimed to investigate the following three research questions:

> **Research Questions**
>
> - **RQ$_1$**: Will the foveated FOV restrictor reduce VR sickness more than a fixed FOV restrictor?
> - **RQ$_2$**: Will the foveated FOV restrictor allow for a more unrestricted view of the VE than the fixed FOV restrictor?
> - **RQ$_3$**: Will a foveated FOV restrictor be less noticeable to users than a fixed FOV restrictor?

Because there is some evidence that women are more likely to experience VR sickness [120, 67], as a secondary factor, we evaluate the effect of sex for each research question. In order to do achieve this we balance the sex of participants.

3.4.1   Equipment

We use an HTC Vive Pro Eye HMD with a diagonal FOV of 110°, refresh rate of 90Hz, a combined resolution of 2880×1600 pixels, six degrees of freedom (DoF) for position and orientation tracking, and adjustable interpupillary (IPD) and focal distances. The headset was powered by an AMD Ryzen 7 1700X Eight-Core processor with 16GB of memory and NVIDIA GeForce GTX 1080ti graphics card running Windows 10. We track eye gaze using the HTC Vive Pro Eye's integrated binocular eye trackers which are capable of dark pupil binocular eye tracking with an output frequency of 120 Hz. Eye tracking can be performed in a 110° field of view which is equal to the HMD's field of view. The eye trackers have an estimated accuracy of $0.5° - 1.1°$.

Participants provided input using an XBox controller that we preferred over the Vive's motion sensing controller because participants were likely to be more familiar with this controller and the profile of the thumb stick used for navigation provides better tactile feedback than the Vive's touchpad.

We use Unity3D engine version 2019.1.6 and the Unity3D VR plugin SteamVR version 1.7 to develop the application. HTC's Sranipal SDK version 1.1.0.1 [1] was used to read eye tracking data from the eye trackers. We used the tunneling effect implementation of SixWays [175] to dynamically manipulate the FOV as per the specifications mentioned in Section 3.3.

Figure 3.2: Birdseye view of the virtual environment we used in the experiment sessions, with red dots representing waypoint positions.

3.4.2 Virtual Environment

The VE used was adapted from the Windridge City environment asset [2] from the Unity Asset Store. The environment (Figure 3.2) consists of an urban setting surrounded by lush forests and winding dirt roads. A set of 105 waypoints, each represented by a blue glowing orb, with a surrounding particle effect animation, were added to guide the participant's movement in the VE. The average distance

between successive waypoints was 30m. During the experiment only one way point is shown at a time starting with the first waypoint. A waypoint disappears as a participant approaches within 1.5m of the waypoint, and the next waypoint appears in the environment. Participants used the Xbox controller's thumbstick to navigate the VE at a speed that varied between 0 and 3 m/s. The same thumbstick was used for steering in a direction relative to the head's forward vector.

3.4.3 Measurements

Measurements were collected through our custom virtual environment (VE) and various questionnaires. To investigate **RQ**$_1$, we use the popular simulator sickness questionnaire (SSQ) [90] along with the self-reported discomfort scores in order to measure VR sickness. The discomfort score was collected through the VE by prompting the user to select a score after every five waypoints. This mechanism was pioneered by Fernandes and Feiner [61] and allows a sampling of a VR sickness score during the trial. The discomfort scores were averaged for each participant per FOV condition to obtain an average discomfort score (ADS), and an ending discomfort score was calculated by using the last discomfort score for each participant per condition. The SSQ scores were collected with post-exposure questionnaires using Google forms. Data collected from the SSQ are used to calculate four associated scores, namely: Total Severity, Oculomotor, Nausea, and Disorientation scores. These scores were calculated as per the conversion formulas by Kennedy et al. [90].

To be able to investigate **RQ**$_2$, we measure eye gaze dispersion; a popular method in eye tracking research [110] to measure gaze behaviour and visual at-

tention. The eye gaze data were used to compute participants' gaze dispersion to establish how visual attention was distributed during each of the two FOV restriction conditions [188]. Gaze dispersion is measured as the standard deviation of participant's gaze positions, and is measured separately for the horizontal (yaw) and vertical (pitch) gaze position components. Furthermore, we combine the two components into a single measure of relative distance using the Pythagorean theorem ($x^2 + y^2 = c^2$) [185]. In our study, since we are only concerned with the user's eye movements relative to the viewport, we measure eye tracking data in normalized viewport coordinates. These coordinates consist of (x, y) pairs, where the lower left corner of the viewport is represented by (-1,-1), the center is represented by (0,0), and the upper right corner is represented by (1,1). Thus, the vertical and horizontal coordinates of the eye gaze position are defined with respect to the position of the VR HMD.

To investigate **RQ**$_3$, after completing each session, participants also completed a participant observation questionnaire to assess whether the participants noticed the FOV restrictors during the experiment sessions. This questionnaire was adopted from [61] who adopted it from [170]. The participant observation questionnaire included two questions (bold) that relate to the FOV restrictors and the rest of the questions were distractor questions. Participants were asked to rate the following seven questions on a scale of 1 - 7, where 1 was "Did not notice or did not happen" and 7 was "Very obvious":

- 1. I saw the VE get smaller or larger.

- 2. I saw the VE flicker.

- 3. **I saw the VE get brighter or dimmer.**

- 4. I saw that something in the VE had changed color.

- 5. **I felt like my field of view was changing in size.**

- 6. I felt like I was getting bigger or smaller.

- 7. I saw that something in the VE had changed size.

3.4.4   Experiment Design

A repeated measures mixed design was used for this study, with a within-participant factor of FOV condition (fixed FOV restriction (FX), foveated FOV restriction (FV)) and a between subjects factor of sex (men, women). We inspect the effect of these factors on the following dependent variables: (1) SSQ: total severity score, (2) SSQ: Nausea score, (3) SSQ: Oculomotor score, (4) SSQ: Disorientation score, (5) the average discomfort score (ADS) [61], (6) the ending discomfort score (EDS) [61], (7) the horizontal gaze dispersion score (8) the vertical gaze dispersion score and (9) the combined gaze dispersion score [188]. To account for order effects, half of the participants started with the FX condition (Group A) while the remaining half started with the FV condition (Group B). To minimize the transfer of VR sickness symptoms across sessions, each session was conducted on a separate day with at least 24 hours rest between sessions. To ensure that each group contained an equal number of men and women, we alternated the assignment of men and women across the two groups.

	1	2	3	4	5	
Never						Very frequently
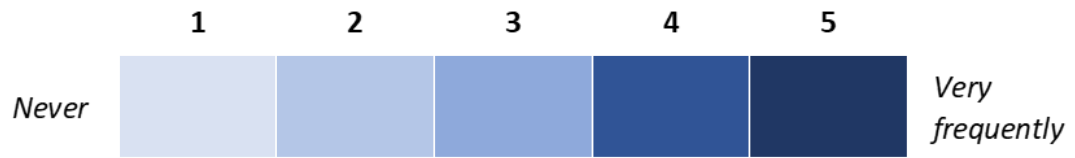
How frequently do you use VR?

	1	2	3	4	5
Women	27.3% (3)	36.4% (4)	18.1% (2)	9.1% (1)	9.1% (1)
Men	36.4% (4)	36.4% (4)	18.1% (2)	0.0% (0)	9.1% (1)
Total	31.8% (7)	36.4% (8)	18.2% (4)	4.5% (1)	9.1% (2)

How frequently do you get motion or VR sick?

	1	2	3	4	5
Women	18.1% (2)	54.6% (6)	0.0% (0)	27.3% (3)	0.0% (0)
Men	72.8% (8)	18.1% (2)	9.1% (1)	0.0% (0)	0.0% (0)
Total	45.5% (10)	36.4% (8)	4.5% (1)	13.6% (3)	0.0% (0)

Figure 3.3: Summary of participants ratings of their frequency of using VR and their tendency of getting motion or VR sick on a scale of 1 (never) to 5 (very frequently). The results are reported in the form of *percentage (count)*.

3.4.5 Procedure

When participants arrived for the first session they were given a short presentation explaining the goal of the study, the outline of the experiment, the risks involved, the data collected, and the details of the training and experiment sessions. The interpupillary distance (IPD) of the participants was measured and was used to set the IPD of the VR headset. Participants were then asked to stand in the middle of the tracking space and were assisted with putting on the VR headset and holding the controller so that they could start the training session.

The goal of the training session was to familiarize the participant with the con-

trols used to provide input and the eye tracker's calibration procedure and to give them an opportunity to practice a short task that was similar to the experiment task. Before starting the training session, participants were asked to complete the eye tracker's calibration procedure. They were then asked to complete a task involving one block of five waypoints, after which they were asked to select a discomfort score from the discomfort score panel. The tunneling effect was not activated during the training session.

During the experiment sessions participants were instructed to follow a set of waypoints at their own pace. After every five waypoints, participants were asked to rate their level of discomfort and were shown a slider from which they had to select their level of discomfort from 0 to 10, with level 10 representing the highest level of discomfort. Participants were encouraged to look around and enjoy the environment around them. After completing each session participants were asked to fill out a SSQ [90] and a participant observation questionnaire to assess if they noticed the FOV restrictors [61] during the experiment sessions.

Finally, participants were asked to fill out a post-study questionnaire which was used to collect demographic information that included their age, sex, frequency of using VR (five-point Likert scale), and tendency of being motion and/or VR sick (five-point Likert scale). On average, the whole study took 1 hour to complete.

3.4.6   Participants

We recruited 25 participants, but three participants (1 man and 2 women) left due to severe VR sickness. 22 participants (11 males/11 females) attended and completed both sessions, and their data were used in the analysis. Participant ages

ranged from 20 to 32 years (average = 23.73, SD = 3.9). Participants were recruited by flyers on a local campus. Participants were asked to rate their frequency of using VR and their tendency to get motion or VR sick on a scale of 1 (never) to 5 (very frequently). The results are summarized in Table 3.3. All participants were compensated with a $15 Amazon gift card. The user study was approved by an IRB.

	Fixed (FX) Restrictor			Foveated (FV) Restrictor		
	Total	Women	Men	Total	Women	Men
Discomfort Scores (Max 10)						
Average	0.62 (.7)	0.87 (.9)	0.38 (.5)	1.14 (1.5)	1.00 (.9)	1.27 (1.9)
Ending	1.23 (1.8)	1.27 (1.4)	1.18 (2.2)	1.64 (2.2)	1.36 (1.6)	1.91 (2.7)
Simulator Sickness Questionnaire						
Nausea	13.44 (16.0)	14.74 (19.7)	12.14 (12.1)	16.04 (20.9)	16.48 (22.6)	15.61 (20.1)
Oculomotor	14.82 (15.6)	19.98 (19.3)	9.65 (9.0)	21.36 (22.2)	21.36 (25.3)	21.36 (19.7)
Disorientation	18.35 (26.3)	22.78 (33.1)	13.92 (17.6)	28.47 (36.8)	34.17 (41.0)	22.78 (33.1)
Total	17.51 (19.5)	21.76 (25.3)	13.26 (10.9)	24.48 (27.6)	26.18 (31.0)	22.78 (25.1)
Gaze - dispersion						
Combined	.156 (.03)	.142 (.02)	.170 (.04)	.188 (.04)	.193 (.04)	.184 (.03)
Horizontal	.120 (.02)	.121 (.02)	.119 (.03)	.145 (.03)	.142 (0.03)	.148 (.03)
Vertical	.099 (.02)	.093 (.02)	.105 (.02)	.110 (.02)	.114 (0.02)	.107 (.02)

Table 3.1: Quantitative measures of the discomfort scores, simulator sickness questionnaire scores (Nausea, Oculomotor, Disorientation and Total) and gaze dispersion in terms of *mean (standard deviation).*

3.5   Results

Results regarding VR sickness and eye gaze behavior are shown in table 3.1 and we discuss each of these collected metrics in more detail in the following subsections.

3.5.1   VR Sickness

VR sickness was measured using the self-reported discomfort score, from which we calculated averaged discomfort scores (ADS) and ending discomfort scores (EDS), and using the simulator sickness questionnaire, from which we calculated the Nausea, Oculomotor, Disorientation and Total Scores.

Discomfort Scores

A Komogorov-Smirnov test found that our data were normally distributed. Using a 2-way mixed-model ANOVA, we did not find an interaction effect between sex and FOV condition in both the ADS ($F_{1,20} = .39, p = .54, \eta_p^2 = .002$) and the EDS ($F_{1,20} = .75, p = .41, \eta_p^2 = .007$). We found no significant difference between sexes with respect to both ADS ($F_{1,20} = .06, p = .82, \eta_p^2 = .002$) and EDS ($F_{1,20} = .08, p = .77, \eta_p^2 = .008$), and we did not find significant effect of FOV condition on ADS ($F_{1,20} = 1.71, p = .21, \eta_p^2 = .009$) and EDS ($F_{1,20} = 1.25, p = .28, \eta_p^2 = .01$).

Simulator Sickness Questionnaire Scores

Our data were normally distributed as tested using a Komogorov-Smirnov test. Using a 2-way mixed-model ANOVA, we did not find an interaction effect between

sex and FOV condition on all SSQ scores: Total Score ($F_{1,20} = .27, p = .61, \eta_p^2 = .003$), Nausea ($F_{1,20} = .05, p = .83, \eta_p^2 = .001$), Oculomotor ($F_{1,20} = 1.67, p = .21, \eta_p^2 = .020$), and Disorientation ($F_{1,20} = .03, p = .86, \eta_p^2 = .001$). We found that FOV conditions did not result in significant difference in all SSQ scores: Total Score ($F_{1,20} = 2.03, p = .17, \eta_p^2 = .020$), Nausea ($F_{1,20} = .41, p = .530, \eta_p^2 = .005$), Oculomotor ($F_{1,20} = 2.68, p = .12, \eta_p^2 = .030$), and Disorientation ($F_{1,20} = 2.07, p = .17, \eta_p^2 = .030$). We did not find significant differences between men and women in any of the SSQ scores either: Total Score ($F_{1,20} = .43, p = .52, \eta_p^2 = .020$), Nausea ($F_{1,20} = .06, p = .81, \eta_p^2 = .002$), Oculomotor ($F_{1,20} = .52, p = .48, \eta_p^2 = .020$), and Disorientation ($F_{1,20} = .73, p = .40, \eta_p^2 = .030$).

3.5.2 Gaze Dispersion

A Komogorov-Smirnov test found that our data followed a normal distribution. Using a 2-way mixed-model ANOVA, we did not find an interaction effect between sex and FOV condition on all gaze dispersion measures: horizontal ($F_{1,20} = 1.91, p = .18, \eta_p^2 = .010$), vertical ($F_{1,20} = .33, p = .57, \eta_p^2 = .004$), and combined ($F_{1,20} = .20, p = .66, \eta_p^2 = .001$). However, we found a significant main effect of FOV restriction on gaze dispersion, with foveated FOV restriction resulting in significantly higher gaze dispersion on all measures: horizontal ($F_{1,26} = 51.04, p < .05, \eta_p^2 = .020$), vertical ($F_{1,26} = 8.84, p < .05, \eta_p^2 = .090$), and combined ($F_{1,26} = 34.51, p < .05, \eta_p^2 = .190$). Figure 3.4 clearly illustrates this significant difference in eye gaze dispersion using a heatmap for one participant. We did not find a significant difference between sexes with respect to all gaze dispersion measures: horizontal ($F_{1,20} = .004, p = .84, \eta_p^2 = .002$), vertical, ($F_{1,20} = 1.95, p = .18, \eta_p^2 = .070$), and combined ($F_{1,20} = .49, p = .49, \eta_p^2 = .020$). Looking at differences in gaze dispersion
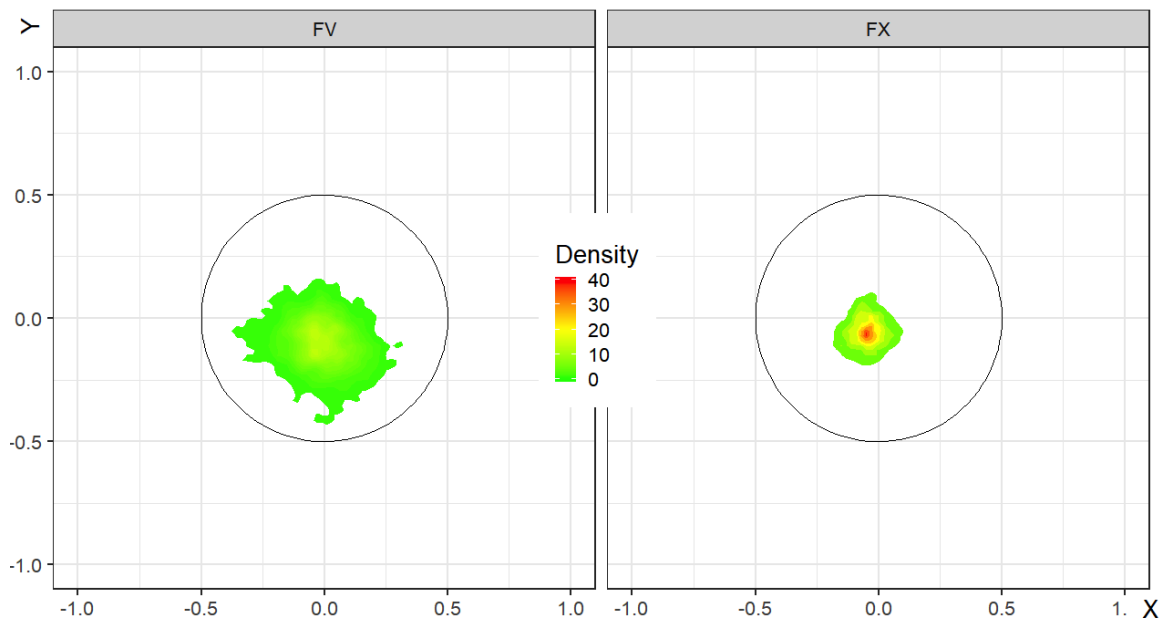
Figure 3.4: Example 2D density contour plot of eye gaze dispersion for one participant under both FOV conditions: FV (left) and FX (right). The plots illustrate the normalized full field of view of the viewport, and the black circle indicates the size of the restrictor at maximum restriction.

between FOV restrictors within each sex, our post hoc analysis using a Bonferroni correction found a statistically significant difference for women for combined ($p < .05$), horizontal ($p < .05$), and vertical ($p < .05$) gaze dispersion. For men, using the same test, we found a statistically significant difference for combined ($p < .05$) and horizontal ($p < .05$) measures, but not for vertical gaze dispersion ($p = .11$).

3.5.3   Participant Observation Questions

Table 3.2 shows the detailed results from the participant observation questionnaire. For FV, the distractor questions' averages ranged from 1.95 to 5.64, which shows that some guessing occurred. Ratings for question 3: ("I saw the VE get brighter or dimmer") (M = 3.59, SD=2.3) and 5: ("I felt like my field of view was changing

	Fixed (FX) Restrictor			Foveated (FV) Restrictor		
	Total	Women	Men	Total	Women	Men
Participant Observation Questionnaire						
VE smaller or larger	3.82 (2.5)	4.82 (2.3)	2.82 (2.4)	4.27 (2.4)	5.27 (2.1)	3.27 (2.4)
VE flicker	4.18 (2.1)	3.55 (2.3)	4.82 (1.7)	5.64 (2.0)	4.91 (2.3)	6.36 (1.3)
Brighter or dimmer	3.91 (2.3)	3.73 (2.3)	4.09 (2.4)	3.59 (2.3)	4.09 (2.4)	3.09 (2.2)
VE change color	3.18 (2.4)	3.64 (2.7)	2.73 (2.1)	2.64 (2.3)	2.91 (2.6)	2.36 (2.1)
FOV Change size	5.27 (2.3)	4.55 (2.3)	6.00 (2.2)	5.45 (2.2)	4.91 (2.7)	6.0 (1.6)
Me smaller/larger	1.55 (1.3)	1.18 (.4)	1.91 (1.8)	1.95 (1.5)	1.91 (2.0)	1.41 (1.6)
Size change in VE	1.55 (1.34)	1.18 (.4)	1.91 (1.8)	1.95 (1.5)	1.91 (1.6)	2.00 (1.41)

Table 3.2: Results from the participant observation questionnaire in terms of means and (stdev). Full content of the questions can be found in section 3.4.3.

in size") (M=5.45, SD=2.2) were all within range of the distractor questions. For FX, some guesswork was involved given that the distractor questions ranged from 1.55 to 4.18. Ratings for question 3: (M = 4.00, SD=2.35) was within range of the distractor questions, but question 5:(M=5.45, SD=2.2) was outside this range.

We used a Wilcoxon Signed-rank test to check if the results for the two relevant questions were significantly different across restrictor types. However, we did not find a statistically significant difference for question 3 ($Z = -0.968$, $p = .332$) or question 5 ($Z = -.578$, $p = .562$). Looking at each sex, for question 3, we did not find a statistically significant difference between restrictors for women ($Z = -.592$, $p > .05$) nor for men ($Z = -.919$, $p = .358$). Likewise, for question 5 we found no statistically significant difference between restrictors for women ($U = 49.5$, $Z = .689$, $p = .490$) nor for men ($U = 53.5$, $Z = -.427$, $p = .667$). Unlike our VR sickness analysis, we did not analyze for differences between sexes.
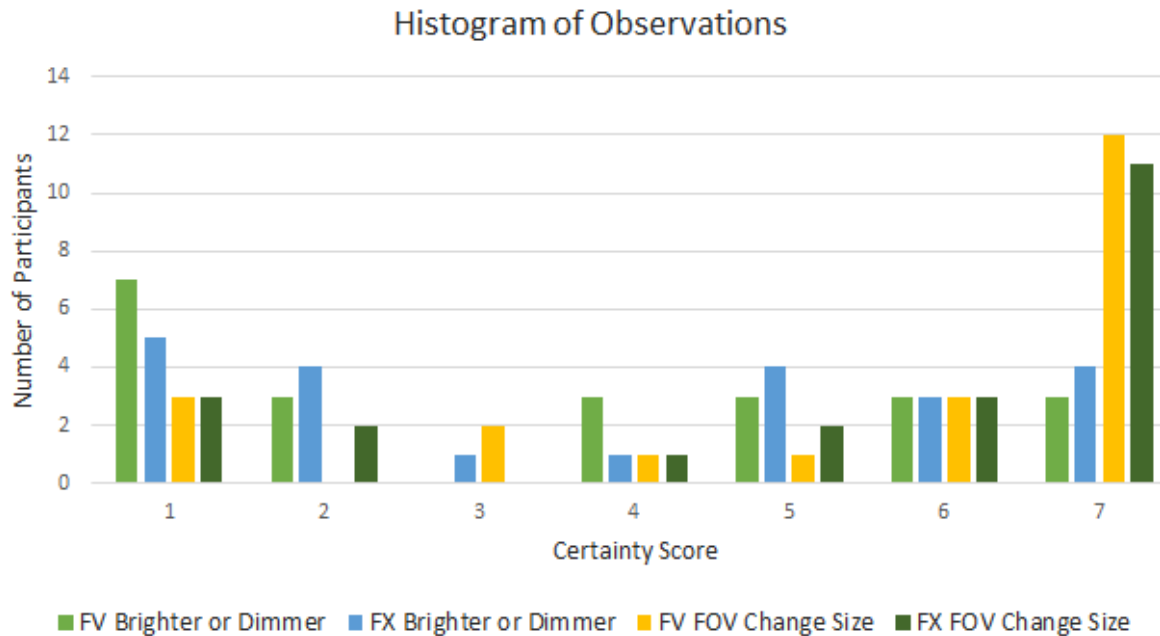
Figure 3.5: Histogram of responses to the participant observation questions relevant to FOV restrictors.

3.6 Discussion and Future Work

3.6.1 RQ$_1$: VR sickness

We did not find a statistically significant difference between the head-fixed and foveated restrictors for VR sickness as measured using discomfort scores and SSQ scores. In general the levels of observed VR sickness were very low with lower scores for the head-fixed restrictor (though this difference was not statistically significant). In addition to our sample size being on the low side, the amount of VR exposure in our experiment might not have been long enough to elicit a difference in VR sickness incidence between a foveated and a head-fixed FOV restrictor. This suggests that if restrictor type does influence VR sickness, the effect is likely to be very small. We did not detect a significant difference in VR sickness between sexes.

Though women are more likely to experience VR sickness [120, 67] the FOV restrictors used were likely successful in suppressing a higher VR sickness incidence in women. A prior study [10] also found FOV restriction to be equally effective in men as in women. Because our study did not use a baseline for comparison, i.e., using no FOV restrictor, no hard claims can be made about the effectiveness of a foveated FOV restrictor to reduce VR sickness, though several studies [159, 106, 27, 93, 61] have found FOV restrictors to be effective in reducing VR sickness.

3.6.2 RQ$_2$: Gaze Behavior

We did detect a statistically significant difference in gaze dispersion between the foveated and the head-fixed FOV restrictor, which indicates that participants covered a larger visual scan area (see Figure 3.4). This result supports **RQ$_2$** and points out an important benefit of using a foveated FOV over a head-fixed FOV restrictor; users have more opportunity to look around (without having to change the orientation of their head). This might allow for taking in more details of the VE they are exploring, which could improve spatial navigation performance. Looking at sex, we noticed that the effect of FOV restriction on gaze dispersion was specially evident in women, where we found significant differences in gaze dispersion in the horizontal, vertical and combined measures. For men we did not detect any significant difference in the vertical gaze dispersion. This is an interesting finding which we speculate that it could be explained by the fact that women rely more on the perception of landmarks for spatial navigation while men rely more on vestibular/geometrical cues. [157].

3.6.3 RQ₃:Noticeability

We did not find statistically significant differences between FOV restrictor types for question 3 (VR getting brighter/dimmer) or question 5 (FOV increase). Compared with Fernandes and Feiner's study [61], which also used this questionnaire to assess noticeability of FOV restriction, we observed much higher values for these responses. We chose 55° as the minimum size of our restrictors to match those found in popular VR experiences like Google Earth VR. Though this size is highly effective in reducing VR sickness it also makes the restrictor quite noticeable to participants. In hindsight, we could have explored using a larger minimum FOV for our restrictor. This would likely have elicited lower scores for the two questions, and higher VR sickness scores. Regarding **RQ₃** we conclude that both FOV restrictors are noticeable but that there was no statistically significant difference between them. It is always possible to use a higher minimum FOV to reduce noticeability at the cost of an increase in VR sickness.

3.6.4 Study Limitations

In our study we did not assess how FOV restriction affects spatial navigation performance or presence though a foveated FOV restrictor could affect both. A prior study [10] already found that FOV restriction does not impede path integration which is a component of spatial navigation. The tradeoff between FOV and presence has been well established [159, 106, 103]. We did not assess presence due to a lack of testing a baseline (e.g., no FOV restrictor). Fernandes and Feiner's study [61] also found that when using a minimum FOV restrictor of 90° this will be barely noticeable to users and a high presence can be maintained.

Another limitation pertains to the low number of subjects in this study which might have impacted our findings. The study compared the effect of two FOV restrictors on VR sickness using a mixed-model design with 22 participants. However, considering that the incidence and severity of VR sickness varies greatly among individuals [45], this small number of participants might not have been sufficient to allow results to reach statistical significance. A larger number of participants would thus have increased the power of our study. Therefore, the findings of this study have to be seen in light of these limitations.

3.6.5   Future Work

In future work we aim to investigate optokinetic nystagmus (OKN), a type of eye movement that can be observed during locomotion. During OKN events, with their head remaining stationary, users smoothly track objects in the VE (the slow phase) until their eye position becomes too eccentric, then the eyes quickly move back to the center of their field of view (the fast phase). One study has suggested that OKN responses [54] are a possible cause of visually-induced motion sickness, but this issue has not been further investigated. Using a head-fixed FOV restrictor, OKN might not be observed as objects disappear in the restrictor fairly quickly. A foveated FOV restrictor would allow participants to follow an object all the way until it goes outside the FOV and thus might lead to higher frequency of OKN.

Chapter 4

GazeMetrics: An Open-Source Tool for Measuring the Data Quality of HMD-based Eye Trackers

4.1 Introduction

Eye tracking has been used as a research tool for decades; however, reliable and easy-to-use HMD-based eye trackers have only recently become widely available. While these newer devices often come with software designed to make eye tracking simple, the settings for collecting, filtering, and analyzing data are not standardized across devices [81, 59]. This makes it difficult to meaningfully compare data collected on different devices, under different circumstances, and by users with differing levels of experience [55, 43, 59]. The most important measures of data quality that facilitate comparison across studies are spatial accuracy and precision.

Accuracy quantifies the average offset between the actual fixation location and the location of the intended target in units of visual angle (Eq. 4.1). It provides a measure of the quality of the calibration and gaze-mapping procedure. Precision quantifies the ability of the eye tracker to reliably reproduce a given result, regardless of intended gaze location; that is, it measures the end-to-end noise in the system (Eq. 4.2, 4.3). Precision therefore captures the aggregate of system-inherent, oculomotor, and environmental noise [81]. Controlling for as many factors as possible allows for better calculation of precision [177, 38].

Many researchers report the manufacturer-determined accuracy and precision when publishing eye tracking data [82, 9, 43, 24], but these metrics are typically calculated under ideal conditions [177]. If manufacturer metrics are used instead of actual measures, the data will be impaired and this can invalidate experimental results and conclusions [43, 81, 128].

To address these issues, we have developed a novel open-source tool, GazeMetrics, that allows for the easy extraction of data samples and calculation of accuracy and precision. GazeMetrics is designed to be comprehensive and universal, while enabling objective, replicable measurements of accuracy and precision [177]. The goal of the project is to enhance user experience, ease of measurement, and current software functionality.

4.2   Related Work

Several open-source tools have been developed for remote eye trackers to make accuracy and precision measurements more reliable. These tools are used for validation of data quality [9], assessment of data quality under non-ideal conditions [38] or with more difficult populations [43], and extend the usability of eye tracking to other software, such as MATLAB [70]. Tools have also been developed for wearable eye trackers to measure accuracy and precision [112, 138] and to assess the effects of non-ideal stimulus presentation on these metrics [100]. These studies emphasize the need to standardize accuracy and precision measurements.

While these tools focus on comprehensive measures of accuracy and precision, they use eye trackers that are not integrated with VR. VR presents its own challenges with calculating correct metrics across depth. Pfeiffer and Latoschik [138]

focus on applications of accuracy and precision in VR, such as depth fixation detection, but mention that their experimental set up is limited by the projection technology and the monitor-based display.

4.3   Motivation

Data quality is vital to the comparability and standardization of experimental results when using eye tracking [128, 9, 82, 55, 24]. Accuracy and precision measured on-site are almost always worse than what is expected based on manufacturer specifications [59, 9, 38]. Furthermore, accuracy and precision will affect how data is collected and how well the results turn out.

During collection, these metrics contribute to factors such as data loss and detection of fixations, saccades, and other eye movement events [81]. While applying filters to the data can help enhance precision, poor accuracy is more difficult to fix [59, 38]. After data have been collected and filtered, any inaccuracy and imprecision will become apparent when assessing the results. While some higher-order measures are robust to inaccuracy and imprecision, most are adversely affected.

Additionally, accuracy and precision can be difficult to assess [24, 9, 126]. Pre-programmed calibration procedures often do not show the outcome of the calibration to the user. For longer sessions, measurements begin to drift over time, causing a decay of data quality, sometimes up to 30% over the span of 4 minutes [55], which may not be noticeable until after the data collection.

Together, these factors highlight the necessity for a tool that is easy to implement and whose results are clear and reproducible. Standardization across devices

allows researchers to compare results meaningfully and assess the actual effectiveness of their own data.

4.4   System Description

4.4.1   General Overview
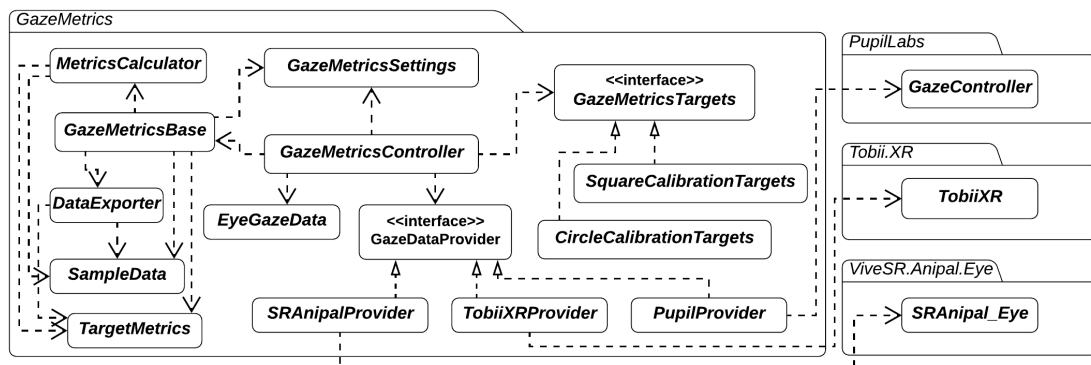
Figure 4.1: High-level UML class diagram of GazeMetrics.

GazeMetrics is a stand-alone package that allows for online quantification of data quality. The most powerful feature is that nearly every functionality can be customized without modification to the source code, making it easy to use for users who are not necessarily experts in coding. All changes can be saved as default settings and multiple settings can be saved for implementation with various eye tracking studies.

4.4.2   Technical Specifications

GazeMetrics is a software package built in Unity. It provides built-in support for three popular eye trackers' Unity software development kits (SDKs), which in turn support multiple HMD-based eye tracking platforms. Moreover, to allow users to add their own implementations to the source code to support other devices or applications, the system was built using an extensible software design pattern, the provider model design pattern [83]. Figure 4.1 shows a high-level class diagram of GazeMetrics. The components of the system will be discussed in detail in this section.

GazeMetrics comes with built-in support for the Tobii XR SDK from Tobii Pro, which can be used in conjunction with the HTC VIVE Pro Eye integrated eye tracker, the Pico Neo 2 Eye integrated eye tracker, and the Tobii Pro VR Integration eye tracker. In addition, the tool supports the Pupil Labs SDK, which works with the Pupil Labs add-on eye trackers that can be installed into the HTC VIVE, VIVE Pro, and VIVE Cosmos headsets. Finally, GazeMetrics supports the VIVE SRAnipal SDK, the native SDK for VIVE Pro Eye. Combined, they comprise most VR HMD-based eye trackers available on the market today.

GazeMetrics was tested for functionality on Unity version 2019.1.6, using the eye tracking SDKs: Tobii XR SDK v1.7.0.160, Pupil labs HMD eyes SDK v1.1 and Vive SRanipal SDK v1.1.0.1. Development and testing of the system was done in Windows 10.

4.4.3 Accuracy and Precision Calculation

GazeMetrics calculates accuracy and precision based on the eye gaze data provided by the selected eye tracker's SDK in Unity. Most HMD-based eye trackers report eye gaze data in the form of a gaze ray or origin and direction vectors from which a gaze ray can be constructed. The gaze ray is anchored at the position of the eye or the head and is directed in the eye gaze direction of the participant. This approach of representing eye gaze as a ray vector is widely used in the literature [50, 19]. Calculating an accurate 3D coordinate of a gaze point in the virtual environment (VE), however, is a challenging problem and is also extensively covered in previous literature [138].

GazeMetrics uses the gaze ray reported by the eye tracking SDK to calculate inaccuracy, or offset, of each sample. This is calculated as the angular difference between the reported gaze ray and an imaginary gaze ray projected from its origin onto the target stimulus (θ_i). The average of all offset angles is taken to calculate the overall accuracy of the eye tracker:

$$Accuracy = \frac{1}{n} \sum_{i=1}^{n} \theta_i \tag{4.1}$$

$$\theta_{RMS} = \sqrt{\frac{1}{n} \sum_{i=1}^{n} \left(\theta_i^2\right)} = \sqrt{\frac{\theta_1^2 + \theta_2^2 + ... + \theta_n^2}{n}} \tag{4.2}$$

$$SD_{precision} = \sqrt{\frac{1}{n} \sum_{i=1}^{n} (x_i - \bar{x})^2} \tag{4.3}$$

Spatial precision metrics quantify variability in gaze measurements. There are two popular ways to measure precision: one involves calculating the root mean square (RMS) of the inter-sample angular distances (Eq. 4.2) and the other involves measuring the standard deviation of the samples (Eq. 4.3) [82]. For HMD-based eye trackers, inter-sample angles can be calculated by measuring the angle between successive gaze ray samples reported by the eye tracking SDK. To calculate precision using standard deviation, data is needed about the x, y, and z coordinates of the gaze point in the VE. However, calculating the gaze point in the VE is a challenging problem, so not all eye tracking SDKs report gaze point coordinates in the VE. Therefore, the tool is designed to report only the RMS precision when gaze-point data is not available. When gaze-point data is available, precision via standard deviation is also calculated and reported separately in each direction. The methods that calculate accuracy and precision are defined in the `MetricsCalculator` class.

4.4.4 Stimulus Target Presentation

After selecting the SDK, the user has the option to alter the calibration targets from the user interface and to change several of the elements, including the presentation geometry (Fig. 4.2); target size, number, and color; and target display length, depth (distance from eyes), and eccentricity. There is also the option to change the background color that the targets will be presented on.

Accuracy tends to be better if the conditions used in the initial calibration procedure are similar to the conditions used in the data quality test [177]. However, different eye trackers use different calibration settings; for instance, Tobii eye track-
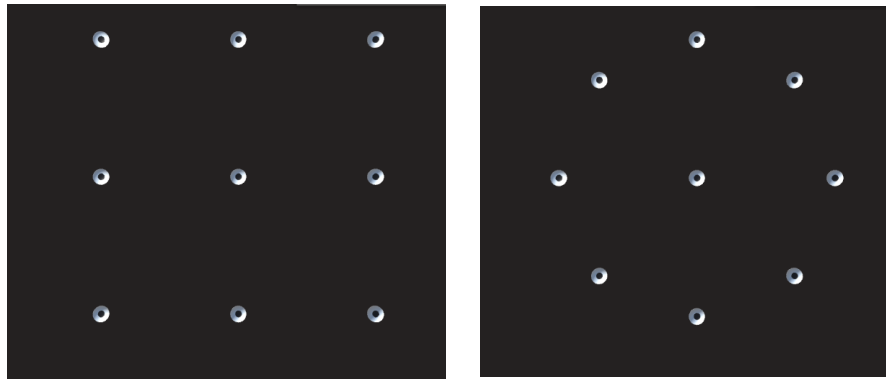
Figure 4.2: Calibration targets can be arranged in a rectangular format (a) or in a circular format (b).

ers use a square calibration point arrangement (Fig. 4.2a) while Pupil Labs eye trackers use a circular arrangement (Fig. 4.2b). GazeMetrics allows the user to choose their desired arrangement by selecting one of the preset settings. Experienced users can also develop their own arrangement by implementing their own classes based on the `GazeMetricsTargets` abstract class.

Desired eccentricity of targets can also be manipulated for different experiments, such as testing foveal versus peripheral acuity. Users can set a different eccentricity, depth, and position of the central target for each arrangement of targets during a single run using settings on the user interface.

The settings can be previewed on the user's screen with a single button press to ensure desired placement before the participant interacts with the experiment. The `GazeMetricsSettings` class is used to create `ScriptableObjects`, which are used to create a data container that is used to store data that persists between sessions. Therefore GazeMetrics settings can be saved for use with other sessions and reported in the methods to allow other users to replicate the procedure.

4.4.5   Data Collection and Reporting

GazeMetrics communicates with the selected eye trackers' Unity SDK to collect real-time data from the eye tracker. The sampling rate at which data is collected can be set by the experimenter using the settings window. It is recommended that the sampling rate be equal to the eye tracker's sampling frequency. GazeMetrics collects binocular data from the selected SDK, which is sufficient for most interactive and analytical uses. If users prefer to use monocular data for the precision and accuracy calculations, they can modify the `GazeDataProvider` implementation of their selected SDK, or write their own implementation of the `GazeDataProvider` interface.

In addition, there is an option to change how the data is collected and thus, how the metrics are calculated. For example, it is possible to include or exclude samples collected within certain time frames during target presentation, such as excluding the first 800ms and last 200ms to ensure fixation without including overshoots or glissades [129, 82]. The targets can be displayed for a selected amount of time, so the amount of data collected from each target can be modified to suit the user's needs.

The tool reports results in two ways: 1) by displaying live results through a panel on the user's view of the VE, and 2) by storing raw data and experiment results on external files. The live data quality results panel (Fig. 4.3) allows the experimenter to check the data quality of the eye tracker under the current experimental conditions without interrupting the experiment.

For more detailed post-hoc analysis, GazeMetrics stores all collected and processed data in the form of CSV files in a storage location that the user chooses on
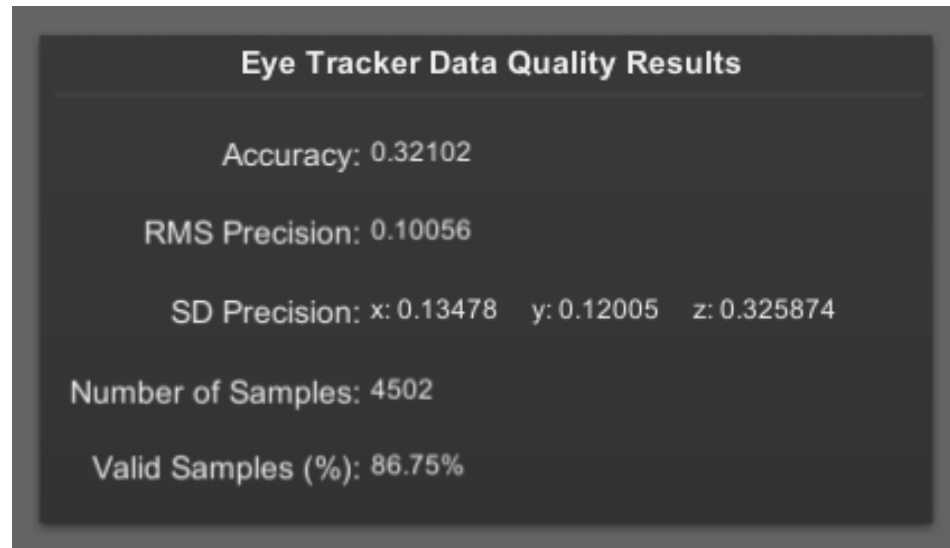
Figure 4.3: Data quality measurement results panel used to display live results.

the settings panel. While the data displayed on the results panel contain only aggregate data, calculated using the formulae in section 4.4.3, the data exported to the files contain: raw gaze samples, the target's position on the VE, the participant's head position, the validity of the collected samples, and the time stamp at which each sample was collected. To allow users to have complete control of the data, the exported data includes all samples that were excluded from the online calculation; that is, it includes time frames that were originally excluded by user preference. Finally, the accuracy and precision for each target position are stored in a separate CSV file. The methods used to export GazeMetrics data are implemented in the `DataExporter` class.

To evaluate the functionality of GazeMetrics, we collected sample data from two users using the HTC Vive Pro Eye headset, and SRAnipal SDK. We used 9 targets with a circular target arrangement, with a radius of 0.3m. The targets were placed at a depth of 1m. We displayed each target for 2 seconds and excluded the first 500 ms from the calculation. After running the accuracy and precision tests

with GazeMetrics, we obtained an average accuracy score of 1.23°, RMS precision score of 0.62°, and SD precision values of 3.95mm, 0.46mm, and 3.34mm respectively on the X, Y and Z directions. The manufacturer of the Vive Pro Eye reports spatial accuracy of $0.5° - 1.1°$ for the eye tracker. The manufacturer does not report spatial precision of the eye tracker. Our accuracy result is worse than the manufacturer reported accuracy. This underscores the importance of testing the data quality of eye trackers under the actual experiment conditions rather than relying on the manufacturer reported metrics. However, we would like to clarify that this test was performed to evaluate the functionality of the tool, and should not be taken as an empirical evaluation of the data quality of the tested eye tracker.

4.5   How to use the Tool

GazeMetrics is prepared as an easy-to-use Unity software package that can be added to a new or existing Unity software project. While it can be used as a stand-alone procedure to assess data quality, it can also be used inside an existing eye tracking experiment to verify data quality. GazeMetrics can be initiated by pressing a single key at any point during an eye tracking experiment. The tool can be run right after the initial calibration procedure or during the experiment to check if the data quality is high enough to continue.

GazeMetrics contains all the required source code and related assets. The user can download the latest version of the tool from its Github page [1]. Once the package has been imported to the assets folder, the developer needs to add the 'Gaze-

---

[1] https://github.com/isayasMatter/GazeMetrics

Figure 4.4: Easy-to-use settings allow the experimenter to customize various aspects of the tool. This figure shows one of the settings windows for the tool.

MetricsController' prefab to the project by dragging-and-dropping it in the hierarchy window.

GazeMetrics comes with preset settings suitable for most experiments. However, the user can also change the settings by clicking on the "Gaze Metrics Settings" or the "Target settings" of the GazeMetricsController object. These settings are self-explanatory and contain pop-up tool-tips for ease of use. Users start by selecting which SDK (eye tracker) to use under the "Eye tracker type" setting and then changing elements of target presentation, data collection, and sampling rate.

After establishing the preferred settings, the procedure can be started by pressing the 'S' key anytime during the experiment. If the user wants to preview the actual positions of the target stimuli inside the VE, they can press the 'P' key to preview the target markers without initiating the procedure. Users have the ability to change the activation keys. Once the procedure is started the results panel will display live results. This panel is visible to the user, but is hidden from the participant in the VE. The tool displays useful status and log messages throughout the procedure to notify the experimenter and the participant about the status of

the experimental procedure.

4.6   Discussion and Future Work

Accuracy and precision are two vital components of data quality that have implications for data collection, data analysis, and validity of results [81, 82]. As such, it is best practice to report correct metrics rather than relying on manufacturer data sheets and have these measures outlined within the methods of a study to ensure reproducible results. GazeMetrics is a free, open-source software made to address these issues. It has a user interface that is customizable without having to alter the source code, making it accessible for users with all levels of coding experience.

As eye tracking in VR develops, addressing the issue of standard accuracy and precision reporting becomes increasingly important. We plan to continue supporting GazeMetrics, and to extend the functionality of GazeMetrics to include other HMD VR devices, such as FOVE, and other platforms for presenting stimuli to enhance data quality and encompass more of the research community.

Chapter 5

VR Sickness Adaptation with Ramped Optic Flow Transfers from Abstract To Realistic Environments

5.1 Introduction

Virtual reality (VR) is currently seen as the next digital frontier. In recent years, various commercial VR head-mounted displays (HMD) have become available at a low cost and VR is currently already widely used for training, rehabilitation, education, work and entertainment. Unfortunately, VR sickness is still considered a major barrier to mass consumer adoption [121]. VR sickness is a type of motion sickness unique to VR and can include symptoms such as nausea, pallor, sweating, stomach awareness, increased heart rate, drowsiness, disorientation, and general discomfort [90]. Not all individuals who are exposed to VR will experience VR sickness, however, those who do may find it debilitating [149, 166].

Several VR sickness mitigation strategies have already been developed, including the use of dynamic or foveated field-of-view (FOV) restriction [61, 8, 195] and vection blurring [31]. In practice though, the bulk of locomotor VR experiences that are currently available rely primarily on the use of teleportation [13] which has been shown in a recent meta review Prithul et al. [143] to result in significantly lower VR sickness incidence but at the cost of lower presence and potential spatial disorientation. The reason for the success of teleportation may be in part due to the lack of optic flow generated during use [143]. Optic flow can contribute

to both vection [131, 160] and sensory conflict [30, 131], which cause sickness in certain contexts [30].

A current challenge with VR sickness is that available mitigation strategies aren't 100% effective since the effectiveness of any particular mitigation strategy varies across individuals [147]. This makes it difficult to create a one-size-fits-all strategy for mitigation. A better strategy may be to supplement existing mitigation techniques by investigating how the user might best prepare themselves for continued VR use.

Research which focuses on using adaptation to the virtual environment has shown promising results for VR sickness mitigation [146, 39, 80, 18, 48, 21]. The general assumption is that this repeated exposure facilitates adaptation to sensory conflict in the virtual environment, reducing sickness. However, much of this success is dependent on the researchers exposing users to the *same* virtual environment. Development of a training paradigm which facilitates the transfer of adaptation effects between multiple environments has proven even more difficult to achieve [119, 163, 52]. These issues may be in part a result of the dissimilarities between the environments [146, 147]; Adaptation to sensory conflict is thought to be largely dependent on the user becoming accustomed to the conflict which arises in a particular environment through developing the appropriate expectations for sensory input in that environment [146, 147, 92]. Therefore, facilitating more general adaptation may require training through exposure to factors that are consistent between all VR environments, for example, optic flow stimuli.

Therefore, we aimed to develop a training technique that facilitates the transfer of adaptation effects across environments. Our study borrows concepts from motion sickness mitigation work by emphasizing gradual exposure to sickness-

inducing stimuli [172, 155] such as expanding optic flow [54, 30] and graphic realism [73, 46] to facilitate adaptation. To this end, we use a simplified training environment consisting only of the walls and floor of a labyrinth that users navigate. Over successive days, we gradually adapt users to increasing optic flow by incrementally increasing luminance contrast of the visual stimulus. We show that adaptation that is achieved using this simplified environment with gradual increases in optic flow strength successfully transfers to a richer, more naturalistic environment. Results of this study suggest that it should be possible to develop standardized training paradigms to reduce and possibly even eliminate VR sickness in susceptible individuals.

5.2 Related work

There are three main theories aimed at explaining VR sickness: postural instability theory, eye movement theory, and sensory conflict theory [151, 54, 146]. Postural instability [151] theory attributes VR sickness to a disruption of postural stability caused by unnatural or unexpected motion in the virtual environment. Eye movement theory [54] postulates that optic flow drives rapid reflexive eye movement to stabilize the image (optokinetic nystagmus) and that the associated sensory and motor signals innervate the vagal nerve, leading to VR sickness. Sensory conflict theory [146] seems to be the most widely accepted [91, 99] and attributes VR sickness to the conflicting signals between the visual, vestibular, and somatosensory senses causing discomfort and nausea among other symptoms. These theories are not mutually exclusive, and this list does not encompass all efforts to explain VR sickness [94].

One element these theories have in common is that they all seek to explain how sickness may be caused by exposure to full-field visual motion, or optic flow. Optic flow is thought to cause VR sickness [46, 176] particularly when the visually-simulated self-motion does not match natural self-motion of the user, i.e. when there is sensory conflict [30]. Many mitigation strategies, including FOV restriction, aim to reduce optic flow during movement [61, 8]. Other strategies instead try to reduce conflict by providing some form of vestibular or efferent feedback [137], for example, by walking-in-place [178]. It is important to note that optic flow is not the same as vection; optic flow refers to the visual motion stimulus itself while vection refers to the visually-induced perception of self-motion [66]. Optic flow can cause vection [132, 161], so their separate effects can be easily confounded during discussions of VR sickness [34]. Like optic flow, vection has been linked to feelings of VR sickness [94, 133], however the relationship is still not perfectly understood [94, 133] nor should it be oversimplified. As vection may be experienced without inducing VR sickness, vection alone is not sufficient to induce sickness[95]. Instead, it must be paired with other factors such as sensory conflict, postural instability, etc. This makes it difficult to disentangle the distinct effects of the optic flow versus vection when investigating sickness.

Other work related to the current study has investigated adaptation to VR sickness. Prior studies have argued that repeated exposure to an aversive stimulus allows developing an altered expectation of sensory input [146, 92], with the required length of exposure increasing as the stimuli become more complex [147]. It has been suggested that this makes it unlikely for adaptation effects in one virtual environment to transfer to another. The degree of transfer may depend on *the degree of dissimilarity* between two environments [146, 147]. Previous research in similar environments has been rather consistent in demonstrating effec-

tive adaptation, with reports of symptoms decreasing over the course of exposure [80, 84, 18, 48, 21], even on timescales as low as 45 minutes [162]. In one study by Lampton et al. [102], the researchers saw VR sickness decrease following repeated exposure to a training environment, however, these effects disappeared when the participants entered the mission environment [102]. Another study by Hill and Peter [80] had participants view a game being played through an HMD on five consecutive days. Results also demonstrated significantly less nausea on the fifth day, compared to the first. More recently, a study by Beadle et al. [21] had participants perform a shooting task in an HMD over 3 sessions. SSQ scores significantly decreased following each session. This is not an exhaustive list of VR adaptation studies (for review, we recommend Duzmanska et al. [52]), but they do demonstrate a common theme; adaptation to a single VR environment is possible for mitigating VR sickness. In this experiment, we hope to expand upon this research by examining whether adaptation can transfer between VR environments.

Other relevant prior work has examined how various methods of training against sickness may offer a potential solution to VR sickness more generally, rather than to a single environment [119, 163]. One such study by Smither et al. [163] showed that when participants were pre-exposed to simulated rotary stimulation they experienced less symptoms of VR sickness than individuals who had no prior exposure [163]. Similarly, an experiment by Mouloua et al. [119] demonstrated cross-platform training was possible, but that it was only successful when using optokinetic nystagmus (OKN) training, and not a VR HMD [119]. Another study by PÃ¶hlmann and colleagues (2021) found that individuals that spend extensive amounts of time playing action video games (not on HMDs) experienced less VR sickness when exposed to a simple virtual environment compared to individuals that do not play any video games [141]. All of these experiments were exam-

ining transfer in a way that used a non-VR device as their training mechanism. It is possible that these experiments were training against motion sickness more broadly, rather than adaptation to VR specifically. While this may be another effective methodology for sickness mitigation, it stands to reason that this would not be readily available for the average user. Here, we seek to facilitate adaptation solely through the use of a VR HMD.

Specifically, we explicitly aim to facilitate adaptation between distinct VR environments. This means that experiencing one environment will lead to a reduction in VR sickness in a dissimilar environment. Additionally, we hypothesize that this adaptation can occur without exposing participants to the full optic flow and luminance contrast normally experienced in the VR environment. In other words, training can be tailored to act as a "ramp up" period for the participants. Studies which center on training against motion sickness have suggested that adaptation should be facilitated through a gradual increase of the provocative stimulus [172, 155]. Similarly, if we want to train participants against VR sickness, best practice may be to increase intensity over time such that adaptation has time to take place while avoiding extreme illness.

5.3   Materials and Methods

Our study aims to answer two research questions:

- **RQ 1**. Does ramped exposure to increased optic flow strength in an abstract environment allow gradual adaptation?

- **RQ 2**. Does the adaptation transfer from abstract to more complex environ-

ments?

5.3.1 Equipment

We used an HTC Vive Pro Eye HMD to present stimuli, and track position and orientation. It has a diagonal FOV of 110 degrees, a refresh rate of 90Hz, and a combined resolution of 2880x1600 pixels. It allows the user to adjust the interpupillary distance (IPD) and focal distance of the HMD to their comfort. The HMD was powered by an AMD Ryzen 7 1700x Eight-Core processor with NVIDIA GeForce GTX 1080ti graphics card and 16GB of memory.

An Empatica E4 wristband was used to read Electrodermal Activity (EDA) from participants. We use the Empatica's lead wire extension to collect data using Ag/AgCl electrodes attached to the palmar surface. Participants navigated the environment and provided discomfort score input using an XBox 360 controller. This controller is preferred over the Vive touchpad given its familiarity to new users. The tracking space was set to 2.2 by 2.4 meters.

Our system included stimulus presentation and data acquisition components. Stimulus presentation was accomplished through a custom application developed in Unity3D engine version 2019.4.28, using SteamVR version 1.7 plugin. For data acquisition, we used lab streaming layer (LSL) along with LSL LabRecorder version v1.14.2. LSL allows unified and time-synchronized collection of various data streams in an experiment. The Empatica E4 streaming server was used along with a custom built application that used PyLSL version 1.15.0 to stream the EDA data from the wristband to LSL LabRecorder. EDA data was collected at a sampling rate of 4 Hz.

5.3.2 Virtual Environment

To address our two research questions, we developed two separate virtual environments: an adaptation training environment and a test environment. The training environment was an abstract environment developed to help us answer RQ1, and the test environment was a natural and complex virtual environment developed to help us answer RQ2.

The training environment was a custom-built labyrinth. The labyrinth consists of a series of repeating hallways with alternating black and white stripes on the walls, and arrows on the floor to help guide participants to the waypoints. This environment was built to have fewer features than the city environment. Unlike the test environment, the training environment did not change in elevation, all paths were straight, sharp, turns, and not winding, and the appearance stayed relatively constant throughout. Our hope with this environment was to reduce feature richness, as previous research has suggested that virtual environments with greater graphic realism [73, 46] and scene complexity [167, 97] can lead to higher levels of sickness than simple or abstract scenes. Thus, we created an abstract environment that allowed us to maintain and control optic flow strength through manipulation of luminance contrast. Luminance contrast is the ratio between the maximum and minimum luminance values in the environment, and it is calculated using the following formula [158, 135, 77]:

$$C = \frac{(I_{max} - I_{min})}{(I_{max} + I_{min})} \tag{5.1}$$

with I_{max} and I_{min} representing the highest and lowest luminance. In our train-

ing environment, luminance contrast was set to a value of 0.50 during the first day, 0.75 the second, and 1.0 (full contrast) on the final day. Increasing luminance contrast leads to increased optic flow strength and vection [77], and thus serves as a method to gradually increase stimulus intensity over successive training days.

The test environment was adapted from the Windridge City [180] environment. This environment was chosen due to its rich features; it consists of a city surrounded by lush forests, flower fields, and winding dirt roads. This test environment replicates what users may experience in normal VR use, particularly for entertainment. The environment has compelling imagery, changes in elevation, and provides plenty of interesting features for participants to examine as they navigate it. For these reasons, the test environment also works as a direct comparison for real-world applications. Both environments contained a set of waypoints as their main means of navigating the environments for 20 minutes.

In summary, the training and testing environments were very dissimilar. This ensures that any reduction in sickness on the final test day is not simply due to repeated exposure to the same environment. Instead, we examine whether adaptation acquired in the training environment is maintained and transfers to the test environment on the final day. Figure 5.1 shows the baseline and final testing environment used on days 1 and 5 on the left and right, and the training environment with increasing contrast luminance levels used on days 2 through 4 in the center.

5.3.3 Measurements

Measuring VR sickness has proven challenging and best practices are still being debated. Most commonly, researchers have relied on the Simulator Sickness Ques-
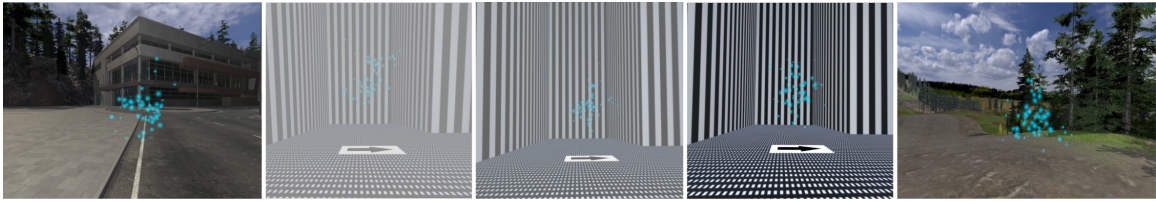
Figure 5.1: Participants were exposed to 2 virtual environments over the course of 5 days. On days 1 and 5, participants navigated a naturalistic environment, which served as the baseline and test for adaptation. On days 2 through 4, participants navigated an optokinetic labyrinth with an increase in the luminance contrast on each day. Participants used blue particle cloud waypoints and arrow textures to help guide their navigation.

tionnaire [90] but updated versions such as the VR Sickness Questionnaire [96] have recently gained some traction. The SSQ measures multiple symptoms using a long questionnaire and is usually collected post exposure. More recently, researchers have developed more simple alternative questionnaires that can be collected during the experiment. The Discomfort Score [61, 8] is a widely used method which asks subjects to rate how sick they are feeling at that moment on a scale of 0 to 10 during the VR experience, with 0 indicating how they felt when the experience started, and 10 indicating that they need to stop usage immediately. This metric has an obvious advantage over the previously mentioned questionnaires; the Discomfort Score allows us to see sickness as it evolves in users over time.

Subjective measurements of VR sickness such as the SSQ and Discomfort scores have some limitations because they rely on the user's subjective judgment which could vary between individuals. In an effort to establish more objective measures of tracking VR sickness, researchers have looked to collect physiological data such as postural sway [78], electrodermal activity (EDA) [113], body temperature [69], and heart rate [195]. Eye blink data has also been suggested as a potential source of valuable sickness information [35]. In this study, to measure the incidence of VR sickness and discomfort we use both subjective and objective methods.

Subjective Sickness Scores

Discomfort scores   The discomfort scores were collected through the VE by prompting the user to select a score every minute. The discomfort score allows a sampling of VR sickness scores during the trial. Discomfort scores were averaged for each participant per session to obtain an average discomfort score (ADS), and an ending discomfort score (EDS) was calculated by using the last discomfort score for each participant per session, similar to Fernandes et al. [61]. This value is 10 if the participant terminated early due to severe discomfort.

SSQ scores   Baseline SSQ data was collected before each session and post-immersion SSQ data was collected after each session. Data collected from the SSQ questionnaires are used to calculate four associated scores, namely: Total Severity, Oculomotor, Nausea, and Disorientation scores. These scores were calculated as per the conversion formulas by Kennedy et al. [90]. We then subtract the baseline SSQ subscores from the post-immersion SSQ subscores to get our relative SSQ subscores.

Objective Sickness Scores

A recent review of the causes and measurements of VR sickness by Chang et al. [34] found that electrodermal activity (EDA) is one of the widely used objective measures of VR sickness. As a result, in this study we chose to use EDA as an objective measurement of VR sickness. EDA was recorded from the medial-phalanges of the index and middle finger of the non-dominant hand's palmar sites. That is, we placed the sensors on the upper-middle portion of the index and middle finger (see Figure 5.2). Baseline EDA data was recorded for 2 minutes before immersion

in VR, and for the full period of each experiment session. There are two main components in EDA signals: the general tonic-level component measured as Skin Conductance Level (SCL) which is thought to reflect general changes in autonomic arousal, and the phasic-level component measures as Skin Conductance Response (SCR) which refers to the fast changing elements of the signal.

Figure 5.2: Placement of the Empatica E4 wristband and the EDA electrodes.

To decompose the EDA signal into the phasic and tonic components we applied a high pass filter with a cut-off frequency of 0.05 Hz, and we compute the SCL of the tonic component and Amplitude Root Mean Square (RMS) from the phasic component as these metrics have been shown to be promising VR sickness indicators in previous studies [68, 47]. Similar to previous studies [68, 47] we divide the recorded data into blocks of 1 minute each, and for the purpose of statistical analysis the tonic SCL and the RMS amplitude are averaged for these blocks. To remove individual variability, our tonic SCL scores are standardized by dividing all exposure values by the baseline score [47, 29], and our EDA signal was standardized using Z-score standardization prior to extracting the phasic component [29].

Optic Flow

To understand the amount of optic flow experienced by participants during each day of the experiment, we measured the magnitude of optic flow during each session. To measure optic flow we recorded video streams of participants navigating the virtual environment during each condition. Similar to previous studies, the video streams were recorded from the left stereoscopic camera [85]. The streams were recorded at a rate of 30 frames per second and at the full resolution of 2220x1450. The video frames were preprocessed by re-scaling them to 392 x 256 resolution, as calculating dense optic flow with the full resolution would be computationally expensive. We use the dense optic flow calculation algorithm developed by Farneback [56] to calculate the magnitude and direction of optic flow in each frame. Optic flow for each frame is expressed as a 2D vector field where each vector represents displacement of image points between successive frames. We then average the magnitude of optical flow, measured as pixels per frame, over all pixels of each frame to get the average magnitude of optic flow per frame. The data for all frames of each session video is then averaged to get the average magnitude of optic flow exposure for that session. For convenience, we refer to this average magnitude below as optic flow strength.

5.3.4 Procedure

When participants arrived for the first day of testing, they were provided information explaining the procedures of the experiment, the risks involved, and the types and handling procedures of the data collected in the experiment. Following this, participants were asked to fill out a pre-study demographic questionnaire. The

participants were shown a 2 minute video explaining the virtual environments and the experiment task, and were given an overview of the controller used in the study and how to use it.

Participants started by filling in a baseline SSQ. They were then assisted with putting the physiological sensor wristband on their non-dominant hand. Following this, two minutes of resting baseline EDA data outside the VR environment was collected from the participants. Participants were asked to sit and avoid movement of the hand wearing the wristband during baseline data collection. Following this, participants were assisted with putting on the VR headset. We made sure the HMD and wristband were well-fitted, but comfortable.

Participants were asked to navigate the Windridge City environment by following a set of waypoints to the end of the environment. On days 2 through 4, participants navigated an optokinetic labyrinth at increasing luminance contrast values: 0.5 on day 2, 0.75 on day 3, full contrast on day 4. On the final day of testing, participants navigated the Windridge city environment as they had on the first day. During the experiment, participants were also asked to provide a discomfort score (see section 5.3.3) [61] at one minute intervals. Participants completed the navigation tasks while standing. They controlled their forward and lateral movements with the XBox 360 controller and steered with their head. To prevent transfer of symptoms between sessions, a minimum of 12 hours (maximum 48 hours) and a full night's rest were required between sessions. Each experiment session took around 30 minutes, with 20 minutes of VR exposure.

After each session, participants were asked to fill out a Simulator Sickness Questionnaire (SSQ, [90]) in order to assess their level of post-exposure sickness. The room was kept at 20 degrees Celsius to prevent interference with SSQ data

(i.e. sweating due to temperature, rather than sickness) and ensure participants all experience the same air temperature [16].

5.3.5 Participants

Potential participants were recruited by online flyers from the local campus community. Participants who expressed interest in the study were given a questionnaire to determine their eligibility. The questionnaire (Supplementary Materials, Figure 1) was adapted from Golding [72] and Kinsella [98]. As we are interested in users who experience VR sickness symptoms, participants were excluded from participating if they satisfied any of the following conditions: are frequent users of VR, never experience VR sickness or motion sickness, suffer from inner ear problems or vertigo. Initially, 49 people showed interest in the study, out of whom 12 were excluded because they had frequent experience with VR, 2 were excluded because they have inner ear problems or vertigo, 13 chose not to participate in the study after getting contacted for participation. 22 participants were recruited for the experiment (11 male, 11 female, mean age: 23.45, SD: 3.9).

Out of the 22 participants who participated in the study, two participants, both female, were unable to complete the study reporting that they were too sick to continue after day 2. One additional female participant experienced data loss during a session due to equipment failure. The analyses included were conducted on the remaining 19 participants (11 male, 8 female. mean age: 22.8, SD: 3.6). The number of participants was chosen based on similar previous studies [8, 14, 62].

5.4 Results

To align our results with our research questions, we report the results in two parts: the first subsection reports results for the test sessions (days 1 and 5) and the second subsection reports the results for the training sessions (days 2, 3, and 4). The results for the test sessions aim to address RQ2 - whether the adaptation training was transferred from the abstract training environment to the complex testing environment.

For all statistical tests, we use Shapiro-Wilk tests to test the normality of our data, and we used the box plot method to identify outliers outside the Q1 - 1.5 x IQR to Q3 + 1.5 x IQR range. Q1 and Q3 are the first and third quartile, respectively. IQR is the interquartile range (IQR = Q3 - Q1). There were outliers in some of our results due to participants showing high levels of discomfort, especially during the early days. We retained these outliers because they are a natural part of the data, rather than errors. A significance level of 0.05 was set for all analysis. All our statistical tests were performed in R version 4.1.0 using the rstatix package, and results were verified on SPSS.

5.4.1 Testing Sessions

In this section we report the results for day 1 (pre training) and day 5 (post training). We report summary results of the discomfort scores and the SSQ subscales in table 5.1 and we discuss the results and our statistical tests in more detail in the following subsections.

	Day 1	Day 5
Discomfort Score		
Average	3.08 (2.2)	1.71 (1.5)
Ending	3.84 (3.3)	2.32 (2.2)
SSQ Subscores		
Nausea	40.67 (35.7)	12.05 (24.4)
Oculomotor Discomfort	26.33 (17.2)	13.96 (21.9)
Disorientation	51.28 (38.3)	32.24 (39.1)
Total Severity	42.72 (30.8)	20.28 (27.4)
Optic flow		
Mean Magnitude	1.31 (.4)	1.35 (.3)
Electrodermal Data		
Ampl. RMS Baseline	0.43 (.3)	.44 (.4)
Ampl. RMS End	.51 (.3)	.33 (.3)
Tonic SCL End	5.00 (5.4)	3.66 (3.5)

Table 5.1: Summary results of discomfort scores, simulator sickness questionnaire, optic flow, and electrodermal data for the testing days in terms of *mean (standard deviation).*
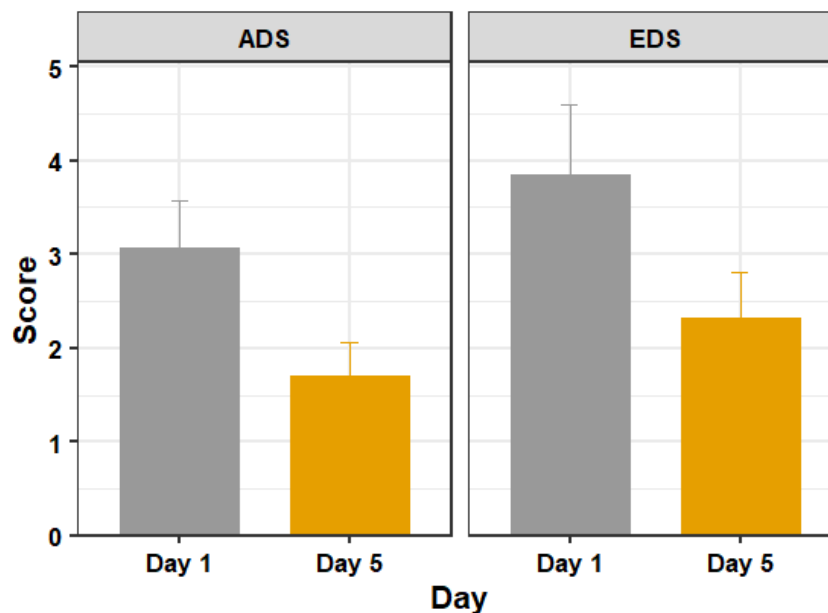
Discomfort Scores

Figure 5.3: The average discomfort score (ADS) and ending discomfort score (EDS) of participants on days 1 (before training) and 5 (after training). Figure shows mean and standard error.

Figure 5.3 shows the mean ADS and EDS scores of the testing days 1 and 5.

A Shapiro-Wilk test found that our data were normally distributed. Our outlier

test showed that we had one outlier, but no extreme outliers. We retained the identified outlier in each score, as we considered that they were a natural part of the data, rather than errors.

Using a paired t-test we found significant differences in discomfort measures between days 1 and 5 with respect to both ADS ($t(18) = 3.297, p = 0.004, d = 0.756$) and EDS ($t(18) = 2.635, p = 0.017, d = 0.605$).

SSQ Sub-scores
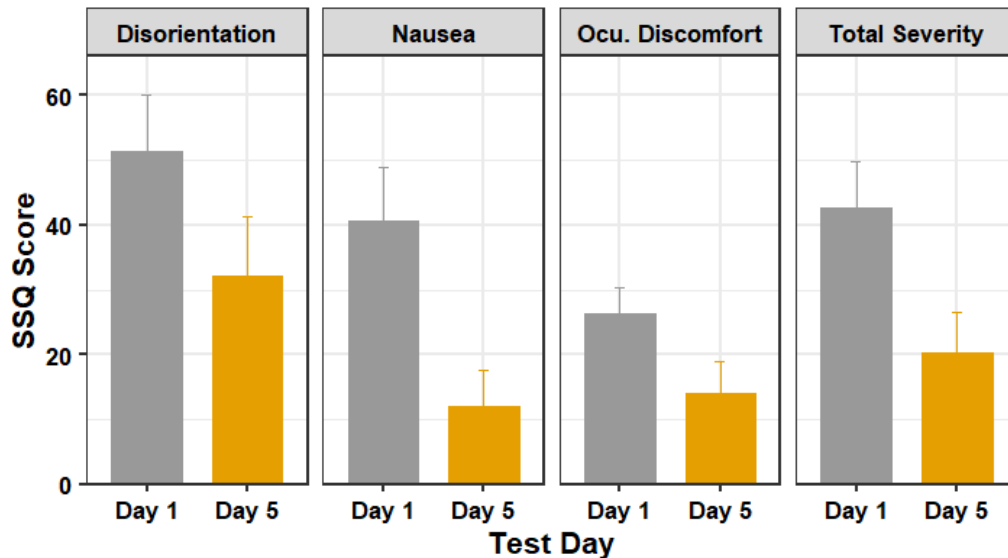
Figure 5.4: The SSQ subscores of participants in days 1 (before training) and 5 (after training). Figure shows mean and standard error.

Figure 5.4 shows the average SSQ subscores for the testing days. A Shapiro-Wilk test found that our data were not normally distributed. Our outlier test showed that we had some outliers. We retained the identified outliers in each sub-score, as these scores were from users who felt severe discomfort during the experiment and were not extreme outliers. Since our data violates the assumptions

of the paired t-test, we used a Wilcoxon signed-rank test - the non-parametric alternative to the paired t-test.

A Wilcoxon signed-rank test showed that there was statistically significant change in nausea score ($Z = 16, p = 0.001$) and the total severity score ($Z = 14, p = 0.031$), but there was no statistically significant change in the disorientation score ($Z = 12, p = 0.143$) or the oculomotor discomfort score ($Z = 13, p = 0.096$) between days 1 and 5.

EDA Data
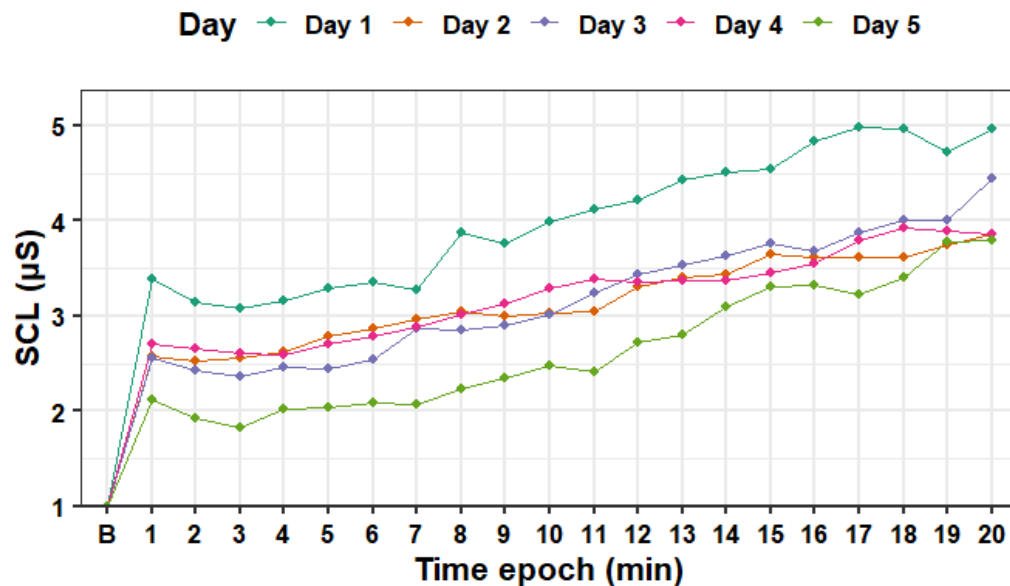
Figure 5.5: Standardized tonic skin conductance level data averaged for each epoch (minute) during the experiment days. B - baseline SCL.

A wilcoxon signed rank test showed that, on day 1, the phasic amplitude RMS values did not differ significantly when compared to the baseline values ($Z = 115, p = 0.322$). On day 5, there was no significant increase in phasic amplitude RMS values during the session ($Z = 174, p = 0.0.322$). Comparing between days,

while there were no significant differences at the baseline between days 1 and 5 ($Z = 146, p = 0.973$), the phasic amplitude RMS was significantly lower on day 5 compared to day 1 ($Z = 215, p = 0.015$) indicating a decrease of VR sickness symptoms in day 5, after completing the training sessions.

Figure 5.5 shows how the average tonic SCL values changed over time during each session. Although the SCL plot shows a decrease on the tonic SCL level between days 1 and 5, a Wilcoxon signed-rank test showed that the difference was not significant ($Z = 18, p = 0.648$).

Optic Flow Magnitude

A Shapiro-Wilk test found that our optic flow magnitude data for the testing days were not normally distributed, therefore we used the Wilcoxon-signed ranks test to analyze the data.

Our analysis of optic flow magnitude data with the Wilcoxon-signed rank test for the testing days (days 1 and 5) found that participants did not experience a significantly different magnitude of optic flow ($Z = 0.648, p = 0.517$) during the test days.

5.4.2 Training Sessions

In this section we report our results for the training days (days 2,3 and 4). We report summary results of the discomfort scores and the SSQ subscales in table 5.2 and we discuss the results and our statistical tests in more detail in the following subsections.

	Day 2	Day 3	Day 4
Discomfort Score			
Average	2.27 (2.1)	1.6 (1.5)	1.66 (1.4)
Ending	2.63 (2.4)	2.4 (2.6)	2.32 (2.2)
SSQ Subscores			
Nausea	20.59 (21.9)	19.58 (26.9)	12.55 (18.2)
Oculomotor Discomfort	23.94 (25.2)	13.96 (21.6)	17.16 (20.8)
Disorientation	37.36 (36.6)	33.70 (40.5)	33.70 (34.8)
Total Severity	29.92 (28.6)	23.62 (29.4)	22.44 (24.6)
Optic flow			
Mean Magnitude	4.83 (.7)	7.79 (1.2)	11.57 (1.1)
Electrodermal Data			
Ampl. RMS Baseline	.44 (.3)	.37 (.4)	.34 (.3)
Ampl. RMS End	.5 (.4)	.38 (.4)	.44 (.3)
Tonic SCL End	3.65 (3.1)	4.06 (4.2)	4.01 (2.9)

Table 5.2: Summary results of discomfort scores, simulator sickness questionnaire, optic flow, and electrodermal data for the training days in terms of *mean (standard deviation).*
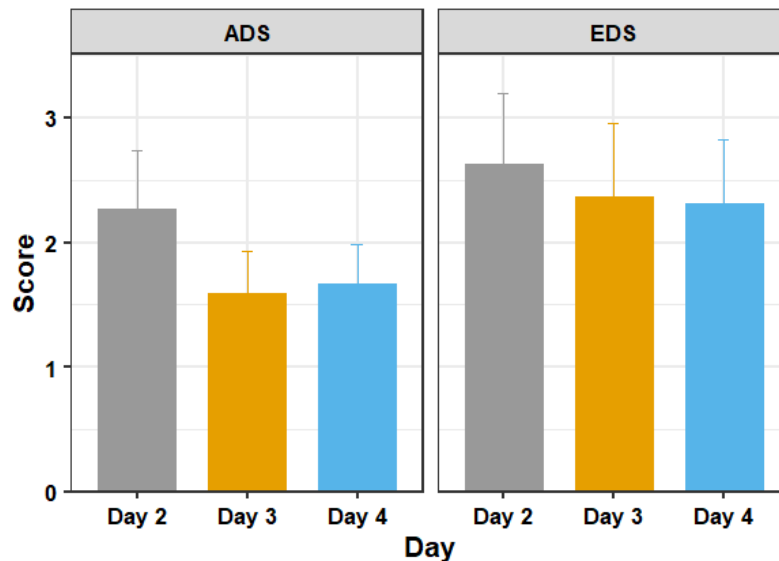
Discomfort Scores

Figure 5.6: The average discomfort score (ADS) and ending discomfort score (EDS) of participants in days 2, 3 and 4 of adaptation training. Figure shows mean and standard error.

Figure 5.6 shows the mean ADS and EDS scores of the training days 2, 3 and 4. A Shapiro-Wilk test found that our data were normally distributed. We did not have extreme outliers in our data.

A one way repeated measures ANOVA showed that there were significant differences in discomfort measures between the training days with respect to ADS ($F = 4.086, p = 0.042$) but not with respect to EDS ($F = 0.503, p = 0.609$). Post hoc analysis with paired t-tests was conducted and Bonferroni adjustment applied. The post hoc tests revealed that ADS was statistically significantly decreased from day 2 to day 3 ($t(18) = 3.38, p = 0.010$), but not from days 3 to 4 ($t(18) = -0.31, p = 1.000$). EDS did not show any statistically significant decreases between day 2 and day 3 ($t(18) = 0.96, p = 1.000$) or from day 3 to day 4 ($t(18) = 0.15, p = 1.000$).

SSQ Sub-Scores
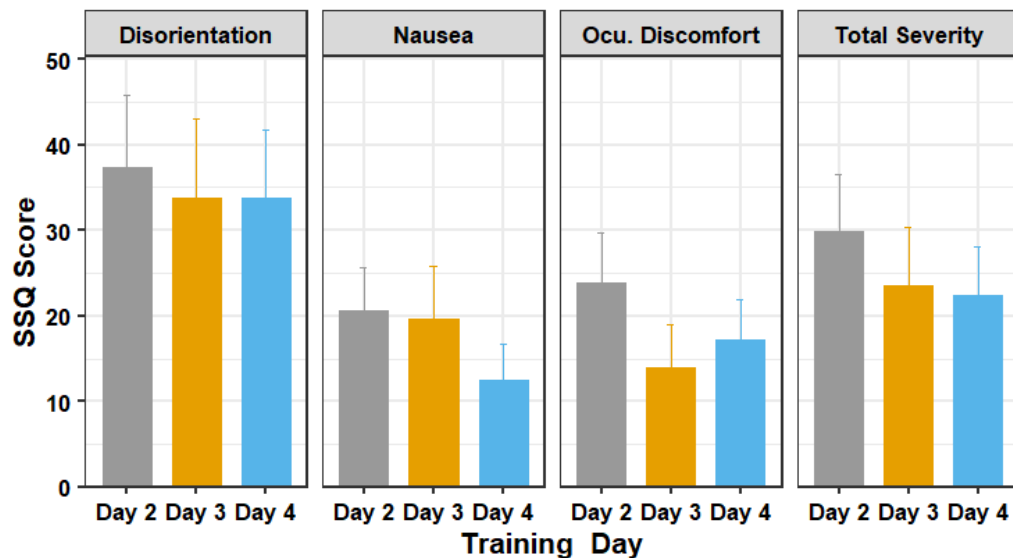
Figure 5.7: The SSQ subscores of participants in days 2 through 4 of the training session. Figure shows mean and standard error.

Figure 5.7 shows the average SSQ subscores for the training days. A Shapiro-Wilk test found that our data were not normally distributed. Our outlier test also showed that we had some outliers from users who felt extreme discomfort during the experiment. Since our data violates the assumptions of the one way repeated

measures ANOVA, we used the Friedman test - the non-parametric alternative to the one way repeated measures ANOVA.

The Friedman test showed that there was a statistically significant difference in the oculomotor discomfort score among the training days, ($\chi^2(2) = 8.38, p = 0.015$). The test showed that there was no significant difference in the nausea score ($\chi^2(2) = 2.76, p = 0.251$), disorientation score ($\chi^2(2) = 2.52, p = 0.284$) and the total severity score ($\chi^2(2) = 3.65, p = 0.161$). Post-hoc analysis with Wilcoxon signed-rank tests was conducted with a Bonferroni correction applied, and showed that there was no significant difference in scores between the training days.

EDA Data

Wilcoxon signed rank tests showed that the phasic amplitude RMS values did not increase significantly at the end of the session for days 2 ($Z = 147. p = 0.945$), 3 ($Z = 145.5. p = 0.986$) and 4 ($Z = 109. p = 0.231$) when compared to the baseline values. Comparing between days 2, 3, and 4, a Friedman test showed that there were no significant differences for the baseline ($\chi^2(2) = 2.471, p = 0.291$) or the session end ($\chi^2(2) = 0.471, p = 0.790$) values of the phasic amplitude RMS. A Friedman test showed that the tonic SCL data also does not show significant difference between days 2, 3 and 4 ($\chi^2(2) = 1.529, p = 0.465$).

Optic flow Magnitude

Figure 5.8 shows the average optic flow magnitude for the training days, and figure 5.9 shows a visualization of the optic flow a typical user experienced during the training days. A Shapiro-Wilk test found that our data for both the training days
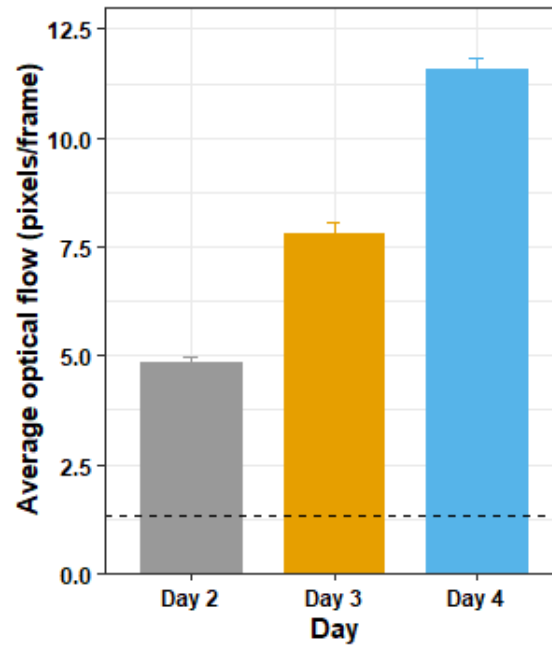
Figure 5.8: The average optic flow magnitude by day for the training days. The horizontal dotted line shows the average optic flow magnitude of the two testing days (days 1 and 5) for comparison. The figure shows mean and standard deviation.

were not normally distributed, therefore we used the Friedman test to analyze the results for the training days.

The Friedman test showed that there was a substantially significant difference in optic flow magnitude between the training days ($\chi^2(2) = 38, p < 0.05$). Post hoc analysis with Wilcoxon signed-rank tests was conducted with a Bonferroni correction applied, and showed that there was significant difference in optic flow magnitude between days 2 and 3 ($Z = 0, p < 0.05$), between days 3 and 4 ($Z = 0, p < 0.05$) and between days 2 and 4 ($Z = 0, p < 0.05$).
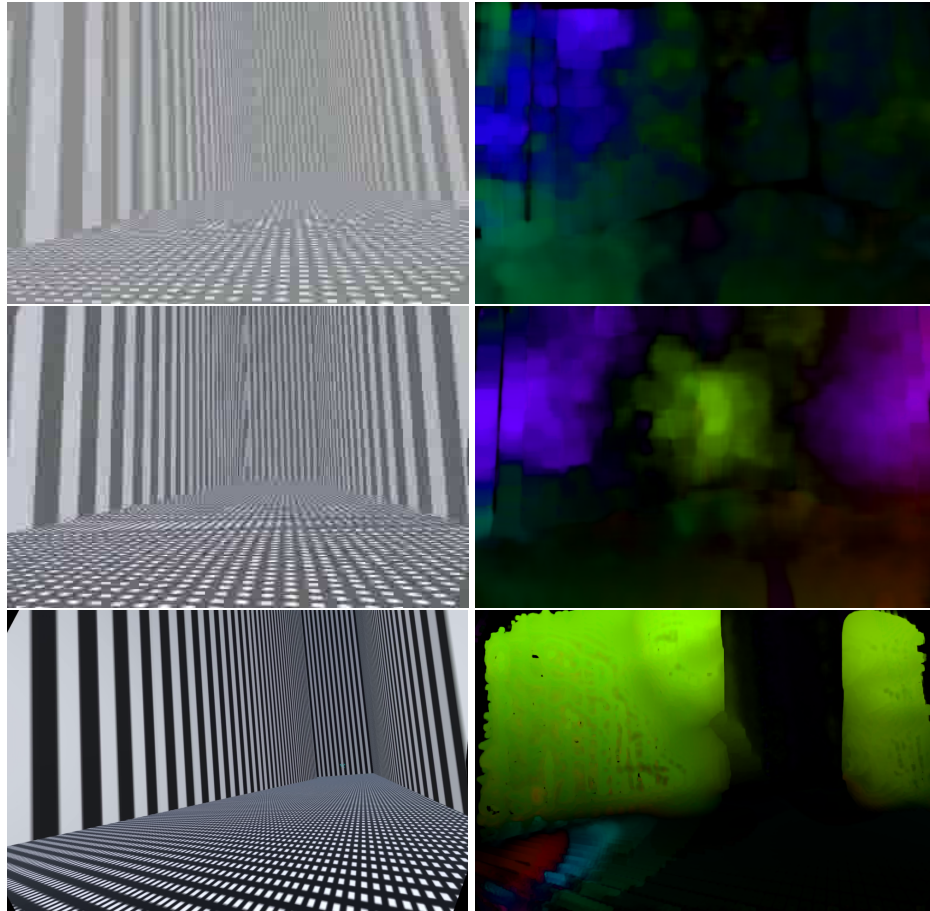
Figure 5.9: Frames captured in days 2,3 and 4 of training days along with their corresponding optic flow visualization. The frames show the view a typical participant saw traveling through the same spot at the same speed in the three separate days of the experiment, along with their optic flow visualizations.

5.5 Discussion

This study had two aims, to investigate VR sickness adaptation methods that allow gradual exposure to increasing optic flow and the transferability of adaptation from one environment to another. To avoid floor effects, we explicitly recruited individuals that reported susceptibility to VR sickness and limited VR use. Subjects were tested over five days, consisting of a baseline on day 1, three consecutive training days, and a final test session on day 5. The test environment consisted

of a cityscape, while the training environment was a less realistic labyrinth with black and white striped walls. Contrast and thus optic flow strength was gradually increased over consecutive training days. Results indicate that, despite the increase in optic flow strength, subjective sickness reports and objective physiological measures did not increase, but instead tended to remain constant or even decrease over consecutive training days, though this decrease was generally not significant. Comparison between measures obtained on days 1 and 5, on the other hand, tended to show significant decreases in sickness. These results suggest that exposure to ramped optic flow strength supports gradual adaptation of VR sickness and its symptoms. Additionally, adaptation that is developed in more abstract and impoverished environments can transfer to richer and more naturalistic environments. These results suggest that carefully controlled adaptation procedures can be a successful mitigation strategy for VR sickness.

5.5.1 RQ$_1$: Ramped Optic Flow Exposure

One of the primary aims of this study was to investigate whether exposure to ramped optic flow strength in an abstract environment allows for gradual adaptation to VR sickness. Prior studies have shown that reducing overall optic flow strength, for example, by restricting the FOV to eliminate faster motion at the periphery [61] can lead to reduced sickness. In addition, reducing contrast has recently been shown to reduce vection magnitude and duration, and to increase vection onset latency [77]. However, to our knowledge, no prior studies have explicitly demonstrated that scene contrast directly impacts VR sickness. It is reasonable to hypothesize that decreased contrast, and thus decreased optic flow strength, should lead to decreased severity of sickness. For this reason, we chose to begin

training on day 2 with a reduced contrast version of the training environment. The drop in reported sickness between days 1 and 2 suggests that the low-contrast labyrinth was indeed less provocative than the full-contrast test environment, and thus a well-chosen training stimulus. We believe this reduction is due in part to the impoverished nature of the training environment [167, 152, 46] and the reduced contrast, but it may also be a manifestation of the typical day-1-to-day-2 learning rate reported previously [122]. Regardless, contrast manipulation provided a convenient method to parametrically increase optic flow strength (Fig. 5.8), vection [77], and thus (presumably) the provocative nature of the VR experience, over successive training days. Despite this increase, we did not observe an increase in reported sickness. To the contrary, reported sickness either remained constant or decreased over successive training days. These results suggest that manipulating optic flow via contrast manipulation may be a straightforward way to maintain sickness at manageable levels while still allowing training.

5.5.2 RQ$_2$: Adaptation Transfer

Another primary aim of this study was to investigate whether adaptation to VR sickness that was developed in a more abstract environment can transfer to a richer and more complex environment. Prior research has demonstrated that VR sickness is more pronounced with increasing graphic realism [73, 46] and scene complexity [167, 97]. This was our motivation for training using an impoverished environment, as a way to limit sickness during training. But for such a method to be effective, the results of any adaptation must be shown to transfer from more impoverished to richer environments. To our knowledge, no other study has demonstrated the transfer of adaptation between VR environments using VR as its train-

ing mechanism. We take the reduction in sickness observed on Day 5 relative to Day 1 in our experiment to be evidence that adaptation developed in the labyrinth environment effectively transferred to the richer test environment. An alternative explanation for the reduced sickness on day 5 relative to day 1 is that this is simply a manifestation of the reduction in sickness due to prior exposure to the test environment on day 1. We believe this is unlikely because the sickness scores on day 4 with the training stimulus (ADS, EDS, and SSQ) are generally very similar to the sickness scores observed on day 5 with the test stimulus. This similarity is consistent with the idea of adaptation transfer and seems unlikely to occur by chance. Not all subscores from the SSQ indicated decreased sickness, specifically, the oculomotor and disorientation scores were not significantly different between Day 1 and Day 5. This would indicate that the change in total severity score is driven mostly by a change in nausea. It is worth noting that research also suggests that an increased sense of presence can lead to a decrease in VR sickness [190]. While we did not collect information on subjects' feelings of presence, we take the drop in sickness between days 1 and 2 to demonstrate that regardless of presence, subjects did experience greater sickness in the original, complex, environment.

5.6 Limitations and Future Works

The conclusions of the study would be strengthened by collection of additional data to control for both ramping optic flow as well as the transfer of adaptation between abstract and rich natural environments. For example, the drop in sickness and EDA observed between days 1 and 5 could be compared against the drop in sickness observed in a comparison group exposed to the test stimulus on consecutive days without being exposed to the training environment. Similarly,

the levels of sickness observed on training days 2 through 4 could be compared against sickness observed in a comparison group for which contrast and optic flow were held constant over the three days. These avenues were not explored for two reasons; First, these measurements were not possible because they would have required tripling the number of subjects enrolled in our study. Due to our restrictive inclusion criteria (see methods) and COVID-19 concerns it was already a challenge to recruit the current pool of subjects. Second, these methodologies were already largely exploratory, with previous literature already investigating much of the aforementioned control results. As mentioned in the related works section, it is well-known that consistent exposure to the same VR environment results in adaptation [146, 39, 80, 18, 48, 21], but these effects have also been known to dissipate in as little the same day [102]. This makes it unlikely that the results from day 5 are solely due to exposure to the city environment on the first day. Similarly, investigations into adaptation transfer have been largely unsuccessful or conflicting, so it is noteworthy that scores between days 4 and 5 were so similar. We suggest that this methodology was successful because it borrows concepts from motion sickness training such as gradually increasing exposure [172, 155] to a root cause of VR sickness (i.e. optic flow or the associated vection).

From our results, we concluded that subjects experienced lower levels of sickness over time, and these effects persisted between environments. The mechanisms behind this change, whether they be through the actions of the subjects or via some neurological mechanism, are unfortunately beyond the scope of this study. However, future works exploring changes in behavior in subjects in VR over time would be a worthy follow-up to this study.

Subjective feelings of vection were not directly measured during this experi-

ment. However, previous research has shown increasing luminance contrast increases feelings of vection [158, 135, 77], and so it is logical to assume the same effect was experienced in our experiment. Independent of this matter, further research has shown that increases in optic flow lead to greater feelings of VR sickness [46]. Therefore, regardless of vection, we can assume that the increase in luminance contrast and optic flow did lead to greater stimulus intensity as intended.

Regarding physiological data, we used the Empatica E4 watch, which is limited to a sampling rate of 4 Hz for EDA data. It is important to note that EDA signals are particularly sensitive to motion artifacts. Because our subjects were using their hands in order to manipulate the controller for locomotion, these artifacts were likely present in our data.

Chapter 6

Conclusion

The current thesis examines three research questions 1) how sex differences influence susceptibility to VR sickness and the effectiveness current of VR sickness mitigation strategies; 2) how eye-gaze-based adaptive VR sickness mitigation strategies can be developed that adapt to the individual user's behaviour; and 3) how systems that facilitate perceptual adaptation to VR sickness can be developed thereby reducing the need to consistently modify the virtual environment.

In chapter 2, we studied the impact of dynamic FOV restriction - a widely used VR sickness mitigation strategy - on sex differences in spatial learning and VR sickness. We found that there is a sex difference in spatial learning. Nevertheless, our results suggest that FOV restriction is an effective solution to mitigate VR sickness in both sexes, and it does not impede spatial learning above and beyond pre-existing sex differences in spatial learning ability. We consider these outcomes to be valuable to VR interaction designers who aim to make their virtual experiences inclusive for women.

In chapter 3, we introduced a new type of FOV restrictor - foveated FOV restrictor - which differs from current implementations in that the restrictor is rendered around the user's eye gaze location. This implementation assures optimal blocking of peripheral optical flow, users cannot look at the restrictor itself and it allows users to see more of the VE during locomotion. We analyzed the effectiveness of the foveated FOV restrictor on VR sickness, gaze behavior and noticeability by comparing it to a head-fixed FOV restrictor. The results showed no significant dif-

ference in VR sickness or noticeability incidence between FOV restrictors, but we did find that participants had a wider gaze dispersion indicating wider visual scan area when using the foveated restrictor.

In chapter 4, we introduced a new tool - GazeMetrics - to measure the accuracy and precision of VR-based eye trackers. Accuracy and precision are two vital components of eye tracker data quality that have implications for eye-gaze-based interaction, data collection, data analysis, and validity of results [81, 82]. As such, it is best practice to report correct metrics rather than relying on manufacturer data sheets and have these measures outlined within the methods of a study to ensure reproducible results. GazeMetrics is free, open-source software made to address these issues. It has a user interface that is customizable without having to alter the source code, making it accessible for users with all levels of coding experience. As eye tracking is being increasingly utilized in VR systems, addressing the issue of standard accuracy and precision reporting becomes increasingly important, and GazeMetrics promises to address that issue.

Finally, in chapter 5, we introduced a new paradigm for VR sickness mitigation - adaptation through training. We used an abstract environment and reduced stimulus contrast to limit sickness during training. We showed that sickness remained constant or decreased on consecutive training days, even though contrast and optic flow strength were increasing. We also showed that adaptation developed in an abstract training environment transferred to a richer test environment. These results demonstrate that adaptation to VR sickness via careful and gradual exposure to successively more provocative VR stimuli shows promise as a VR sickness mitigation strategy.

In summary, in this dissertation, we drew on knowledge originating in human-

computer interaction, cognitive neuroscience, and computer graphics to develop new techniques for the mitigation of VR sickness with the goal of making VR more accessible for people who suffer from VR sickness. We also address the biased effects of VR sickness on specific populations, such as women, that currently face inequitable barriers to engage with immersive technologies because of these . Increased access to VR can improve the well being of these populations by opening the door to a variety of VR applications including in healthcare [86, 164, 156], clinical skills training [124], and STEM education [194, 101] to name a few.

6.1 Future Directions

In the future, I aim to design, develop and evaluate accessible VR systems that take into consideration the multitude of human factors involved in inducing or exacerbating VR sickness. This can best be achieved by rethinking the design of VR systems to make them personalized through dynamic adaptation of the virtual environment. To realize this, motivated by user-adaptive systems, I aim to explore the theoretical and empirical foundation for an adaptive VR sickness mitigation framework. The framework would be designed to learn the characteristics of the user interacting with a VR system and change features of the environment to provide the user with a dynamically personalized and targeted experience, with the aim of reducing sickness and discomfort. To realize this, I would focus my work on the following three key research objectives:

6.1.1 Developing objective measures of VR sickness

Measuring and quantifying VR sickness and discomfort is especially challenging in the context of real-time adaptive systems since sickness and discomfort in VR are typically measured by collecting self-reported data from the user post-exposure through various questionnaires. Due to their subjective nature, such self-assessments have various drawbacks, including being unreliable and non real-time. Alternative measurement techniques for VR sickness rely on the physiological symptoms that accompany VR sickness. Various physiological measures that aim to measure these symptoms have been explored as potential indicators of VR sickness [34]. In the future, I aim to develop computational models that combine physiological sensor data, subjective self-reports and historical data about a user to build an objective measure of VR sickness. These computational models can then be used to measure the onset and severity of VR sickness symptoms in real-time.

6.1.2 Identifying optimal and adaptable features of VR systems

Various features of VR systems have been shown to affect VR sickness in previous research, including latency, hardware field of view (FOV), visual fidelity, and virtual travel velocity [34]. Naturally, adjusting these features have been shown to reduce VR sickness. However, not all those features can be manipulated in real time to reduce the severity of VR sickness. For example, manipulating the hardware FOV or the latency of a VR system in real time is challenging. Instead the FOV of the content could be manipulated to reduce VR sickness. In my our previous research [6, 11], my colleagues and I have investigated the effectiveness of dynamic and gaze-contingent field-of-view (FOV) restriction to reduce VR sick-

ness. In the future,k I aim to expand my recent research to empirically identify the most optimal features of VR systems that can be modified in real time to mitigate VR sickness.

6.1.3 Exploring adaptive prediction models

Given a quantitative measurement of a user's VR sickness symptoms at a particular point in time, the ultimate goal of an adaptive VR sickness mitigation system is to manipulate the virtual environment to reduce the symptoms. Towards this goal, I aim to explore predictive approaches for exploiting the adaptable features of the environment. These predictive approaches need be lightweight so that they don't rely on heavy offline analysis. Concretely, the predictive approaches will be based on optimal decision theory to minimize real-time changes to the environment while maximizing efficiency (i.e., minimizing VR sickness).

BIBLIOGRAPHY

[1] Sranipal sdk, https://developer.vive.com/resources/knowledgebase/vive-sranipal-sdk/.

[2] https://assetstore.unity.com/packages/3d/environments/roadways/windridge-city-132222.

[3] Daydream elements, vr guidelines, https://developers.google.com/vr/elements/overview#locomotion, June 2017.

[4] Daydream elements, vr guidelines, https://developers.google.com/vr/elements/overview#locomotion. https://developers.google.com/vr/elements/overview#locomotion, 2017.

[5] Google earth vr. https://vr.google.com/earth/, 2018.

[6] Isayas Berhe Adhanom, Nathan Navarro Griffin, Paul MacNeilage, and Eelke Folmer. The effect of a foveated field-of-view restrictor on vr sickness. *2020 IEEE Conference on Virtual Reality and 3D User Interfaces (VR)*, pages 645–652, March 2020.

[7] Isayas Berhe Adhanom, Nathan Navarro Griffin, Paul MacNeilage, and Eelke Folmer. The Effect of a Foveated Field-of-view Restrictor on VR Sickness. In *2020 IEEE Conference on Virtual Reality and 3D User Interfaces (VR)*, number February, pages 645–652. IEEE, 3 2020.

[8] Isayas Berhe Adhanom, Nathan Navarro Griffin, Paul Macneilage, and Eelke Folmer. The Effect of a Foveated Field-of-view Restrictor on VR Sickness. *Proceedings - 2020 IEEE Conference on Virtual Reality and 3D User Interfaces, VR 2020*, pages 645–652, 2020.

[9] Deepak Akkil, Poika Isokoski, Jari Kangas, Jussi Rantala, and Roope Raisamo. TraQuMe: A tool for measuring the gaze tracking quality. In *Eye Tracking Research and Applications Symposium (ETRA)*, 2014.

[10] Majed Al Zayer, Isayas B Adhanom, Paul MacNeilage, and Eelke Folmer. The effect of field-of-view restriction on sex bias in vr sickness and spatial navigation performance. In *Proceedings of the 2019 CHI Conference on Human Factors in Computing Systems*, pages 1–12, 2019.

[11] Majed Al Zayer, Isayas B. Adhanom, Paul MacNeilage, and Eelke Folmer. The effect of field-of-view restriction on sex bias in vr sickness and spatial navigation performance. *Proceedings of the 2019 CHI Conference on Human Factors in Computing Systems*, pages 1–â12, 2019.

[12] Majed Al Zayer, Paul MacNeilage, and Eelke Folmer. Virtual locomotion: a survey. *IEEE transactions on visualization and computer graphics*, 2018.

[13] Majed Al Zayer, Paul MacNeilage, and Eelke Folmer. Virtual Locomotion: A Survey. *IEEE Transactions on Visualization and Computer Graphics*, 26(6):2315–2334, 2020.

[14] Majed Al Zayer, Sam Tregillus, Jiwan Bhandari, Dave Feil-Seifer, and Eelke Folmer. Exploring the use of a drone to guide blind runners. In *Proceedings of the 18th International ACM SIGACCESS Conference on Computers and Accessibility*, pages 263–264. ACM, 2016.

[15] Imtiaz Muhammad Arafat, Sharif Mohammad Shahnewaz Ferdous, and John Quarles. Cybersickness-provoking virtual reality alters brain signals of persons with multiple sclerosis. pages 1–120, 2018.

[16] Josh T. Arnold, Kate O'Keeffe, Chloe McDaniel, Simon Hodder, and Alex Lloyd. Effect of virtual reality and whole-body heating on motion sickness severity: A combined and individual stressors approach. *Displays*, 60(August):18–23, 2019.

[17] Robert S Astur, Maria L Ortiz, and Robert J Sutherland. A characterization of performance by men and women in a virtual morris water task: A large and reliable sex difference. *Behavioural brain research*, 93(1-2):185–190, 1998.

[18] J. N. Bailenson and N. Yee. A Longitudinal Study of Task Performance, Head movements, subjective report, simulator sickness, and transformed social interaction in collaborative virtual environments. *Presence*, 15(6):699–716, 2006.

[19] James Barabas, Robert B. Goldstein, Henry Apfelbaum, Russell L. Woods, Robert G. Giorgi, and Eli Peli. Tracking the line of primary gaze in a walking simulator: Modeling and calibration. *Behavior Research Methods, Instruments, and Computers*, 2004.

[20] Shaowen Bardzell. Feminist hci: taking stock and outlining an agenda for design. In *Proceedings of the SIGCHI conference on human factors in computing systems*, pages 1301–1310. ACM, 2010.

[21] Sarah C. Beadle, Eric R. Muth, and Christopher C. Pagano. Using head-mounted displays to examine adaptation and calibration under varying perturbations. *Displays*, 66(December 2020):101985, 2021.

[22] Jiwan Bhandari, Paul MacNeilage, and Eelke Folmer. Teleportation without spatial disorientation using optical flow cues. In *Proceedings of Graphics Interface 2018*, GI 2018, pages 162 – 167. Canadian Human-Computer Communications Society / Société canadienne du dialogue humain-machine, 2018.

[23] Frank Biocca. Will simulation sickness slow down the diffusion of virtual environment technology? *Presence: Teleoperators & Virtual Environments*, 1(3):334–343, 1992.

[24] Pieter Blignaut and Tanya Beelders. TrackStick: A data quality measuring tool for Tobii eye trackers. In *Eye Tracking Research and Applications Symposium (ETRA)*, 2012.

[25] Mark Bolas, J Adam Jones, Ian McDowall, and Evan Suma. Dynamic field of view throttling as a means of improving user experience in head mounted virtual environments, May 9 2017. US Patent 9,645,395.

[26] Frederick Bonato, Andrea Bubka, and Stephen Palmisano. Combined pitch and roll and cybersickness in a virtual environment. *Journal of Aviation, space, and environmental medicine*, 80(11):941–945, 2009.

[27] Jelte E Bos, Sjoerd C de Vries, Martijn L van Emmerik, and Eric L Groen. The effect of internal and external fields of view on visually induced motion sickness. *Applied ergonomics*, 41(4):516–521, 2010.

[28] Doug Bowman, David Koller, and Larry F. Hodges. Travel in immersive virtual environments: An evaluation of viewpoint motion control techniques. In *Virtual Reality Annual International Symposium, 1997., IEEE 1997*, pages 45–52. IEEE, 1997.

[29] JJ Jason J Braithwaite, Dr Derrick, G Watson, Robert Jones, Mickey Rowe, DG Watson, Jones Robert, and Rowe Mickey. A Guide for Analysing Electrodermal Activity (EDA) & Skin Conductance Responses (SCRs) for Psychological Experiments. . . . , pages 1–42, 2013.

[30] Andrea Bubka, Frederick Bonato, and Stephen Palmisano. Expanding and contracting optical flow patterns and simulator sickness. *Aviation Space and Environmental Medicine*, 78(4 I):383–386, 2007.

[31] Pulkit Budhiraja, Mark Roman Miller, Abhishek K. Modi, and David Forsyth. Rotation Blurring: Use of Artificial Blurring to Reduce Cybersickness in Virtual Reality First Person Shooters, 2017.

[32] Neil Burgess. Spatial memory: how egocentric and allocentric combine. *Trends in cognitive sciences*, 10(12):551–557, 2006.

[33] Chih-Hui Chang, Wu-Wen Pan, Li-Ya Tseng, and Thomas A Stoffregen. Postural activity and motion sickness during video game play in children and adults. *Experimental brain research*, 217(2):299–309, 2012.

[34] Eunhee Chang, Hyun Taek Kim, and Byounghyun Yoo. Virtual Reality Sickness: A Review of Causes and Measurements. *International Journal of Human-Computer Interaction*, 36(17):1–25, 2020.

[35] Eunhee Chang, Hyun Taek Kim, and Byounghyun Yoo. Predicting cybersickness based on user's gaze behaviors in HMD-based virtual reality. *Journal of Computational Design and Engineering*, 8(2):728–739, 2021.

[36] Lucia A Cherep, Alex F Lim, Jonathan W Kelly, Devi Acharya, Alfredo Velasco, Emanuel Bustamante, Alec G Ostrander, and Stephen B Gilbert. Spatial cognitive implications of teleporting through virtual environments. *Journal of Experimental Psychology: Applied*, 2020.

[37] Stacy A Clemes and Peter A Howarth. The menstrual cycle and susceptibility to virtual simulation sickness. *Journal of biological rhythms*, 20(1):71–82, 2005.

[38] A. Clemotte, M. Velasco, D. Torricelli, R. Raya, and R. Ceres. Accuracy and precision of the tobii X2-30 eye-tracking under non ideal conditions. In *NEUROTECHNIX 2014 - Proceedings of the 2nd International Congress on Neurotechnology, Electronics and Informatics*, 2014.

[39] Sue V. G. Cobb, Sarah Nichols, Amanda Ramsey, and John R. Wilson. Virtual Reality-Induced Symptoms and Effects (VRISE). *Presence*, 8(2):169–186, 1999.

[40] Jacob Cohen. A power primer. *Psychological bulletin*, 112(1):155, 1992.

[41] Mary Czerwinski, Desney S Tan, and George G Robertson. Women take a wider view. In *Proceedings of the SIGCHI conference on Human factors in computing systems*, pages 195–202. ACM, 2002.

[42] James M Dabbs, E-Lee Chang, Rebecca A Strong, and Rhonda Milun. Spatial ability, navigation strategy, and geographic knowledge among men and women. *Evolution and Human Behavior*, 19(2):89–98, 1998.

[43] Kirsten A. Dalrymple, Marie D. Manner, Katherine A. Harmelink, Elayne P. Teska, and Jed T. Elison. An examination of recording accuracy and precision from eye tracking data from toddlerhood to adulthood. *Frontiers in Psychology*, 2018.

[44] Rudolph P Darken, William R Cockayne, and David Carmein. The omni-directional treadmill: a locomotion device for virtual worlds. In *Proceedings of UIST'97*, pages 213–221. ACM, 1997.

[45] Simon Davis, Keith Nesbitt, and Eugene Nalivaiko. A systematic review of cybersickness. In *Proceedings of the 2014 Conference on Interactive Entertainment*, pages 1–9. ACM, 2014.

[46] Simon Davis, Keith Nesbitt, and Eugene Nalivaiko. Comparing the onset of cybersickness using the Oculus Rift and two virtual roller coasters. *11th Australasian Conference on Interactive Entertainment (IE 2015)*, (January):27–30, 2015.

[47] Mark S. Dennison, A. Zachary Wisti, and Michael D'Zmura. Use of physiological signals to predict cybersickness. *Displays*, 44:42–52, 2016.

[48] Joshua E. Domeyer, Nicholas D. Cassavaugh, and Richard W. Backs. The use of adaptation to reduce simulator sickness in driving assessment and research. *Accident Analysis and Prevention*, 53:127–132, 4 2013.

[49] Ira Driscoll, Derek A Hamilton, Ronald A Yeo, William M Brooks, and Robert J Sutherland. Virtual navigation in humans: the impact of age, sex, and hormones on place learning. *Hormones and behavior*, 47(3):326–335, 2005.

[50] Andrew Duchowski, Eric Medlin, Nathan Cournia, Hunter Murphy, Anand Gramopadhye, Santosh Nair, Jeenal Vorah, and Brian Melloy. 3-D eye movement analysis. *Behavior Research Methods, Instruments, and Computers*, 2002.

[51] Henry Been-Lirn Duh, Donald E Parker, and Thomas A Furness. An independent visual background reduced simulator sickness in a driving simulator. *Presence: Teleoperators & Virtual Environments*, 13(5):578–588, 2004.

[52] Natalia Duzmanska, Pawel Strojny, and Agnieszka Strojny. Can simulator sickness be avoided? A review on temporal aspects of simulator sickness, 2018.

[53] Sheldon M Ebenholtz. Motion sickness and oculomotor systems in virtual environments. *Presence: Teleoperators & Virtual Environments*, 1(3):302–305, 1992.

[54] Sheldon M Ebenholtz. Motion sickness and oculomotor systems in virtual environments. *Presence: Teleoperators & Virtual Environments*, 1(3):302–305, 1992.

[55] Benedikt V. Ehinger, Katharina Groß, Inga Ibs, and Peter König. A new comprehensive eye-tracking test battery concurrently evaluating the Pupil Labs glasses and the EyeLink 1000. *PeerJ*, 2019(7), 2019.

[56] Gunnar Farneback. Two-Frame Motion Estimation Based on Polynomial Expansion. *Lecture Notes in Computer Science*, 2749(1):363–370, 2003.

[57] Franz Faul, Edgar Erdfelder, Albert-Georg Lang, and Axel Buchner. G* power 3: A flexible statistical power analysis program for the social, be-

havioral, and biomedical sciences. *Behavior research methods*, 39(2):175–191, 2007.

[58] Steven K Feiner and Ajoy Savio Fernandes. Imperceptible automatic field-of-view restrictors to combat vr sickness and cybersickness, September 7 2017. US Patent App. 15/447,986.

[59] Anna Maria Feit, Shane Williams, Arturo Toledo, Ann Paradiso, Harish Kulkarni, Shaun Kane, and Meredith Ringel Morris. Toward everyday gaze input: Accuracy and precision of eye tracking and implications for design. In *Conference on Human Factors in Computing Systems - Proceedings*, 2017.

[60] Thomas D Ferguson, Sharon A Livingstone-Lee, and Ronald W Skelton. Incidental learning of allocentric and egocentric strategies by both men and women in a dual-strategy virtual morris water maze. *Behavioural brain research*, 364:281–295, 2019.

[61] Ajoy S Fernandes and Steven K Feiner. Combating VR sickness through subtle dynamic field-of-view modification. In *2016 IEEE Symposium on 3D User Interfaces (3DUI)*, pages 201–210. IEEE, 2016.

[62] Ajoy S. Fernandes and Steven K. Feiner. Combating VR sickness through subtle dynamic field-of-view modification. *2016 IEEE Symposium on 3D User Interfaces, 3DUI 2016 - Proceedings*, pages 201–210, 2016.

[63] Kiran J Fernandes, Vinesh Raja, and Julian Eyre. Cybersphere: the fully immersive spherical projection system. *Communications of the ACM*, 46(9):141–146, 2003.

[64] Moira B Flanagan, James G May, and Thomas G Dobie. Sex differences in tolerance to visually-induced motion sickness. *Aviation, space, and environmental medicine*, 76(7):642–646, 2005.

[65] Sebastian Freitag, Benjamin Weyers, and Torsten W Kuhlen. Assisted travel based on common visibility and navigation meshes. In *Virtual Reality (VR), 2017 IEEE*, pages 369–370. IEEE, 2017.

[66] Yoshitaka Fujii and Takeharu Seno. The Effect of Optical Flow Motion Direction on Vection Strength. *i-Perception*, 11(1), 2020.

[67] Andre Garcia, Carryl Baldwin, and Matt Dworsky. Gender differences in simulator sickness in fixed-versus rotating-base driving simulator. In *Proceedings of the Human Factors and Ergonomics Society Annual Meeting*, volume 54, pages 1551–1555. SAGE Publications Sage CA: Los Angeles, CA, 2010.

[68] Alireza Mazloumi Gavgani, Keith V. Nesbitt, Karen L. Blackmore, and Eugene Nalivaiko. Profiling subjective symptoms and autonomic changes associated with cybersickness. *Autonomic Neuroscience: Basic and Clinical*, 203:41–50, 2017.

[69] Gregor Geršak, Huimin Lu, and JoÅ¾e Guna. Effect of VR technology matureness on VR sickness. *Multimedia Tools and Applications*, 79(21-22):14491–14507, 2020.

[70] Agostino Gibaldi, Mauricio Vanegas, Peter J. Bex, and Guido Maiello. Evaluation of the Tobii EyeX Eye tracking controller and Matlab toolkit for research. *Behavior Research Methods*, 2017.

[71] John F Golding. Motion sickness susceptibility. *Autonomic Neuroscience: Basic and Clinical*, 129(1):67–76, 2006.

[72] John F. Golding. Predicting individual differences in motion sickness susceptibility by questionnaire. *Personality and Individual Differences*, 41(2):237–248, 7 2006.

[73] John F. Golding, Kim Doolan, Amish Acharya, Maryame Tribak, and Michael A. Gresty. Cognitive cues and visually induced motion sickness. *Aviation Space and Environmental Medicine*, 83(5):477–482, 2012.

[74] Claire C Gordon, Cynthia L Blackwell, Bruce Bradtmiller, Joseph L Parham, Patricia Barrientos, Stephen P Paquette, Brian D Corner, Jeremy M Carson, Joseph C Venezia, Belva M Rockwell, Michael Mucher, and Shirley Kristensen. 2012 anthropometric survey of u.s. army personnel: Methods and summary statistics. *U.S. Army Natick Soldier Research Development & Engineering Center*, 2014.

[75] David A Graeber and Kay M Stanney. Gender differences in visually induced motion sickness. In *Proceedings of the Human Factors and Ergonomics Society Annual Meeting*, volume 46, pages 2109–2113. SAGE Publications Sage CA: Los Angeles, CA, 2002.

[76] Nathan Navarro Griffin and Eelke Folmer. Out-of-body locomotion: Vectionless navigation with a continuous avatar representation. *25th ACM Symposium on Virtual Reality Software and Technology on - VRST '19*, 2019.

[77] Xuanru Guo, Shinji Nakamura, Yoshitaka Fujii, Takeharu Seno, and Stephen Palmisano. Effects of luminance contrast, averaged luminance and spatial frequency on vection. *Experimental Brain Research*, (0123456789), 2021.

[78] Jukka Häkkinen, Tero Vuori, and Monika Puhakka. Postural stability and sickness symptoms after HMD use. *Proceedings of the IEEE International Conference on Systems, Man and Cybernetics*, 1(April):147–152, 2002.

[79] David B Henson. *Visual fields*. Butterworth-Heinemann Medical, 2000.

[80] K J Hill and Peter A Howarth. Habituation to the side effects of immersion in a virtual environment. *Displays*, 21(1):25–30, 2000.

[81] Kenneth Holmqvist, Marcus Nyström, Richard Andersson, Richard Dewhurst, Halszka Jarodzka, and Joost Van de Weijer. Eye tracking: A comprehensive guide to methods and measures. In *Eye Tracking: A comprehensive guide to methods and measures*, chapter 2, pages 9–64. OUP Oxford, 2011.

[82] Kenneth Holmqvist, Marcus Nyström, and Fiona Mulvey. Eye tracker data quality: What it is and how to measure it. *Eye Tracking Research and Applications Symposium (ETRA)*, 1(212):45–52, 2012.

[83] Rob Howard. Provider model design pattern and specification. http://msdn.microsoft.com/en-us/library/ms972319.aspx, 2006. [Online; accessed 7-April-2020].

[84] Peter A. Howarth and Simon G. Hodder. Characteristics of habituation to motion in a virtual environment. *Displays*, 29(2):117–123, 2008.

[85] Rifatul Islam, Kevin Desai, and John Quarles. Cybersickness Prediction from Integrated HMDâs Sensors: A Multimodal Deep Fusion Approach using Eye-tracking and Head-tracking Data. In *2021 IEEE International Symposium on Mixed and Augmented Reality (ISMAR)*, number August, pages 31–40. IEEE, 10 2021.

[86] Mohd Javaid and Abid Haleem. Virtual reality applications toward medical field. *Clinical Epidemiology and Global Health*, 8(2):600–605, 2020.

[87] Valen E Johnson. Revised standards for statistical evidence. *Proceedings of the National Academy of Sciences*, 110(48):19313–19317, 2013.

[88] Jonathan W Kelly, Alec G Ostrander, Alex F Lim, Lucia A Cherep, and Stephen B Gilbert. Teleporting through virtual environments: Effects of path scale and environment scale on spatial updating. *IEEE Transactions on Visualization and Computer Graphics*, 26(5):1841–1850, 2020.

[89] Andras Kemeny, Paul George, Frédéric Mérienne, and Florent Colombet. New vr navigation techniques to reduce cybersickness. *Electronic Imaging*, 2017(3):48–53, 2017.

[90] Robert S Kennedy, Norman E Lane, Kevin S Berbaum, and Michael G Lilienthal. Simulator sickness questionnaire: An enhanced method for quantifying simulator sickness. *The international journal of aviation psychology*, 3(3):203–220, 1993.

[91] B Keshavarz, H Hecht, and BD Lawson. Visually induced motion sickness: characteristics, causes, and countermeasures. *Handbook of Virtual Environments: Design, Implementation, and Applications*, pages 648–697, 2014.

[92] Behrang Keshavarz. Exploring behavioral methods to reduce visually induced motion sickness in virtual environments. In *Virtual, Augmented and Mixed Reality*, pages 147–155. Springer International Publishing, 2016.

[93] Behrang Keshavarz, Heiko Hecht, and Lisa Zschutschke. Intra-visual conflict in visually induced motion sickness. *Displays*, 32(4):181–188, 2011.

[94] Behrang Keshavarz, Bernhard E Riecke, Lawrence J Hettinger, and Jennifer L Campos. Vection and visually induced motion sickness: how are they related? *Frontiers in psychology*, 6:472, 2015.

[95] Behrang Keshavarz, Bernhard E. Riecke, Lawrence J. Hettinger, and Jennifer L. Campos. Vection and visually induced motion sickness: How are they related? *Frontiers in Psychology*, 6(APR):1–11, 2015.

[96] Hyun K. Kim, Jaehyun Park, Yeongcheol Choi, and Mungyeong Choe. Virtual reality sickness questionnaire (VRSQ): Motion sickness measurement index in a virtual reality environment. *Applied Ergonomics*, 2018.

[97] Kelly S Kingdon, Kay M. Stanney, and Robert S. Kennedy. Extreme Responses to Virtual Environment Exposure. In *PROCEEDINGS ofthe HUMANFACTORS AND ERGONOMICS SOCIETY 45th ANNUAL MEETING*, pages 1906–1910, 2001.

[98] Amelia Kinsella. Adaptation to Base Latency in a Head-Mounted Display Using a Performance Task to Facilitate Adaptation. *ProQuest Dissertations and Theses*, page 147, 2018.

[99] Eugenia M Kolasinski. Simulator sickness in virtual environments. Technical report, DTIC Document, 1995.

[100] Michal Kowalik. Do-It-Yourself Eye Tracker: Impact of the Viewing Angle on the Eye Tracking Accuracy. *Proceedings of CESCG 2011: The 15th Central European Seminar on Computer Graphics*, 2011.

[101] Richard Lamb, Pavlo Antonenko, Elisabeth Etopio, and Amanda Seccia. Comparison of virtual reality and hands on activities in science education via functional near infrared spectroscopy. *Computers & Education*, 124:14 – 26, 2018.

[102] Donald Ralph Lampton, Mar Esther Rodriguez, and James Eastham Cotton.

Simulator Sickness Symptoms During Team Training in Immersive Virtual Environments. In *Proceedings of IEA 2000/HFES 2000 Congress*, 2000.

[103] J-F Lapointe and Norman G Vinson. Effects of joystick mapping and field-of-view on human performance in virtual walkthroughs. In *3D Data Processing Visualization and Transmission, 2002. Proceedings. First International Symposium on*, pages 490–493. IEEE, 2002.

[104] Joseph J LaViola Jr. A discussion of cybersickness in virtual environments. *ACM SIGCHI Bulletin*, 32(1):47–56, 2000.

[105] Jiun-Yu Lee, Ping-Hsuan Han, Ling Tsai, Rih-Ding Peng, Yang-Sheng Chen, Kuan-Wen Chen, and Yi-Ping Hung. Estimating the simulator sickness in immersive virtual reality with optical flow analysis. *SIGGRAPH Asia 2017 Posters on - SA '17*, 2017.

[106] JJ-W Lin, Henry Been-Lirn Duh, Donald E Parker, Habib Abi-Rached, and Thomas A Furness. Effects of field of view on presence, enjoyment, memory, and simulator sickness in a virtual environment. In *Virtual Reality, 2002. Proceedings. IEEE*, pages 164–171. IEEE, 2002.

[107] Gerard Llorach, Alun Evans, and Josep Blat. Simulator sickness and presence using hmds: comparing use of a game controller and a position estimation system. In *Proceedings of the 20th ACM Symposium on Virtual Reality Software and Technology*, pages 137–140. ACM, 2014.

[108] J M Loomis, R L Klatzky, and R G Golledge. Navigating without vision: basic and applied research. *Optometry and Vision Science*, 78(5):282–289, May 2001.

[109] Jack M Loomis, Roberta L Klatzky, Reginald G Golledge, Joseph G Cicinelli, James W Pellegrino, and Phyllis A Fry. Nonvisual navigation by blind and sighted: assessment of path integration ability. *Journal of Experimental Psychology: General*, 122(1):73, 1993.

[110] Tyron Louw and Natasha Merat. Are you in the loop? using gaze dispersion to understand driver visual attention during vehicle automation. *Transportation Research Part C: Emerging Technologies*, 76:35 – 50, 2017.

[111] Cayley MacArthur, Arielle Grinberg, Daniel Harley, and Mark Hancock. Youâre making me sick: A systematic review of how virtual reality research considers gender & cybersickness. In *Proceedings of the 2021 CHI Conference on Human Factors in Computing Systems*, CHI '21, New York, NY, USA, 2021. Association for Computing Machinery.

[112] Jeff MacInnes. Wearable Eye-tracking for Research : comparisons across devices. *bioRxiv*, 2018.

[113] Takurou Magaki and Michael Vallance. Developing an accessible evaluation method of VR cybersickness. *26th IEEE Conference on Virtual Reality and 3D User Interfaces, VR 2019 - Proceedings*, pages 1072–1073, 2019.

[114] Michael E McCauley and Thomas J Sharkey. Cybersickness: Perception of self-motion in virtual environments. *Presence: Teleoperators & Virtual Environments*, 1(3):311–318, 1992.

[115] Morgan McCullough, Hong Xu, Joel Michelson, Matthew Jackoski, Wyatt Pease, William Cobb, William Kalescky, Joshua Ladd, and Betsy Williams. Myo arm: swinging to explore a ve. In *Proceedings of the ACM SIGGRAPH Symposium on Applied Perception*, pages 107–113, 2015.

[116] Omar Merhi, Elise Faugloire, Moira Flanagan, and Thomas A Stoffregen. Motion sickness, console video games, and head-mounted displays. *Human Factors*, 49(5):920–934, 2007.

[117] Betty J Mohler, William B Thompson, Sarah H Creem-Regehr, Herbert L Pick, and William H Warren. Visual flow influences gait transition speed and preferred walking speed. *Experimental brain research*, 181(2):221–228, 2007.

[118] Richard GM Morris. Spatial localization does not require the presence of local cues. *Learning and motivation*, 12(2):239–260, 1981.

[119] Mustapha Mouloua, Janan Smither, Robert C. Kennedy, Robert S Kennedy, Daniel E Compton, and Julie M Drexler. Training effects in a sickness-inducing environment. In *Proceedings of the Human Factors and Ergonomics Society*, pages 2206–2210, 2005.

[120] Justin Munafo, Meg Diedrick, and Thomas A Stoffregen. The virtual reality head-mounted display oculus rift induces motion sickness and is sexist in its effects. *Exp. Brain Research*, pages 1–13, 2016.

[121] Noah Nelson. Npr: All tech considered. virtual reality's next hurdle: Overcoming 'sim sickness' http://www.npr.org/sections/alltechconsidered/2014/08/05/338015854/virtual-realitys-next-hurdle-overcoming-sim-sickness, August 2015.

[122] Michael C. Newman, Geoffrey W. McCarthy, Scott T. Glaser, Frederick Bonato, and Andrea Bubka. Motion sickness adaptation to coriolis-inducing head movements in a sustained G flight simulator. *Aviation Space and Environmental Medicine*, 84(2):104–109, 2013.

[123] Tao Ni, Doug A Bowman, and Jian Chen. Increased display size and resolution improve task performance in information-rich virtual environments. In

Proceedings of Graphics Interface 2006, pages 139–146. Canadian Information Processing Society, 2006.

[124] Felix Nickel, Julia A Brzoska, Matthias Gondan, Henriette M Rangnick, Jackson Chu, Hannes G Kenngott, Georg R Linke, Martina Kadmon, Lars Fischer, and Beat P Müller-Stich. Virtual reality training versus blended learning of laparoscopic cholecystectomy: a randomized controlled trial with laparoscopic novices. *Medicine*, 94(20), 2015.

[125] Guangyu Nie, Yue Liu, and Yongtian Wang. Prevention of visually induced motion sickness based on dynamic real-time content-aware non-salient area blurring. In *Mixed and Augmented Reality (ISMAR-Adjunct), 2017 IEEE International Symposium on*, pages 75–78. IEEE, 2017.

[126] Diederick C. Niehorster, Tim H.W. Cornelissen, Kenneth Holmqvist, Ignace T.C. Hooge, and Roy S. Hessels. What to expect from your remote eye-tracker when participants are unrestrained. *Behavior Research Methods*, 2018.

[127] Raffaella Nori, Laura Piccardi, Andrea Maialetti, Mirco Goro, Andrea Rossetti, Ornella Argento, and Cecilia Guariglia. No gender differences in egocentric and allocentric environmental transformation after compensating for male advantage by manipulating familiarity. *Frontiers in neuroscience*, 12:204, 2018.

[128] Marcus Nyström, Richard Andersson, Kenneth Holmqvist, and Joost van de Weijer. The influence of calibration method and eye physiology on eyetracking data quality. *Behavior Research Methods*, 2013.

[129] Marcus Nyström and Kenneth Holmqvist. An adaptive algorithm for fixation, saccade, and glissade detection in eyetracking data. *Behavior Research Methods*, 2010.

[130] Oculus. Oculus best practices: Motion, https://developer.oculus.com/design/latest/concepts/bp-locomotion/, June 2017.

[131] Stephen Palmisano, Robert S. Allison, Juno Kim, and Frederick Bonato. Simulated viewpoint jitter shakes sensory conflict accounts of vection. *Seeing and Perceiving*, 24(2):173–200, 2011.

[132] Stephen Palmisano, Robert S. Allison, Mark M. Schira, and Robert J. Barry. Future challenges for vection research: Definitions, functional significance, measures, and neural bases. *Frontiers in Psychology*, 6(FEB):1–15, 2015.

[133] Stephen Palmisano, Rebecca Mursic, and Juno Kim. Vection and cybersick-

ness generated by head-and-display motion in the Oculus Rift. *Displays*, 46:1–8, 2017.

[134] George D Park, R Wade Allen, Dary Fiorentino, Theodore J Rosenthal, and Marcia L Cook. Simulator sickness scores according to symptom suscepti- bility, age, and gender for an older driver assessment study. In *Proceedings of the Human Factors and Ergonomics Society Annual Meeting*, volume 50, pages 2702–2706. Sage Publications Sage CA: Los Angeles, CA, 2006.

[135] Frederick Patterson and Yancy York. VECTION AND MOTION THRESH- OLDS AS A FUNCTION OF CONTRAST. 2009.

[136] Denis Pelisson and Alain Guillaume. Eye-head coordination. *Encyclopedia of Neuroscience*, pages 1545–1548, 2009.

[137] Yi Hao Peng, Carolyn Yu, Shi Hong Liu, Chung Wei Wang, Paul Taele, Neng Hao Yu, and Mike Y. Chen. WalkingVibe: Reducing Virtual Reality Sickness and Improving Realism while Walking in VR using Unobtrusive Head-mounted Vibrotactile Feedback, 2020.

[138] Thies Pfeiffer and Marc Erich Latoschik. Evaluation of Binocular Eye Track- ers and Algorithms for 3D Gaze Interaction in Virtual Reality Environments. *Journal of Virtual Reality and Broadcasting*, 2008.

[139] Dominique Piber, Jan Nowacki, Sven C Mueller, Katja Wingenfeld, and Christian Otte. Sex effects on spatial learning but not on spatial memory retrieval in healthy young adults. *Behavioural brain research*, 336:44–50, 2018.

[140] Jérémy Plouzeau, Damien Paillot, Jean-Rémy Chardonnet, and Frédéric Me- rienne. Effect of proprioceptive vibrations on simulator sickness during nav- igation task in virtual environment. 2015.

[141] Katharina Margareta Theresa Pöhlmann, Louise OâHare, Patrick Dickinson, Adrian Parke, and Julia Föcker. Action Video Game Players Do Not Differ in the Perception of Contrast-Based Motion Illusions but Experience More Vection and Less Discomfort in a Virtual Environment Compared to Non- Action Video Game Players, 2021.

[142] Nicholas F Polys, Seonho Kim, and Doug A Bowman. Effects of information layout, screen size, and field of view on user performance in information- rich virtual environments. *Computer Animation and Virtual Worlds*, 18(1):19– 38, 2007.

[143] Aniruddha Prithul, Isayas Berhe Adhanom, and Eelke Folmer. Teleportation in Virtual Reality; A Mini-Review. *Frontiers in Virtual Reality*, 2, 10 2021.

[144] Jerrold D Prothero, Mark H Draper, D E Parker, M J Wells, and others. The use of an independent visual background to reduce simulator side-effects. *Aviation, space, and environmental medicine*, 70(3 Pt 1):277–283, 1999.

[145] Jerrold D Prothero, Mark H Draper, DE Parker, MJ Wells, et al. The use of an independent visual background to reduce simulator side-effects. *Aviation, space, and environmental medicine*, 70(3 Pt 1):277–283, 1999.

[146] James T Reason and Joseph John Brand. *Motion sickness.* Academic press, 1975.

[147] Reason J. Motion sickness adaptation: a neural mismatch model! *Journal of the Royal Society of Medicine*, 71(November):819–829, 1978.

[148] Lisa Rebenitsch and Charles Owen. Review on cybersickness in applications and visual displays. *Virtual Reality*, 20(2):101–125, 2016.

[149] E. C. Regan. Some evidence of adaptation to immersion in virtual reality. *Displays*, 16(3):135–139, 1995.

[150] Gary E Riccio and Thomas A Stoffregen. An ecological theory of motion sickness and postural instability. *Ecological psychology*, 3(3):195–240, 1991.

[151] Gary E Riccio and Thomas A Stoffregen. An ecological theory of motion sickness and postural instability. *Ecological psychology*, 3(3):195–240, 1991.

[152] Bernhard E. Riecke, JÃ¶rg Schulte-Pelkum, Heinrich H. Bülthoff, and Markus von der Heyde. Cognitive Factors Can Influence Self-Motion Perception (Vection) in Virtual Reality. *ACM Transactions on Applied Perception*, 3(3):194–216, 2006.

[153] John J Rieser, D Guth, and E Hill. Mental processes mediating independent travel: Implications for orientation and mobility. *Journal of Visual Impairment and Blindness*, 1982.

[154] Rose Marie Rine, Michael C Schubert, and Thomas J Balkany. Visual-vestibular habituation and balance training for motion sickness. *Physical therapy*, 79(10):949–957, 1999.

[155] Rose Marie Rine, Michael C Schubert, and Thomas J Balkany. Visual-vestibular habituation and balance training for motion sickness. *Physical Therapy*, 79(10):949–957, 1999.

[156] Giuseppe Riva and Luciano Gamberini. Virtual reality in telemedicine. *Telemedicine Journal and e-Health*, 6(3):327–340, 2000.

[157] Noah J Sandstrom, Jordy Kaufman, and Scott A Huettel. Males and females use different distal cues in a virtual environment navigation task. *Cognitive Brain Research*, 6(4):351–360, 1998.

[158] Xavier M. Sauvan and Claude Bonnet. Properties of curvilinear vection. *Perception & Psychophysics*, 53(4):429–435, 1993.

[159] A Fleming Seay, David M Krum, Larry Hodges, and William Ribarsky. Simulator sickness and presence in a high fov virtual environment. In *Virtual Reality, 2001. Proceedings. IEEE*, pages 299–300. IEEE, 2001.

[160] Takeharu Seno, Kayoko Murata, Yoshitaka Fujii, Hidetoshi Kanaya, Masaki Ogawa, Kousuke Tokunaga, and Stephen Palmisano. Vection Is Enhanced by Increased Exposure to Optic Flow. *i-Perception*, 9(3), 2018.

[161] Takeharu Seno, Kayoko Murata, Yoshitaka Fujii, Hidetoshi Kanaya, Masaki Ogawa, Kousuke Tokunaga, and Stephen Palmisano. Vection Is Enhanced by Increased Exposure to Optic Flow. *i-Perception*, 9(3), 2018.

[162] E. Sinitski, A. A. Thompson, P. Capt Godsell, J. Lt(N) Honey, and M. Besemann. Postural stability and simulator sickness after walking on a treadmill in a virtual environment with a curved display. *Displays*, 52(December 2017):1–7, 2018.

[163] Janan Al Awar Smither, Mustapha Mouloua, and Robert Kennedy. Reducing symptoms of visually induced motion sickness through perceptual training. *International Journal of Aviation Psychology*, 18(4):326–339, 2008.

[164] Kalpana Srivastava, RC Das, and S Chaudhury. Virtual reality applications in mental health: Challenges and perspectives. *Industrial psychiatry journal*, 23(2):83, 2014.

[165] Kay Stanney, Cali Fidopiastis, and Linda Foster. Virtual reality is sexist: but it does not have to be. *Frontiers in Robotics and AI*, 7(4), 2020.

[166] Kay M Stanney, Kelly S Hale, Isabelina Nahmens, and Robert S Kennedy. What to expect from immersive virtual environment exposure: Influences of gender, body mass index, and past experience. *Human Factors*, 45(3):504–520, 2003.

[167] Kay M. Stanney, Kelly S. Hale, Isabelina Nahmens, and Robert S. Kennedy. What to Expect from Immersive Virtual Environment Exposure: Influences of Gender, Body Mass Index, and Past Experience. *Human Factors*, 45(3):504–520, 2003.

[168] Kay M Stanney and Phillip Hash. Locus of user-initiated control in virtual environments: Influences on cybersickness. *Presence*, 7(5):447–459, 1998.

[169] Michael J Starrett and Arne D Ekstrom. Perspective: Assessing the flexible acquisition, integration, and deployment of human spatial representations and information. *Frontiers in human neuroscience*, 12, 2018.

[170] Evan A Suma, Seth Clark, David Krum, Samantha Finkelstein, Mark Bolas, and Zachary Warte. Leveraging change blindness for redirection in virtual environments. In *2011 IEEE Virtual Reality Conference*, pages 159–166. IEEE, 2011.

[171] David Swapp, Julian Williams, and Anthony Steed. The implementation of a novel walking interface within an immersive display. In *2010 IEEE Symposium on 3D User Interfaces (3DUI)*, pages 71–74. IEEE, 2010.

[172] Noriaki Takeda, Masahiro Morita, Arata Horii, Suetaka Nishiike, Tadashi Kitahara, and Atsuhiko Uno. Neural mechanisms of motion sickness. *The Journal of Medical Investigation*, 48:44–59, 2001.

[173] Desney S Tan, Mary P Czerwinski, and George G Robertson. Large displays enhance optical flow cues and narrow the gender gap in 3-d virtual navigation. *Human Factors*, 48(2):318–333, 2006.

[174] Nobuhisa Tanaka and Hideyuki Takagi. Virtual reality environment design of managing both presence and virtual reality sickness. *Journal of physiological anthropology and applied human science*, 23(6):313–317, 2004.

[175] Luke Thompson. Unity vr tunneling, https://github.com/SixWays/UnityVrTunnelling.

[176] Nana Tian, Phil Lopes, and Ronan Boulic. A review of cybersickness in head-mounted displays: raising attention to individual susceptibility. *Virtual Reality*, 3 2022.

[177] Tobii Technology. Accuracy and precision test method for remote eye trackers. *Test*, 2011.

[178] Sam Tregillus and Eelke Folmer. VR-STEP: Walking-in-place using inertial sensing for hands free navigation in mobile vr environments. In *Proceedings of the 2016 CHI Conference on Human Factors in Computing Systems*, pages 1250–1255. ACM, 2016.

[179] Michel Treisman. Motion sickness: an evolutionary hypothesis. *Science*, 197(4302):493–495, 1977.

[180] UnityTechnologies. Windridge City, 2021.

[181] Martin Usoh, Kevin Arthur, Mary C Whitton, Rui Bastos, Anthony Steed, Mel Slater, and Frederick P Brooks Jr. Walking> walking-in-place> flying, in virtual environments. In *Proc. of the 26th conference on Computer graphics and interactive techniques*, pages 359–364, 1999.

[182] Robert J van Beers, Anne C Sittig, and Jan J Denier van Der Gon. Integration of proprioceptive and visual position-information: An experimentally supported model. *J. of neurophysiology*, 81(3):1355–1364, 1999.

[183] Roshan Venkatakrishnan, Rohith Venkatakrishnan, Ayush Bhargava, Kathryn Lucaites, Hannah Solini, Matias Volonte, Andrew Robb, Sabarish V Babu, Wen-Chieh Lin, and Yun-Xuan Lin. Comparative evaluation of the effects of motion control on cybersickness in immersive virtual environments. In *2020 IEEE Conference on Virtual Reality and 3D User Interfaces (VR)*, pages 672–681. IEEE, 2020.

[184] Isabelle Viaud-Delmon, Yuri P. Ivanenko, Alain Berthoz, and Roland Jouvent. Sex, lies and virtual reality. *Nature Neuroscience*, 1(1):15–16, May 1998.

[185] Trent W. Victor, Joanne L. Harbluk, and Johan A. Engström. Sensitivity of eye-movement measures to in-vehicle task difficulty. *Transportation Research Part F: Traffic Psychology and Behaviour*, 8(2):167 – 190, 2005. The relationship between distraction and driving performance: towards a test regime for in-vehicle information systems.

[186] Vive. Htc vive survey. http://u3915321.viewer.maka.im/pcviewer/R1HEHKCZ, 2017.

[187] Daniel Voyer, Susan Voyer, and M Philip Bryden. Magnitude of sex differences in spatial abilities: a meta-analysis and consideration of critical variables., 1995.

[188] Ying Wang, Bryan Reimer, Jonathan Dobres, and Bruce Mehler. The sensitivity of different methodologies for characterizing drivers' gaze concentration under increased cognitive demand. *Transportation research part F: traffic psychology and behaviour*, 26:227–237, 2014.

[189] Nicholas A Webb and Michael J Griffin. Eye movement, vection, and motion sickness with foveal and peripheral vision. *Aviation, space, and environmental medicine*, 74(6):622–625, 2003.

[190] Séamas Weech, Sophie Kenny, and Michael Barnett-Cowan. Presence and Cybersickness in Virtual Reality Are Negatively Related: A Review. *Frontiers in Psychology*, 10(FEB):1–19, 2 2019.

[191] Maxwell J Wells and Michael Venturino. Performance and head movements using a helmet-mounted display with different sized fields-of-view. *Optical Engineering*, 29(8):870–878, 1990.

[192] David Matthew Whittinghill, Bradley Ziegler, T Case, and B Moore. Nasum virtualis: A simple technique for reducing simulator sickness. In *Games Developers Conference (GDC)*, 2015.

[193] Daniel G Woolley, Ben Vermaercke, Hans Op de Beeck, Johan Wagemans, Ilse Gantois, Rudi D'Hooge, Stephan P Swinnen, and Nicole Wenderoth. Sex differences in human virtual water maze performance: Novel measures reveal the relative contribution of directional responding and spatial knowledge. *Behavioural brain research*, 208(2):408–414, 2010.

[194] Yoav Yair, Rachel Mintz, and Shai Litvak. 3d-virtual reality in science education: An implication for astronomy teaching. *Journal of Computers in Mathematics and Science Teaching*, 20(3):293–306, 2001.

[195] Hiroo Yamamura, Holger Baldauf, and Kai Kunze. Pleasant Locomotion - Towards Reducing Cybersickness using fNIRS during Walking Events in VR. *UIST 2020 - Adjunct Publication of the 33rd Annual ACM Symposium on User Interface Software and Technology*, (2):56–58, 2020.